POLITECNICO DI MILANO

School of Industrial and Information Engineering

Energy department

Master of Science in Energy Engineering

Micro-grid effective design exploiting PV and wind sources

Supervisor: Prof. Marco Merlo

Co-advisor: Eng. Matteo Moncecchi

Tutors: Eng. Alessandro Bertani (CESI)

Eng. Stefano Mandelli (CESI)

Master thesis of:

Fabio Scazzosi, 876341

Academic Year 2017 - 2018

Ringraziamenti

Un sentito ringraziamento va al Professor Marco Merlo che mi ha prontamente seguito e supportato lungo il percorso di stesura della tesi.

Ringrazio tutti coloro che hanno permesso la mia esperienza formativa presso CESI e in particolare Stefano Mandelli che mi ha guidato e aiutato durante lo svolgimento dello stage.

Ringrazio inoltre tutti i colleghi conosciuti al CESI che mi hanno accompagnato durante questa importante esperienza ed in particolare Giulia che nelle prime settimane di stage mi ha dato importanti consigli su come affrontare il lavoro da svolgere.

Infine, non posso dimenticare la mia famiglia e i gli amici di una vita che mi sono stati vicini in questi mesi di lavoro.

Index

Abstract

Today micro-grids are considered the best choice to face the problem of the rural electrification in developing countries. Therefore, it is important to study a method to optimize the system and to size the components of the grid in order to minimize investment and management costs.

In this thesis micro-grids that exploits renewable energy sources have been analyzed, in particular optimization methods for off-grid systems that adopt photovoltaic (PV) panels and wind turbines have been studied.

The optimization procedure has been implemented in Excel VBA and constitutes a tool that allows to compare different configurations and to choose the optimal one for the considered case. The aim of the tool is to help the decision-making process of an investor providing the best configuration, that is the one with the lowest cost (calculating NPC and LCoE) fixing a constraint on the reliability of the system (maximum acceptable LLP).

To optimize and properly size the components of a micro-grid it is necessary to accurately model the battery. The battery model is fundamental to estimate the energy fluxes within the system. Therefore, an advanced model has been implemented.

One of the configurations analyzed is a micro-grid composed by wind turbines and batteries. Implementing this configuration, it was necessary to study an algorithm that considers different turbines with different power curves and that is able to evaluate which and how many turbines to install to reduce the costs and to better exploit the wind resource.

The exploitation of different energy sources and the study of the optimal mix allow to minimize the battery size and, as a consequence, the costs of the micro-grid. Indeed, the procedure developed analyzes the configuration that adopts PV panels, wind turbines and battery. Therefore, at first it is necessary to optimize the mix of the sources and then to calculate the suitable sizes of battery and generation.

The implemented procedure was validated applying it to a case study: the St. Mary's Lacor Hospital in Uganda. The data relative to the load were provided by measurements taken at the hospital, while the data regarding the solar and wind resource were taken by online databases.

Key words: rural electrification; micro-grid optimization; wind turbines; multi-generation optimization.

Sommario

Oggi le micro reti sono considerate la scelta migliore per affrontare il problema dell'elettrificazione rurale nei paesi in via di sviluppo. È quindi importante studiare un metodo per ottimizzare il sistema e dimensionare i componenti della rete in modo da minimizzare i costi di investimento e di gestione.
In questa tesi sono state analizzate micro reti che sfruttano fonti rinnovabili, in particolare sono stati studiati metodi di ottimizzazione per reti isolate che adottano pannelli fotovoltaici e turbine eoliche.
La procedura di ottimizzazione è stata implementata in Excel VBA e costituisce un tool che permette di confrontare diverse configurazioni e di scegliere quella ottimale per il caso considerato. Lo scopo del tool è quello di aiutare il processo decisionale di un investitore fornendo la configurazione migliore, cioè quella a minor costo (calcolando NPC e LCoE) mantenendo un vincolo sull'affidabilità del sistema (massimo LLP accettabile).
Per ottimizzare e dimensionare correttamente le componenti di una micro rete è necessario modellare accuratamente la batteria. Il modello della batteria è fondamentale per stimare i flussi energetici all'interno del sistema. Per questa ragione è stato implementato un modello avanzato.
Una delle configurazioni analizzate è una micro rete composta dalle turbine eoliche e dalla batteria. Implementando questa configurazione è stato necessario studiare un algoritmo che consideri diverse turbine con diverse curve di potenza e che sia in grado valutare quali e quante turbine installare per ridurre i costi e meglio sfruttare la risorsa eolica.
Lo sfruttamento di diverse fonti energetiche e lo studio del mix ottimale permettono di minimizzare la taglia della batteria e, di conseguenza, i costi della micro rete. Infatti, la procedura sviluppata analizza la configurazione che adotta pannelli fotovoltaici, turbine eoliche e batteria. È quindi necessario prima ottimizzare il mix delle risorse e poi calcolare le taglie adatte di batteria e generazione.
La procedura implementata è stata poi validata applicandola ad un caso studio: il St. Mary's Lacor Hospital in Uganda. I dati relativi al carico provengono da misurazioni fatte presso l'ospedale, mentre i dati delle risorse solare e eolica sono stati presi da database online.

Parole chiave: elettrificazione rurale; ottimizzazione micro-reti; turbine eoliche; ottimizzazione multigenerazione.

Chapter 1

1 Introduction

1.1 Rural electrification in Africa

Even if in the last decade the opportunity to use modern energy services has been strongly promoted and improvements in the field of electrification have been remarkable, part of the humanity is still not able to access to reliable electricity and is affected by energy poverty. That is why one of the aims of the United Nation Sustainable Development Goals (UNSDG) is to reach the universal access by 2030 with the support of the global community [1]. In particular, estimates show a large deficit in access to energy for the world's poorest people, located mostly in sub-Saharan Africa.

According to the World Bank, in 2014 two out of ten people in the world still lacked electricity access. Although the global electricity access deficit has declined since 2000, still 15% of the world population do not have electricity. These numbers do not fully represent the problem, since other issues are important, such as quality, reliability and affordability of electricity.

The access deficit is overwhelmingly concentrated in Sub-Saharan Africa: 609 million people, that is 57% of global deficit, do not have access to electricity [2].

Moreover, the trend of population lacking access to electricity is negative for Sub-Saharan Africa, since the population growth is so high that the people without electricity access increased in the period 2000-2014 unlike the other world's regions (see Figure 1.1).

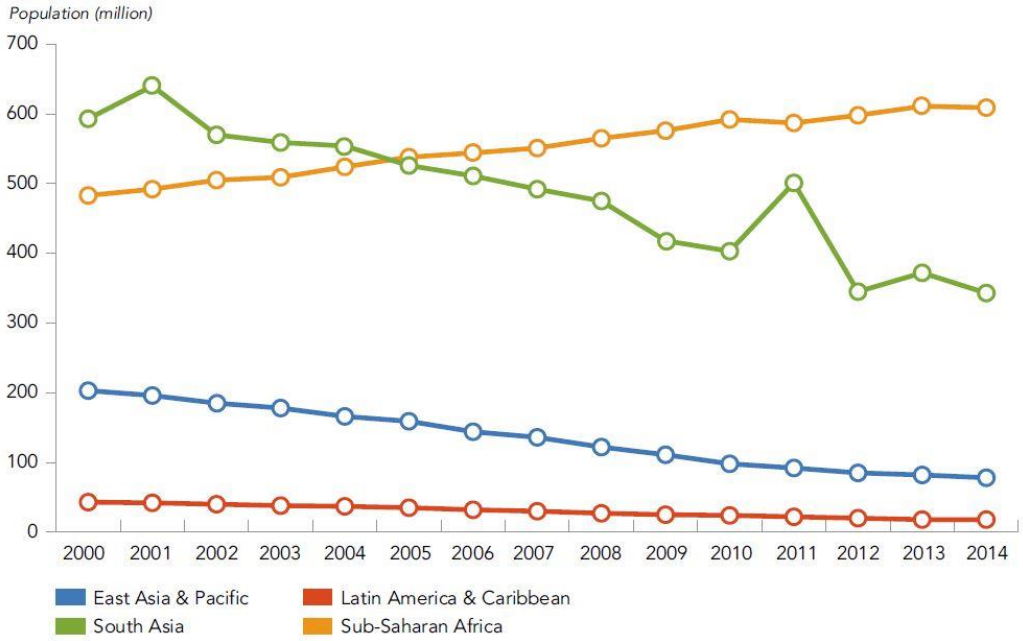

Figure 1.1 Trend in population lacking access to electricity between years 2000-2014

Access to energy can be considered a necessary condition for development but still not enough: experience has shown that electrification and the use of more modern technologies alone are unable to implement change. Anyway, the growing evidence of economic-environment-socio benefits due to electricity, motivates programs to improve the usage of cleaner and more reliable forms of energy. Indeed in Figure 1.2 is evident the relationship between energy consumption and Gross National Income.

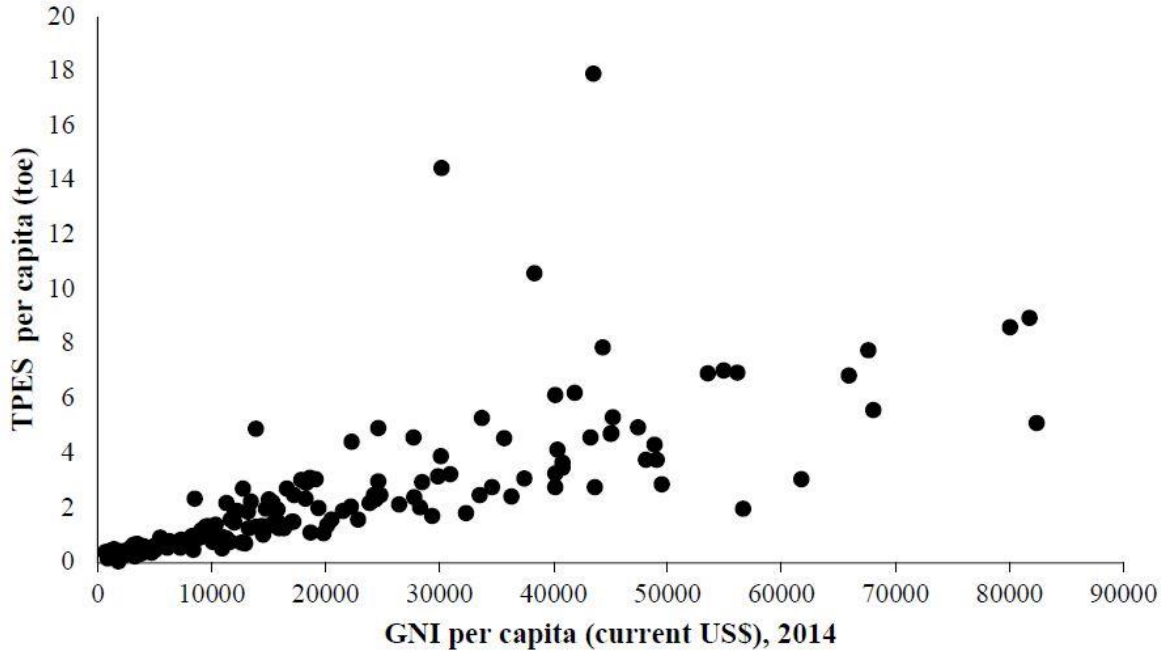

Figure 1.2 Correlation between Gross National Income and Total Primary Energy Supply

At household level, for example, electricity guarantees the extension of working hours, reading and studying, as well as the use of new technologies such as radio and television. In addition, cleaner fuel access decreases the child mortality rate, increases overall health, reduces the time that women and children use to collect wood and coal, avoids exposure to smoke from bad fuels. Rural electrification influences agriculture and small industries, raising their income and productivity using new tools and machines.

Another effect is to reduce transport and communication costs, thus expanding the size and accessibility of the market. In countries with low Gross National Income various sectors like industry, services and exchanges are not developed also because they do not fully exploit their potential, remaining dependent on expensive and inefficient processes. Other issues such as blackouts may dramatically affect the country's economy [3].

The World Bank also estimates that in 2014 the electrification rate stands globally at 85%, with 96% in urban areas and 73% in rural areas and the access deficit is overwhelmingly rural, at about 87%. So, the main efforts have to be done to reach sparsely populated areas, often characterized by small villages far from the main cities and the electric grid [2].

So, two approaches need to be considered when supplying electricity to rural areas. These are grid extensions and off-grid systems.

In developed countries electrification is usually related to grid extension and centralized power generation, distribution and transmission systems. National grid extensions may lower the electricity cost due to more efficient power production, but the cost of connecting sparsely populated regions can be significantly higher. Long distance transmission systems may also have high technical losses [4].

More affordable electricity could be supplied to rural communities using off grid power systems, which also integrate renewable energy sources: micro-grid/off-grid plants are capable to promote rural electrification according to local needs, relying on local resources [5]. However, this approach comes with high investment costs. Off grid power systems are modular, ranging from small home-based systems (that typically rely on a single source), to micro-grids that can integrate more energy sources providing electricity to an entire community. In particular, micro-grids showed the most promising results to face the issue of rural electrification [6].

In developing countries, where the energy system is still under development, it could be sensible to consider small scale decentralized systems as a sustainable alternative to the traditional development of the energy system, based on a centralized approach. Nevertheless, the distributed approach has evident limits: high investment costs and the inherent uncertainty of supply, and the associated problems of stability and management.

1.2 Off-grid systems

In the previous paragraph the importance of the off-grid systems in order to guarantee the electricity access for rural areas was discussed. It is now necessary to classify the different off-grid systems: they can be divided in decentralized and distributed systems [7] [8] [9] [10].

The decentralized systems are composed by autonomous units where conversion and distribution have no interaction with other units. Such systems are usually designed for the specific local energy needs and they often rely only on renewable energy sources. The decentralized systems can be divided into stand-alone and micro-grid systems. The former refers to systems which supply power to nearby single consumers, the latter to systems which supply power to several, similar or different, consumers by means of a distribution grid.

The distributed systems are made by more than one decentralized conversion unit which are connected and interact with each other by means of a distribution grid. This results in several generation points equipped with centralized control that receives data about the operational status of the system and determines how to manage it. These systems are called hybrid micro-grids since they combine conventional fossil energy sources with non-conventional renewable sources.

The present thesis deals only with micro-grids based on renewable sources. The main components of the grid are:

- PV panels: they are composed by cells made of different semi-conductor materials that are able to transform sunlight into direct current.
- Maximum power point tracker (MPPT): it modifies the operating voltage of the PV system in order to maximize its power generation.
- Wind turbines: they exploit the kinetic energy of the wind to generate alternating current.
- AC/DC converter: it transforms the alternating current from the wind turbines in direct current. The wind turbines cannot be directly connected to the AC load since the electric frequency depends on the generator rotational speed, so it depends on wind velocity.
- Batteries: they are electrochemical devices that are able to store energy.
- Charge controller: it is a device that manages the battery and regulates their charge and discharge.
- Inverter: it transforms the DC electricity from the generation and the battery into AC current given to the load, so it connects the DC bus to the AC load.
- Grid: it is constituted by the cables that connect the inverter with all the users.

All these components are summarized in the following figure that represents an example of micro-grid.

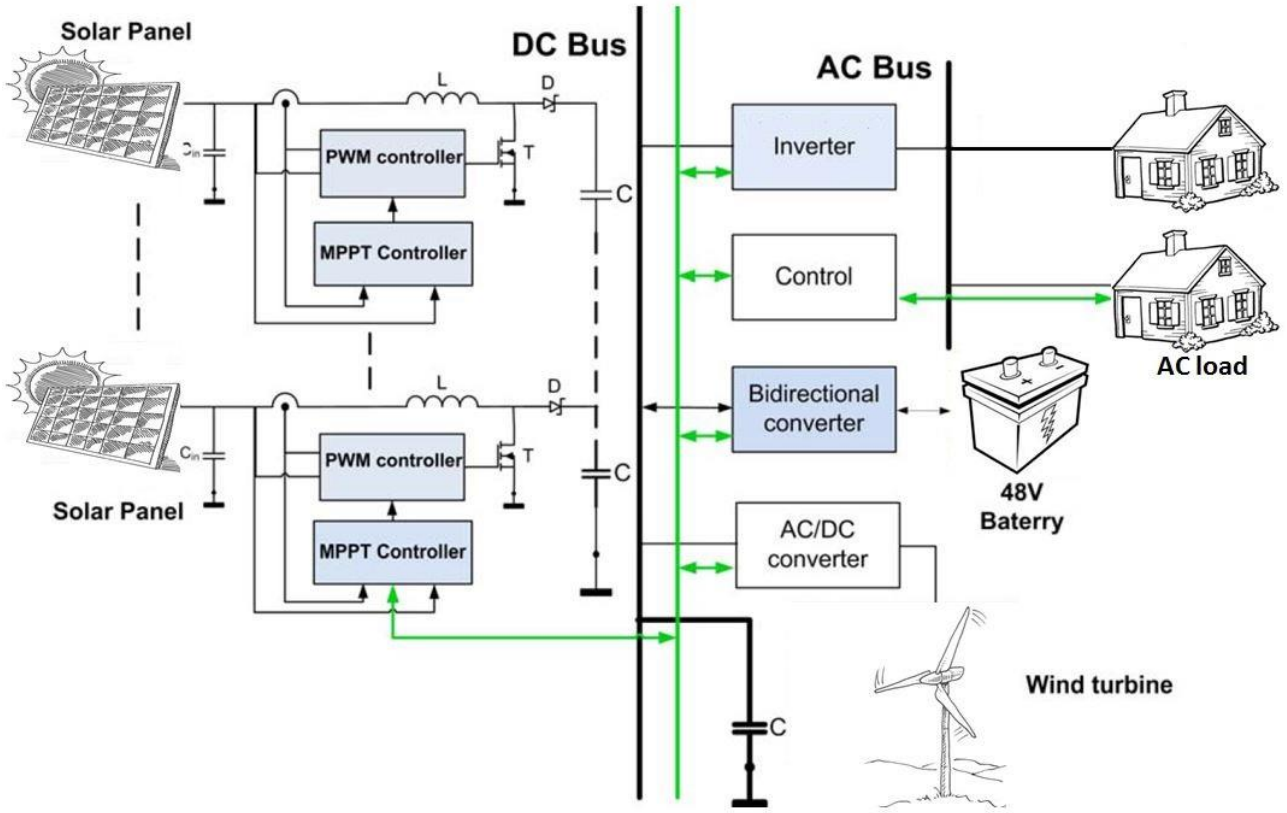

Figure 1.3 Example of micro-grid's components

The micro-grids, even when they rely only on a few energy sources, can have quite complex configurations with different DC voltage levels [11].

1.3 Review on micro-grid optimization software tools

It is now clear that, in order to face the electrification of rural areas in the short-medium scenario, it is necessary to relay on off-grid systems, and so it is necessary to apply specific procedures to size the micro-grid components.

The technical and economic analyses of a micro-grid system are essential for the efficient utilization of renewable energy resources and to avoid too high installation costs. Especially when more than a renewable energy source is considered, the system optimization is complex to be solved. This requires software tools and models which can be used for the design, analysis, optimization and economic planning. A number of software tools have been developed to assess the technical and economic potential of various hybrid renewable technologies to simplify the hybrid system design process and maximize the use of the renewable resources. In the following, a review on some of the software tools developed is reported [12] [13].

HOMER

The Hybrid Optimization of Multiple Energy Resources is the most widely used software. It was developed by the National Renewable Energy Laboratory (NREL) USA and it can carry out quick prefeasibility, optimization and sensitivity analysis in several possible system configurations. It models any combination of wind turbines, PV arrays, hydro power, biomass power, internal combustion engine generators, microturbines, fuel cells, batteries, and hydrogen storage, serving both electric and thermal loads.

It uses inputs like various technology options, components costs and resource availability. It simulates different configurations and generates a list of feasible configurations with many tables and graphs to compare them. HOMER can suggest the best configuration basing on economic parameters.

The main limitations are that it does not consider the depth of discharge of the battery and its relationship with the lifetime. It also does not consider the intra-hour variability and the variations of the bus voltage.

HYBRID 2

It is a probabilistic computer model and uses statistical methods to account for variations within a time step. It can perform long term performance and economic analysis. It can provide time series simulations with time steps between 10 minutes and 1 hour. HYBRID 2 has a limited access to parameters and lack of flexibility but it has a library with various resource data files. It allows to simulate systems based on three buses containing wind turbines, PV, diesel and battery.

RETScreen

It is developed for evaluating both financial and environmental costs and benefits of different renewable energy technologies for any location in the world. It has a global climate database, energy resource maps and grid components' data. It also studies water pumping. This tool can study the technical and financial feasibility of projects involving renewable energies, energy efficiency and cogeneration. The project analyses are performed by means of cost analysis, emission analysis, financial analysis and risk analysis.

The main limitations of RETScreen are that it does not take into account for the PV dependence on temperature, it does not support advanced calculations and it has limited options for search.

iHOGA

The Improved Hybrid Optimization by Genetic Algorithm is used for optimum sizing of hybrid energy system which may include photovoltaic system, wind turbines, hydroelectric turbines, fuel cells, H2 tanks, and electrolyzers, storage systems, fossil fuel based generating systems with multi or mono objective optimization using a genetic algorithm and sensitivity analysis with a low time-consuming procedure.

It can optimize the PV panel slope and calculate the system emissions. The main limitations of iHOGA are that it can simulate only load with a daily average lower than 10 kWh and that the sensitivity analysis is not included.

INSEL

The Integrated Simulation Environment Language is a software tool that has the flexibility of creating configurations for planning and monitoring of electrical and thermal energy systems. It has its own database of meteorological parameters of almost 2000 locations worldwide.

TRNSYS

The Transient Energy System Simulation Program was initially developed for thermal systems simulation, but now includes photovoltaic, thermal solar and other systems and has become a hybrid simulator.
It is an extremely flexible graphically based software used to simulate transient system behavior.
It simulates the performance of the entire energy system by breaking it down into individual components, and it is primarily used for analyzing single-project, local community or island energy systems. The tool used a user-defined time step and it can analyze the performances of the system in a horizon of many years.

1.4 Stand-alone micro-grid design

The object of this thesis is the study and the development of a new procedure implemented in a software tool that have to give the configuration for the electrification of rural areas by means of a sub-optimal solution for the components sizing. This tool has been studied following the guidelines proposed by CESI, Centro Elettrotecnico Sperimentale Italiano, where the author undertook an internship experience, with the didactic purposes of a thesis development. Instead of adopting one of the software tools existing on the market and reported in the previous paragraph, CESI is interested at developing and using its own software with all the characteristics and functionalities needed. The scope is to have a procedure that can support the decisions of the investors, in particular it has to be fast and simple so that it can help the decision-making also for non-technical personnel.
In order to do so it is required to study and compare different configurations, therefore it is necessary to introduce some parameters: the LLP to evaluate the system reliability and the LCoE to calculate its cost.
The analyzed system may not be able to provide enough electricity to satisfy the load demand. In this case the system faces a loss of load:

$$LL(t) = load(t) - \big(gen(t) + E_{batt}(t)\big) * \eta_{inv}$$

Equation 1.1 Loss of load for each time step t

Where $load(t)$ is the load demand, $gen(t)$ is the energy generated and $E_{batt}(t)$ is the energy given by the battery.

So, the reliability of the system can be calculated by means of the Loss of Load Probability during the all considered lifespan T.

$$LLP = \frac{\sum_{t=0}^{T} LL(t)}{\sum_{t=0}^{T} load(t)}$$

Equation 1.2 Loss of Load Probability

The configurations cost is evaluated calculating the Net Present Cost which provides the amount of capital required to implement the specific scenario throughout the fixed period. It takes into account the initial investment cost $inv(0)$, an estimation of the operations and maintenance costs of each component and the battery replacement cost since its lifetime is shorter than the considered lifespan T.

$$NPC = inv(0) + \sum_{y=1}^{Ny} \frac{O\&M(y) + BatteryReplacement(y)}{(1+r)^y}$$

Equation 1.3 Net Present Cost. y are the years of the simulation

Where Ny are number of years simulated, so that $T = Ny * 8760$.
Knowing the NPC, it is possible of evaluate the Levelized Cost of Energy which expresses the price for electricity that would equalize the sum of discounted costs throughout the lifespan of the considered scenario.

$$LCoE = \frac{NPC}{\sum_{y=1}^{Ny} \frac{load(y) - LL(y)}{(1+r)^y}}$$

Equation 1.4 Levelized Cost of Energy

The sub-optimization procedure has been implemented in Excel VBA (Visual Basic for Applications) and it is composed by many modules, each of them studies a different configuration, so that it is possible to compare them.
When the author started his internship at CESI, some modules were already implemented by other interns [14], in particular they were:

- *PV stand-alone.*
- *PV micro-grid.*
- *PV+genset micro-grid.*
- *Grid extension.*

The general idea for all modules but the grid extension is:

1. Identification of an intuitive sizing of the micro-grid components, by means of simple equations, a starting point for the components sizes can be found.
2. Creation of several configurations (space of analysis), starting from the intuitive sizing the components sizes are varied (Figure 1.4).
3. Evaluation of the system's reliability for each configuration, in a quantitative manner (LLP).
4. Calculation of the costs (LCoE) of each configuration.
5. Selection of the sub-optimum configuration: once the reliability and the cost are known for each configuration in the space of analysis, the solution that the procedure is looking for is the configuration that gives the lowest LCoE among the ones that do not exceed the maximum LLP (here set equal to 5%).

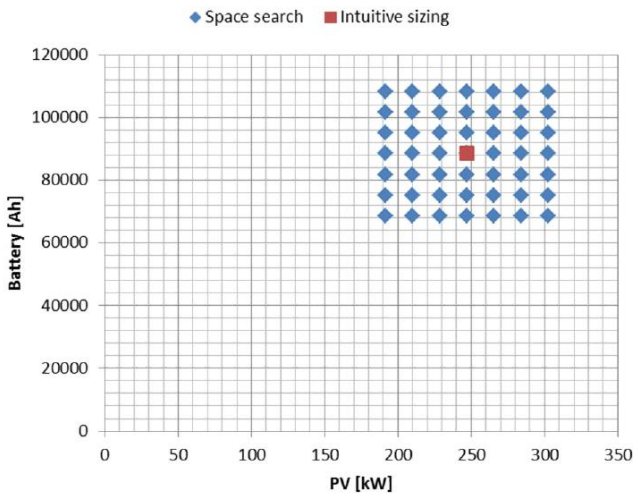

Figure 1.4 Space of analysis for PV-battery sizing

As said, each module studies a different configuration:

- The *PV stand-alone* module studies a scenario in which the grid is not present and so every house in the target village has its own PV plant and battery. Therefore, for each house (or for each type of user) PV and battery have to be sized evaluating LLP and LCoE in a space of analysis based on the load of that specific house.
- The *PV micro-grid* module studies a scenario similar to the previous one, but the PV and the batteries are a unique and centralized plant connected with the village by means of a micro-grid. The size of PV and battery can be found studying a unique space of analysis based on the load of the whole village. From the number of the buildings and the dimension of the village the length of the cables can be estimated, and so also the micro-grid cost.
- The *PV+genset micro-grid* module sizes PV, diesel generator and battery adopting a heuristic procedure. As the previous one it deals with a centralized micro-grid which is sized as before and so

the load is the total one of the village. The PV is set to a certain percentage (PV share) of the peak load while the maximum power of the diesel generator is another percentage (peak shaving) of the peak of the residual load. Therefore, the battery has to cover the energy that is not provided by neither the PV nor the genset. The space of analysis is created varying the values of PV share and peak shaving, giving again a space of analysis with 2 dimensions.

- The *grid extension* module evaluates the costs of the connection of the village micro-grid with the national grid. It has to take into account the investment cost for the construction of the new electric line, the transformer and the house connection and the cost of electricity purchased by the national grid.

To perform the calculations with this last module it is important to know the distance between the village and the existing grid.

As far as the other three modules are concerned it is necessary to know the PV generation. These data concerning the PV generation have been taken from the website database Renewables.ninja. In particular the tool needs the power generated by the PV for each kW of installed peak power for the analyzed location. In this way the values given by Renewables.ninja with a 1-hour time step can be multiplied by the PV size to have the real generated energy.

1.5 Motivations and objectives

The scope of this thesis was to implement new functionalities developed to improve the tool presented in 1.4; in particular the goals were in the study of a proper battery model and in a new optimization procedure capable to handle multi-generation micro-grids, and specifically the PV+wind configuration has been investigated.

The battery is an important element in off-grid systems since is fundamental to provide energy when the unpredictable renewable sources are not working. For this reason, in order to properly size the components, it is important to simulate the battery behavior by means of an accurate model. The model previously implemented was a simple one based on the maximum number of battery cycles. The battery lifetime was given by the maximum number of cycles: it means that when a certain number of cycles (or equivalently a certain value of energy fluxed) was reached the battery had to be replaced. That model was characterized by a constant charge and discharge efficiency and a constant capacity of the battery, which are characteristics that do not really represent the reality. Often the efficiency and the battery lifetime resulted to be underestimated. For this reason an advanced battery model was introduced in the tool.

The micro-grids based on PV have been implemented many times today, so it is a well-known solution. The main problem of this solution is the presence of quite big and expensive batteries that have to cover the load during night and in general the unpredictability of the PV source. Adding a diesel generator can be a solution but the fuel is expensive and may be a problem to be transported to an isolated village. Moreover, there is the

risk of explosion and pollution. An alternative solution is to consider hybrid configurations, combining wind turbines with PV.

Consequently, the addressed topics of this work that result in new elements added to the tool by the author are:

- A new advanced empirical battery model.
- The *wind micro-grid* module.
- The *PV+wind micro-grid* module.

The data necessary to model the wind turbines generation are the velocity of the wind in the analyzed location. These data have been taken from the website database Renewables.ninja where the wind speed at 10 meters from the soil (usual anemometer height) is available.

To model the energy generated by the turbines it is necessary to know the power-velocity curve of a specific turbine. These curves have been taken from the database of HOMER. HOMER is a software tool that has already been presented in the paragraph 1.3. In particular among all the turbines present in its database only the ones with a nominal power lower than 1MW (otherwise too big to deal with a small rural village) and still present in the market have been considered.

In the *wind micro-grid* module the main objective was to study a procedure to select a turbine in the database that best fit the problem according to techno-economic evaluations. This is something new with respect to commercial software, in which typically it is only possible to select the turbine among the available ones and perform the simulation with the turbine chosen by the user [15]. The *wind micro-grid* module is also able to give the optimum size of the battery and the optimum number of turbines.

Once this procedure is defined, it is interesting to combine the PV and the wind sources and to look for the optimum mix of the two. Indeed, the *PV+wind micro-grid* module is a procedure to choose a PV/wind share from which it is possible to size the main component of the grid (PV panels, wind turbines and batteries), while the turbine is chosen among the ones in the database with the same procedure studied in the previous module.

For each of the three main topics just discussed, the author activity can be summarized as follows:

- Literature review on the topic studying the state of the art.
- Comparison of the models or solution proposed in literature to find the most suitable one to be adopted and adapted to the tool purposes.
- Implementation of the chosen procedure in the tool code.
- Search of technical data of the components.
- Comparison and analysis of the results.

The procedures developed have been coded in Excel VBA, and a proper visual interface, whose commands panel is reported in Figure 1.5, has been developed.

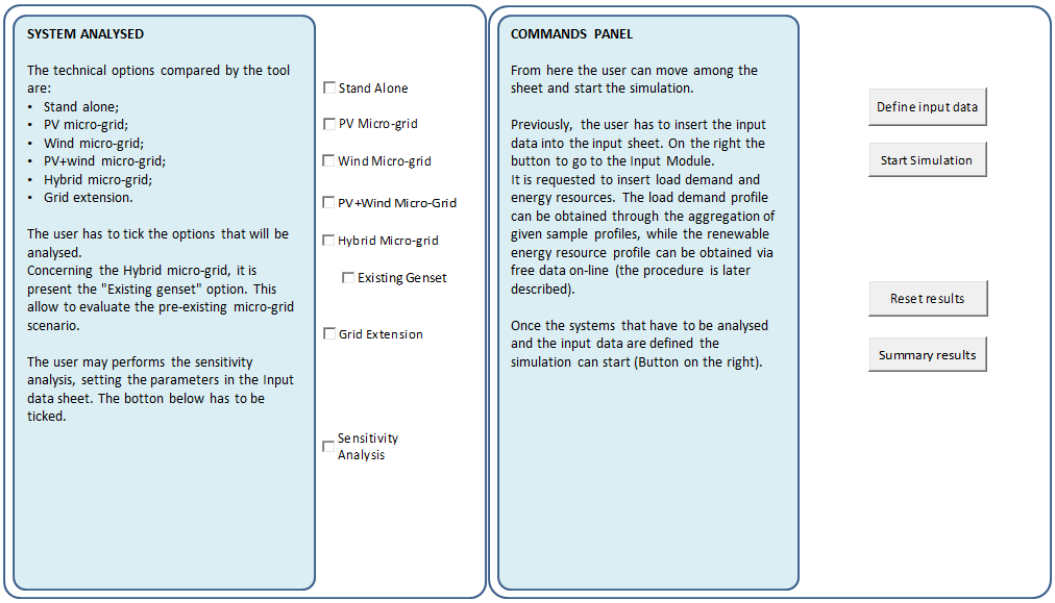

Figure 1.5 Commands panel interface of the developed procedure

1.6 Thesis structure

In the present thesis at first the elements added to the tool are explained, then the results relative to the case study are reported, according to the following structure.

In Chapter 2, after a description of the different models present in literature, the empirical battery model is explained in detail, showing the equations and the algorithm implemented in the tool. After that it is possible to compare the results given by the advanced and the simple model.

Chapter 3 shows the components and the configuration of a micro-grid and it explains how the *wind micro-grid* module is implemented. It shows how the simulated turbines are chosen, how the number of turbine and the battery size is calculated and how the best turbine and the optimum configuration is chosen among all the simulated cases.

Chapter 4 deals with the *PV+wind micro-grid* module. After a literature review of multi-generation optimization in this chapter a way to set a PV/wind share is proposed analyzing different possible objective functions. After the choice of the best turbine (with the procedure shown in Chapter 3) here is explained how the number of turbines and the sizes of the PV plant and the battery are selected in order to find the best configuration. In the end this procedure is validated preforming an analysis of any possible configuration to understand if this module reaches the real optimum.

In Chapter 5 the tool is applied to a real case, the St. Mary's Lacor Hospital in Uganda, to validate the tool and show numerical results.

Chapter 6 reports the author conclusions about the present thesis work and its results.

Chapter 2

2 Battery modelling

This chapter deals with the advanced battery model developed in order to properly estimate the battery behavior and its lifetime. In this way it could be possible to properly estimate the reliability of the system by means of the energy provided by the battery and estimate the cost knowing when the battery has to be replaced.

2.1 Models review

The models presented in the literature can be grouped into four general different approaches.

Electrochemical

The electrochemical models describe the behavior of the elements that composes a battery cell with some simplifications. In Figure 2.1 a simplified schematic of a lithium-ion cell is shown.

These models are based on equations for mass, energy and momentum transport of each species for each phase and component of the cell. A system of partial different equations has to be solved in time and space. Beside current and voltage at external terminals, these models are able to predict local distributions of quantities like reactants concentrations and temperature. Therefore, they are quite complex and they need various parameters to be determined by means of several experiments. This leads to very complex and time-consuming algorithms that cannot be used in micro-grid sizing tools, but it can be useful for the structural design of the battery components [16].

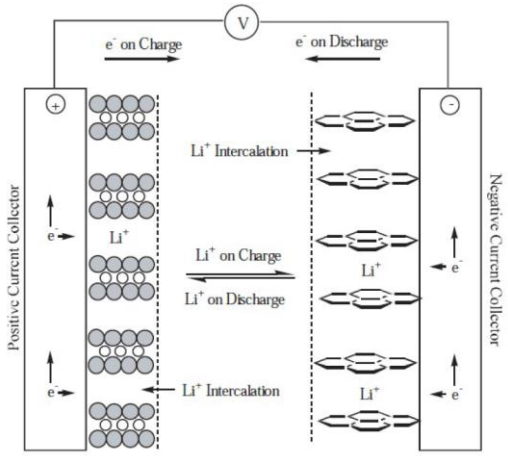

Figure 2.1 Schematic of a Li-ion cell

Analytical

They are based on an abstract vision of the electrochemical cell. The battery is described by analytical equations that do not take into account electrochemical processes, but that are empirically fitted. Among these equations the most important are the empirical correlations to calculate the efficiency and the capacity fade:

$$\eta = f(operating\ conditions)$$
$$cf = f(operating\ conditions)$$

Equations 2.1 Analytical models

In these models the SoC of the battery is based on energy balances and the voltage variation is usually neglected.

Analytical models' complexity can vary but they are in general simpler than others, thus they are often used in sizing tools. However, the simpler models adopted could result inaccurate: the errors in predicting battery performance could be relatively high [17].

Electrical

Batteries can be represented by equivalent electric circuits, that aim to model the voltage and current characteristics at the external terminals.

The equivalent circuit needs to be composed by two parts. The first represents the equilibrium voltage, directly related to the SoC and they can be ideal generators or capacitors. The second part have to represent the overpotential, that is the variation of the voltage once the battery is far from equilibrium. This last part is modelled with resistances.

There is a wide range of equivalent circuits, with very different degrees of complexity. The most complex ones are constituted by many components, so they can reflect the electrochemical characteristics (each

circuital element represents a precise physical phenomenon occurring in the cell). The simplest models have only few elements: a voltage source to represent energy stored and a resistance in series to take into account losses. Two examples of circuits are reported in Figure 2.2.

Although they are not usually implemented in design tools, the simplest ones could match the required characteristics of short computational time and accuracy, while maintaining a physical basis.

Instead, the electric models are used in the Battery Management Systems [18].

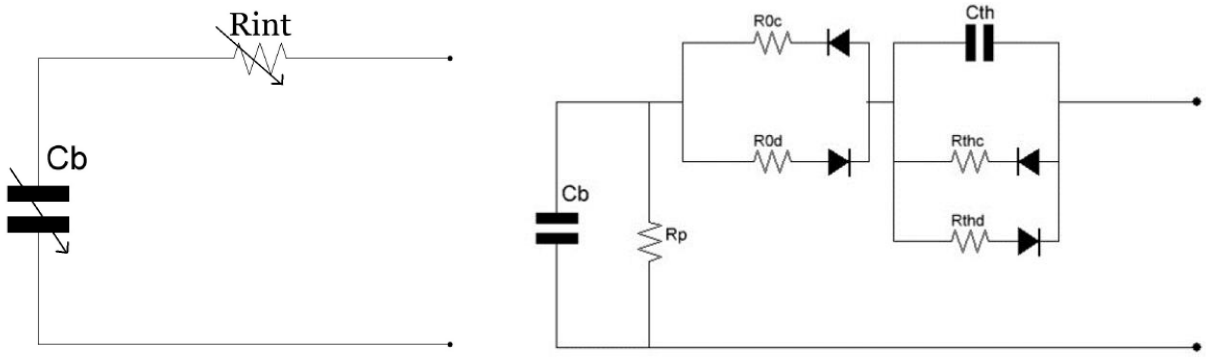

Figure 2.2 Examples of equivalent electric circuits

Stochastic

These models describe the battery system, not only looking at the complex electrochemical reactions, bat also modelling random variables as ambient temperature and usage profiles.

They describe the battery in mathematical terms, employing a high degree of abstraction. For example, the battery can be represented by a Markov chain (a sequence of possible events in which the probability of each event depends only on the state attained in the previous event, as it is represented in Figure 2.3) with N+1 states of charge. The number of the battery's states is linked to the number of units of charge available in the battery.

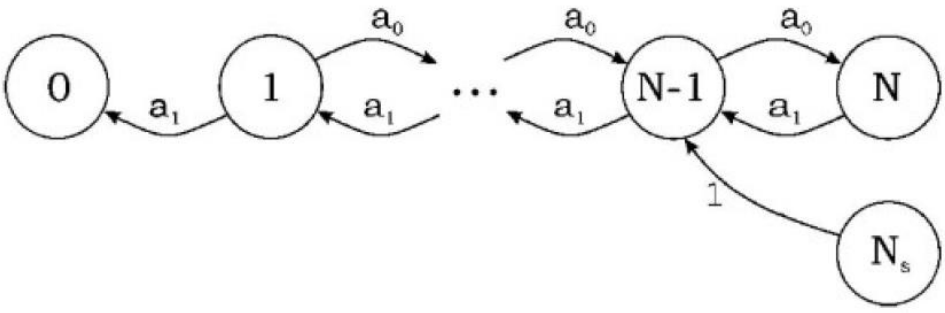

Figure 2.3 Markov chain

Stochastic models are too bounded to specific battery phenomena and cannot represent in a good way battery as a whole, so they cannot be used in sizing tools [19].

The model chosen to be implemented in the tool is the analytical one, in particular an empirical model with variable efficiency and capacity reduction. An easy parametrization has been selected and it takes into account the dependence of battery behavior on operational conditions. This model is simple and accurate enough to be the right compromise needed in design studies like this tool.

Modelling the battery, to understand its behavior and to study its evolution in time, it is necessary to consider two parameters:

- The State of Charge (SoC) allows to calculate the energy that can be stored or provided by the battery and therefore, it is also useful to calculate the amount of energy not provided to the load.
- The State of Health (SoH) describes the reduction of the capacity of the battery due to irreversible degradation processes that occur inside the cell.

2.2 SoC estimation

The empirical model considers the battery as a black box that can store energy with a charge and discharge efficiency. These battery efficiencies together with the inverter efficiency represent the energy losses of the system. In Figure 2.4 the schematic is shown.

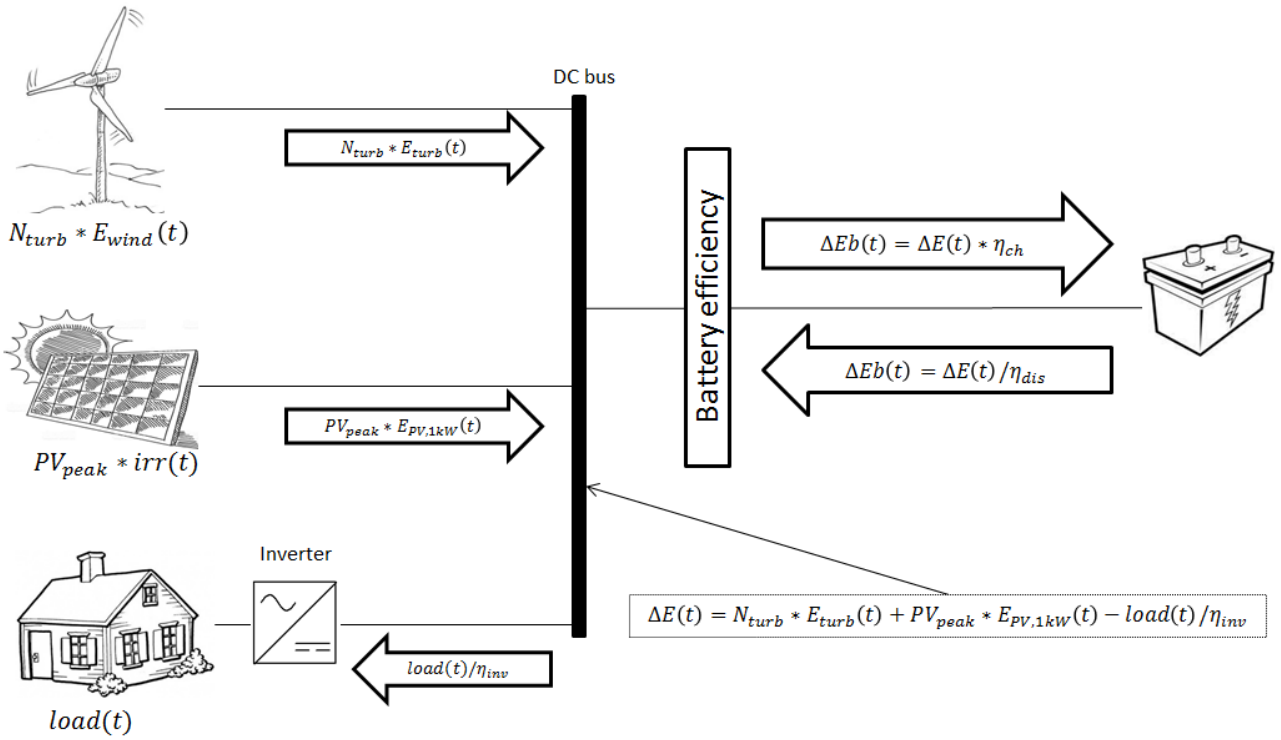

Figure 2.4 Schematic of the battery and the grid

In this model the battery efficiency is assumed to be function of the E_{rate}:

$$E_{rate}(t) = \frac{P(t)}{E_{b,nom}} = \frac{\Delta E(t)}{E_{b,nom}} \left[\frac{1}{h}\right]$$

Equation 2.2 Energy rate

Being the considered time step long 1 hour, the power P in kW and the energy exchanged at the DC bus ΔE in kWh are numerically equivalent. ΔE is the energy balance between the generated energy and the one needed by the load. Therefore, the balance ΔE represents the energy that should be given to the battery charging it (if ΔE is positive) or taken by the battery discharging it (if ΔE is negative) for each time step.
So, the efficiency equation, assuming that the discharge and charge efficiencies are the same, can be written as:

$$\eta_{ch} = \eta_{dis} = a * E_{rate}^3 + b * E_{rate}^2 + c * E_{rate} + d$$

Equation 2.3 Efficiency

Where *a*, *b*, *c* and *d* are coefficient empirically fitted. This equation can be applied to both lithium ion and lead acid batteries by using specific *a*, *b*, *c* and *d* coefficients for each different technology.
Thanks to laboratory campaigns on commercial lithium-ion cells [20], the coefficients for a lithium-ion battery can be fitted and the efficiency correlation is shown in the following figure. The author was not able to find any data for the lead-acid technology.

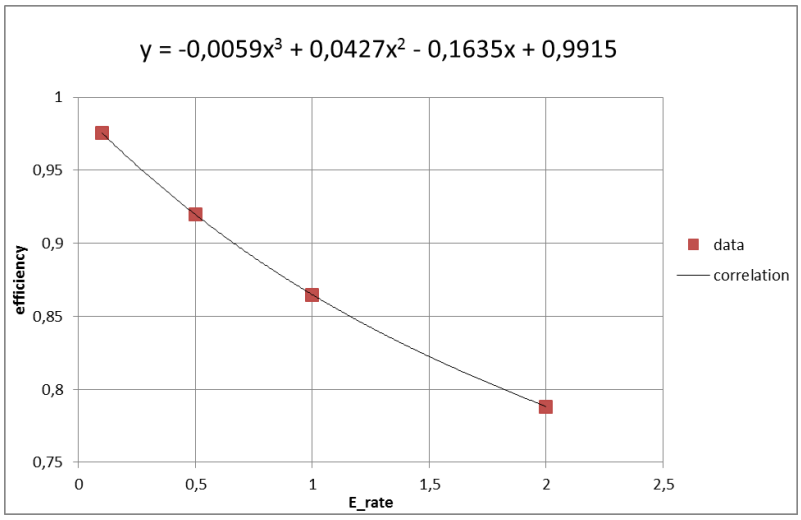

Figure 2.5 Correlation between efficiency and E_{rate}

Known the efficiency, the stored energy variation ΔE_b, according to the energy flow direction, results:

$$\Delta E_b = \begin{cases} \Delta E * \eta_{ch} & if\ charging \\ \Delta E / \eta_{dis} & if\ discharging \end{cases}$$

Equation 2.4 Stored energy variation

But the battery may not be able to exchange ΔE because of technical limitations.

A first limiting parameter is the power/energy fraction limit (PE) that is a limit to the charge/discharge power flowing to/from the battery with respect to its nominal energy value. So, if the generation/load demand balance exceeds $PE * E_{b,nom}$ the energy actually exchanged by the battery is:

$$\Delta E = PE * E_{b,nom}$$

Equation 2.5 PE working logic

When the battery is charging and the energy balance is exceeding the power/energy fraction limit the system is facing an overgeneration. It means that part of the generated energy can be nether stored nor consumed by the load. In the opposite case, when the battery is discharging and the energy balance is overcoming the power/energy fraction limit the system is facing a loss of load.

Moreover, there are limits about the storable energy in order to guarantee a proper and safe utilization of the battery. Those are represented by SoC_{max} and SoC_{min}. Assuming a very small State of Health variation respect to the previous time step (explained in detail in the section 2.3) the limits are:

$$Eb_{max} = E_{b,nom} * SoC_{max} * SoH(t-1)$$
$$Eb_{min} = E_{b,nom} * SoC_{min} * SoH(t-1)$$

Equations 2.6 SoC limits

So, when the battery is charging there may be an overgeneration:

$$E_b(t) = \begin{cases} Eb_{max} & if\ E_b(t-1) + \Delta E_b > Eb_{max} \\ E_b(t-1) + \Delta E_b & if\ E_b(t-1) + \Delta E_b \leq Eb_{max} \end{cases}$$

Equation 2.7 SoC_{max} working logic

While, when the battery is discharging there may be a loss of load:

$$E_b(t) = \begin{cases} E_b(t-1) - |\Delta E_b| & if\ E_b(t-1) - |\Delta E_b| > Eb_{min} \\ Eb_{min} & if\ E_b(t-1) - |\Delta E_b| \leq Eb_{min} \end{cases}$$

Equation 2.8 SoC_{min} working logic

Where $E_b(t)$ is the energy stored in the battery in the time step t.
Once the stored energy is known, it is possible to calculate the usual parameter that is adopted to model battery behavior during operation: the State of Charge.

$$SoC(t) = \frac{E_b(t)}{E_{b,nom} * SoH(t-1)}$$

Equation 2.9 State of Charge

2.3 SoH estimation

The life of the batteries is limited by some aging mechanisms. Indeed, in real operation batteries tend to degrade at a faster rate than the micro-grid system itself, meaning that during the plant lifetime batteries must be replaced and it strongly influences the overall cost. Hence, the degradation model is fundamental.
The first issue that has to be taken into account is the calendar aging that occurs during storage of the battery, when it is at open circuit. It is modelled considering a maximum number of years of working time before replacement.
The second aspect is the cycle aging, that takes place during battery utilization. It is responsible for the capacity fade (cf) that is the decrease of the storable energy. It is caused by loss of useful ions or by loss of electrode active material. It is modeled by means of the State of Health, which by definition is:

$$SoH = \frac{C(t)}{C_{nom}}$$

Equation 2.10 State of Health

Where *C* is the capacity of the battery. Assuming constant nominal voltage it represents the percentage of the maximum storable energy with respect to the nominal value.
The degradation mechanism is strictly related to the chemistry of the cell. So, different models are required for different chemistries.

Lead-acid battery

Battery lifetime decreases with increasing number of cycles and the decline is more rapid the higher the Depth of Discharge (DoD) is. Therefore, the battery life is considered function of the DoD, in particular it is necessary to interpolate the capacity fade as a function of DoD. Being:

$$DoD(t) = 1 - SoC(t)$$

Equation 2.11 Depth of Discharge

And knowing the relationship between the maximum number of cycles and DoD, the capacity fade is calculated:

$$cf(t) = \frac{1 - SoH_{min}}{cycles_{max}\big(DoD(t)\big)}$$

Equation 2.12 Capacity fade for lead-acid batteries

The maximum accepted capacity reduction is usually set to 20% ($SoH_{min} = 0{,}8$), so, fitting some data, the coefficients *a*, *b* and *c* can be found so that the following curve can be implemented in the tool.

$$cf = a * DoD^2 + b * DoD + c$$

Equation 2.13 Capacity fade correlation for lead-acid batteries

Using the data given by the datasheet of a "Sonnenschein A 500" battery cell [21] the coefficients can be fitted resulting in the correlation in Figure 2.6.

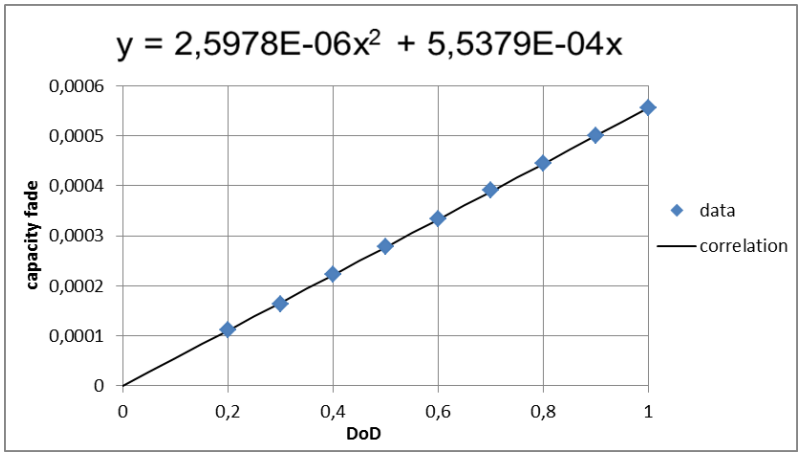

Figure 2.6 Capacity fade correlation for lead-acid batteries

Lithium-ion battery

The battery lifetime decreases with increasing number of cycles and the decline is more rapid the higher the current is. Therefore, the capacity fade is considered as a function of E_{rate}. Applying the same procedure:

$$cf(t) = \frac{1 - SoH_{min}}{cycles_{max}(E_{rate}(t))}$$

Equation 2.14 Capacity fade for lithium-ion batteries

Than it is possible to fit the data and implement in the tool the correlation:

$$cf = a * \exp(b * E_{rate})$$

Equation 2.15 Capacity fade correlation for lithium-ion batteries

The data fitted are given by laboratory results [20] of a "Boston Power Swing5300" battery cell; the implemented correlation is the following one:

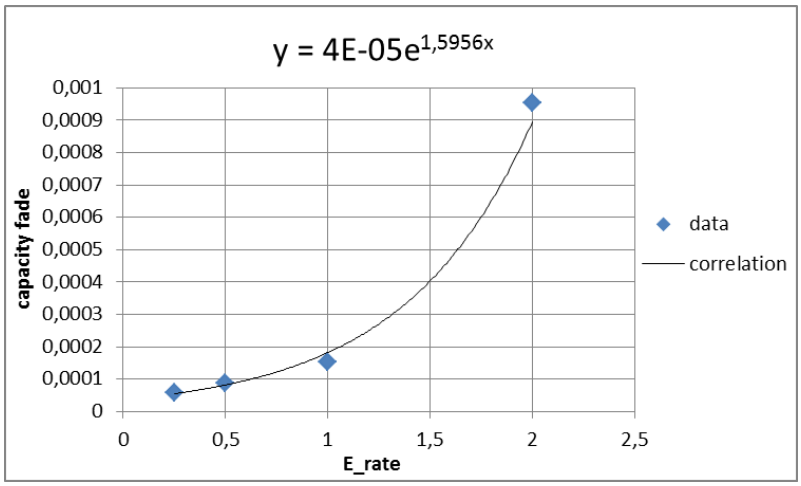

Figure 2.7 Capacity fade correlation for lithium-ion batteries

Independently from battery technology, the state of health indicator is calculated using capacity fade per cycle multiplied by the equivalent cycles. These last are defined considering that if eq_{cycles} is equal to 1, it means the battery has completed a full discharge and charge cycle:

$$eq_{cycles}(t) = \left|\frac{SoC(t) - SoC(t-1)}{2}\right|$$

Equation 2.16 Equivalent cycles

And so:

$$SoH(t) = SoH(t-1) - eq_{cycles}(t) * cf(t)$$

Equation 2.17 State of Health

The battery is considered exhausted and needs to be replaced when SoH = 0,8.
Therefore, the battery replacement takes places when one of the two aging constraints occur: either the maximum number of years is reached (calendar aging) or the State of Health is equal to its minimum (cycle aging).

2.4 Models implementation

The models proposed in this chapter were coded in Excel VBA and implemented in the tool object of this thesis. Therefore, it was possible to perform some simulations to validate the procedure.
As can be seen in Figure 2.8, where the implemented algorithm is shown in detail, the model operates in the following way:

1. It reads the data about load, generation and components sizes (the battery is supposed to be new and fully charged at the beginning).
2. It calculates the energy balance between the generation and the load that is equal to the energy given to or taken from the battery, so the E_{rate} can be evaluated (Equation 2.2).
3. It checks the power/energy fraction limit constraint and in case it is not fulfilled the tool accounts for loss of load or overgeneration (Equation 2.5).
4. Considering the direction of the energy flow, it calculates the stored energy at the end of the time step.
5. If the SoC_{max} (while charging) or the SoC_{min} (while discharging) limits are not fulfilled, it takes into account the loss of load or the overgeneration (Equation 2.7 and Equation 2.8).
6. Once the actual exchanged energy is known, it calculates the SoC neglecting the SoH variation (Equation 2.9).
7. It evaluates the capacity fade with the correct correlation according to the battery technology adopted (Equation 2.13 or Equation 2.15), then it calculates the equivalent cycles and the SoH (Equation 2.16 and Equation 2.17).
8. If the battery is at the end of its life, it is replaced with a new and charged one and its investment cost is considered in the cash flow of that specific year.
9. The points from 2. to 8. are repeated for all the time steps (1 hour) of the analyzed period for the simulation.
10. At the end of the simulation, it calculates the LLP to evaluate the system reliability.

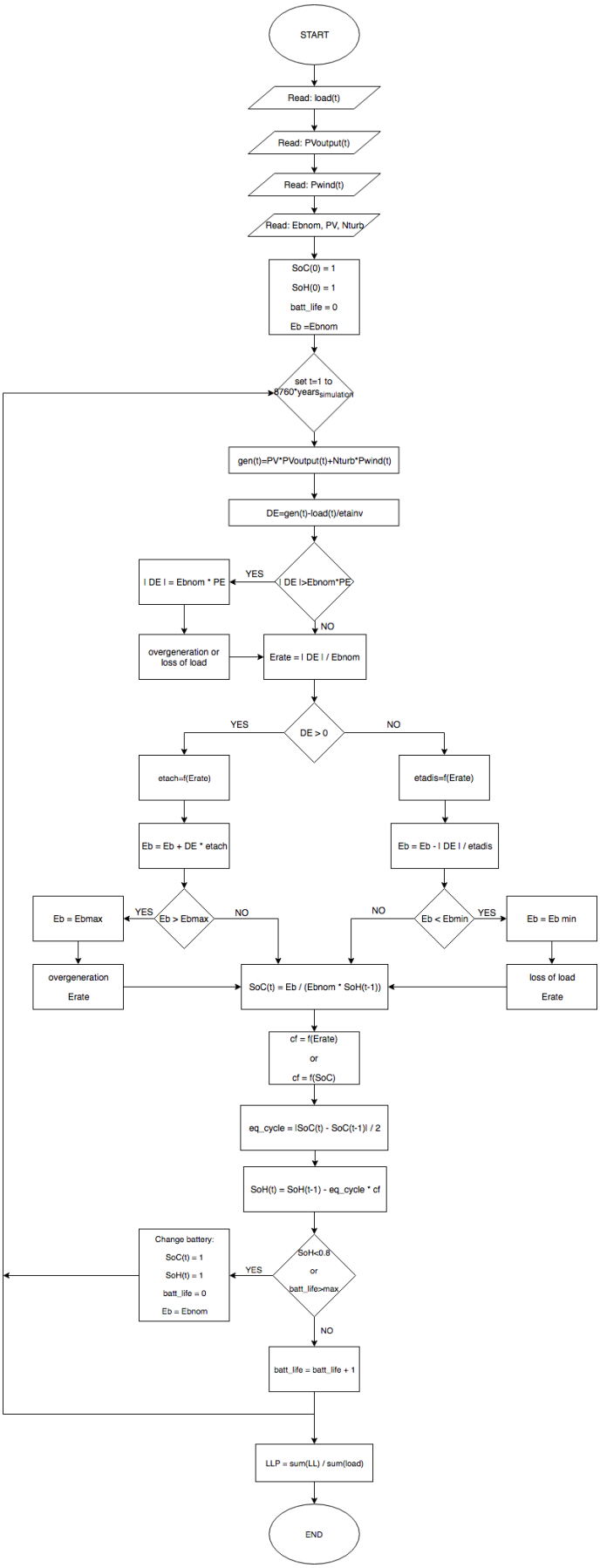

Figure 2.8 Battery model flow chart

2.5 Validation tests

In order to validate this procedure some simulations have been performed with the advanced model and with the simple one so that it is possible to compare them. The tests are related to the design of a PV+storage micro-grid. The data of PV production and load relative to the case study explained in Chapter 5 have been used.

The considered battery is a lithium-ion and for its simple model it has been set a constant charge and discharge efficiency equal to 95% and a maximum number of cycles of 3000. For both models the SoC_{min} has been set to 0% (no degradation effects due to DoD) while the calendar aging has not been considered in order to highlight the SoH effects. The analyzed period is 30 years.

To show the differences some extreme cases are presented.

Case A: small battery

If the battery is small, the E_{rate} is high and efficiency of the advanced model is low. For this reason, the simple model underestimates the LLP. Since a configuration is accepted if it gives an LLP lower than the maximum value (here set equal to 5%), the simple model may lead to accept a battery that would not be accepted if the more precise advanced model was implemented, as it is shown in Table 2.1.

		simple model		advanced model	
PV [kW]	ESS [kWh]	LLP	replacements	LLP	replacements
5000	1400	3,91%	3	10,05%	3

Table 2.1 Case A

When the advanced model is used, the battery is replaced when the SoH reaches 0,8. Indeed:

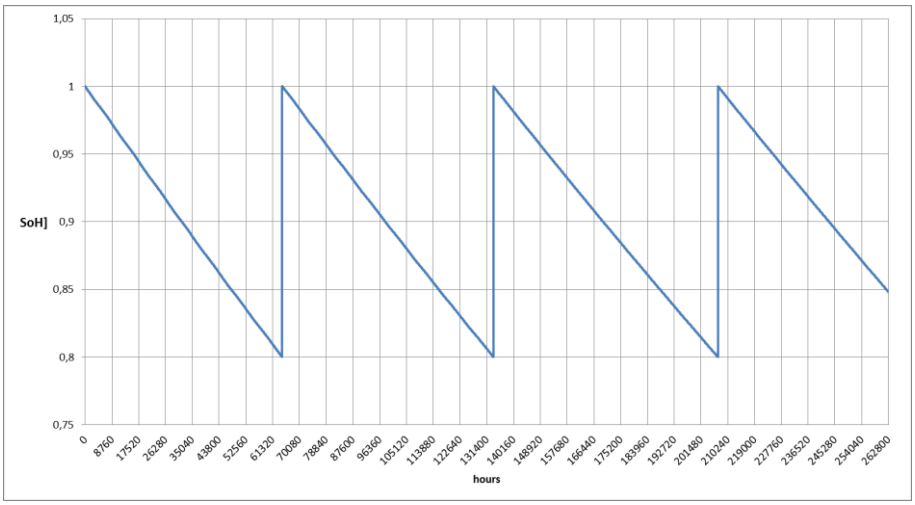

Figure 2.9 Sate of health – case A with advanced model

Instead, when the simple model is used the battery is replaced when the maximum number of cycles is reached. The maximum number of cycles can be easily linked with the maximum energy fluxed by the battery, that is 3000 cycles multiplied by the nominal size of the battery that results 4200 MWh. So, the battery is replaced when it reaches this value. As can be seen in the following figure, in this case the result is not very different from the advanced model simulation.

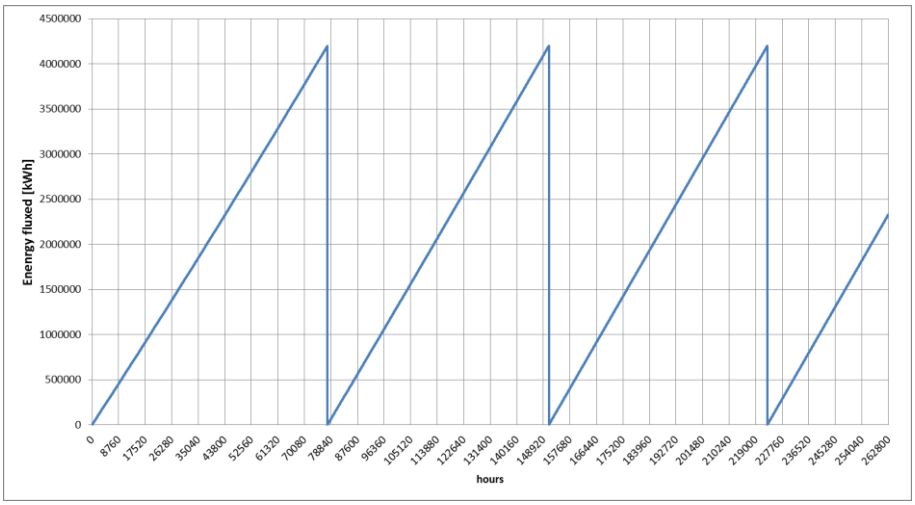

Figure 2.10 Energy fluxed – case A with simple model

Case B: big battery

In Table 2.2 is shown what happens if big batteries are adopted. If the battery is big, the E_{rate} is low and efficiency of the advanced model is high. So, the simple model overestimates the LLP and this may lead to discard a battery that is acceptable according to the maximum LLP.

		simple model		advanced model	
PV [kW]	ESS [kWh]	LLP	replacements	LLP	replacements
1200	10000	5,91%	0	4,73%	0

Table 2.2 Case B

Adopting the advanced model, if the battery is big, also the capacity fade is low. Therefore, if the calendar aging is not considered, the battery never has to be replaced in the last analyzed case. Indeed, in the following figure is shown that the SoH = 0,8 is never reached.

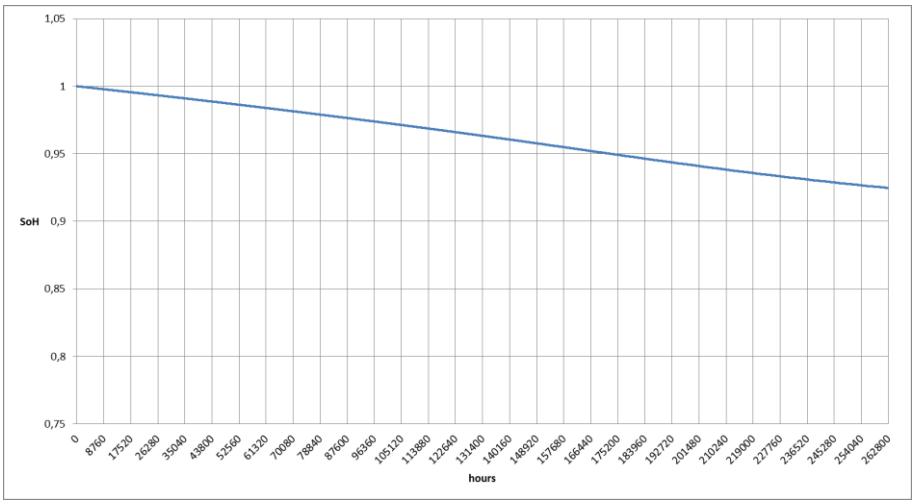

Figure 2.11 Sate of health – case B with advanced model

Similarly, applying the simple model and dealing with a big battery, for each time step the equivalent cycles are very small, so it never reaches the maximum 30000 MWh of fluxed energy that are needed for battery replacement.

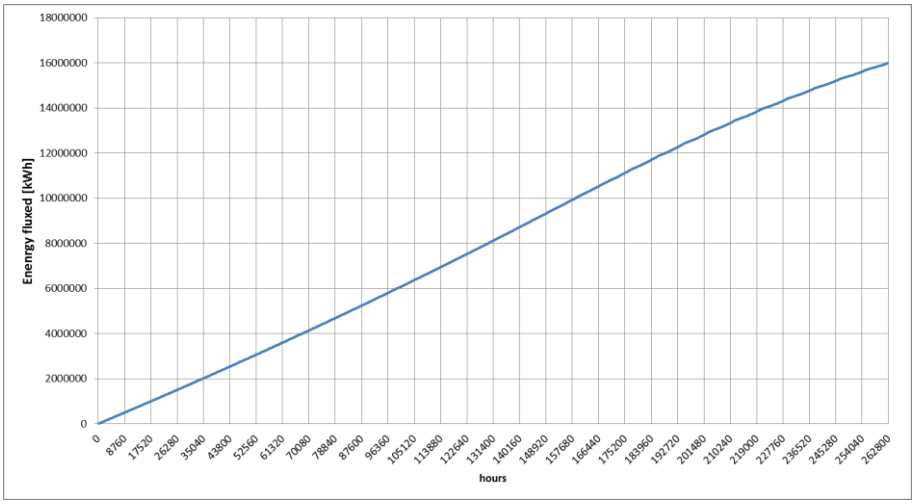

Figure 2.12 Energy fluxed – case B with simple model

The fact that in the two cases presented so far the number of battery replacements are the same applying the two models is not unexpected. Indeed, the value of 3000 maximum cycles was chosen to represent the battery degradation process and its lifetime in a simplified way. In particular, the case of Table 2.1 presents a battery that is not small enough so that it could be possible to notice the differences between the two models in terms of number of battery replacements, but comparing Figure 2.9 and Figure 2.10 it can be seen that the advanced model leads to slightly shorter lifetime. So, it can be interesting to investigate even smaller batteries.

Case C: very small battery

In some cases the simple model can fail to represent correctly the battery lifetime and the replacements. In the case shown the simple model underestimates the number of battery replacements. This happens if the battery is very small, as it is presented in the following table, even though it is not interesting form LLP point of view.

		simple model		advanced model	
PV [kW]	ESS [kWh]	LLP	replacements	LLP	replacements
4000	500	32,09%	3	34,96%	5

Table 2.3 Case C

Here the battery is very small, so the capacity fade is very high and the advanced model reaches SoH = 0,8 more easily then how the simple model reaches the maximum 1500 MWh of fluxed energy. This is shown in the following two figures.

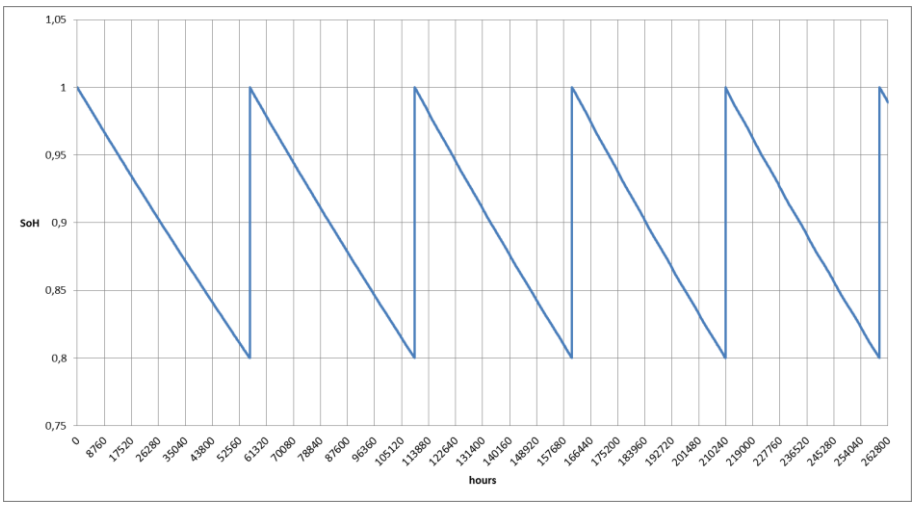

Figure 2.13 Sate of health – case C with advanced model

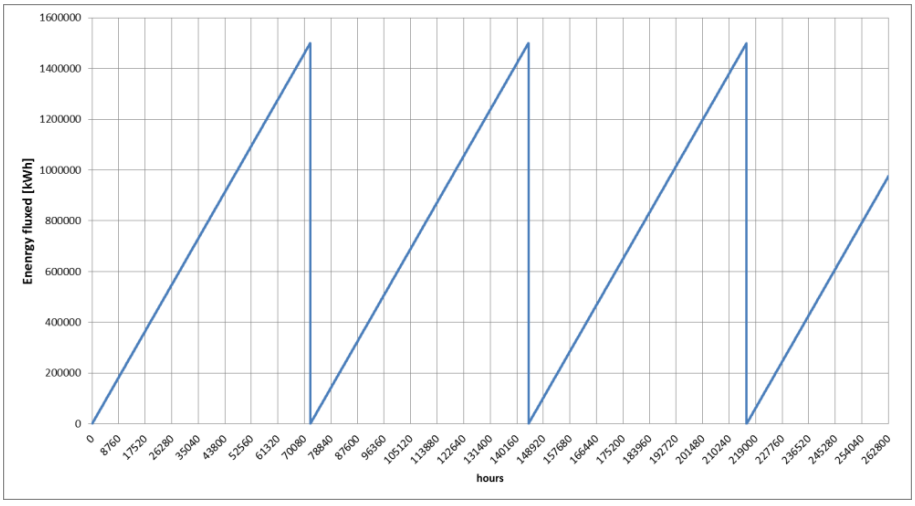

Figure 2.14 Energy fluxed – case C with simple model

The study of the battery replacements is important to correctly evaluate the cost of the plant. So, it is interesting to compare the cash flow of the simulation with the simple model (Figure 2.15) and with the advanced one (Figure 2.16). The replacements of the batteries are represented by the longer bars in the cash flow, excluding the year zero of the initial investment (for example the years 9, 17 and 25 in Figure 2.15 that agree with Figure 2.14).

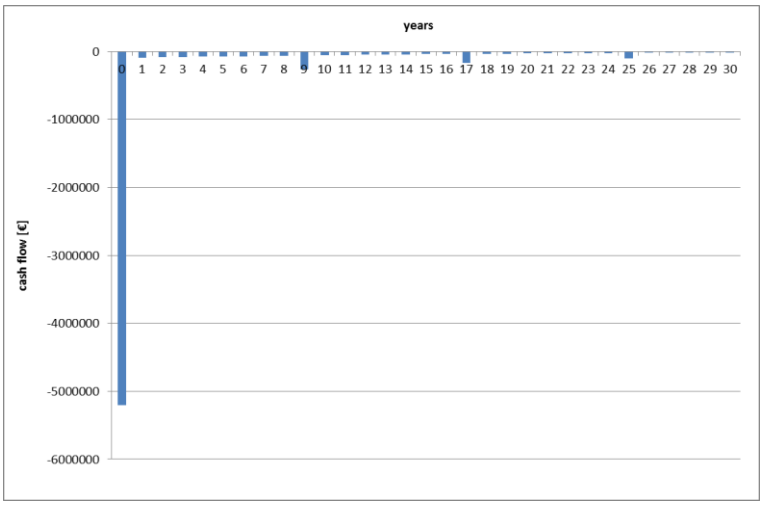

Figure 2.15 Cash flow with simple model

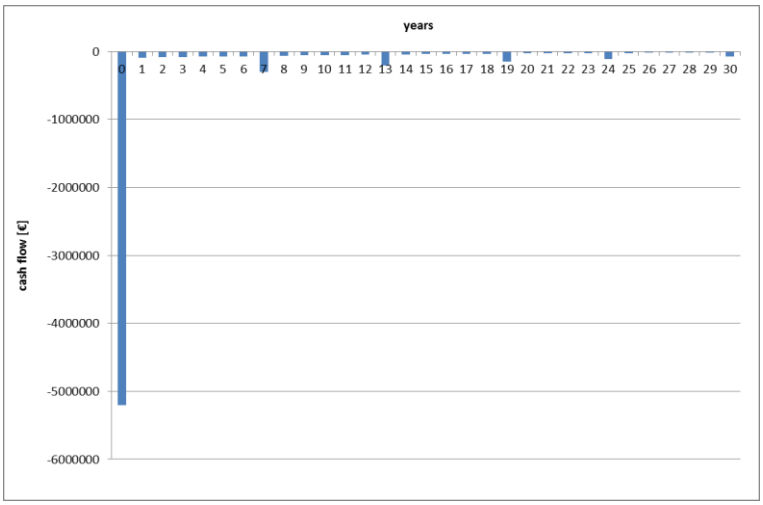

Figure 2.16 Cash flow with advanced model

In conclusion it can be stated that the advanced battery modeling is important in order to avoid wrong estimation of the system cost and reliability, that are important parameters to be considered when searching the optimal configuration of the plant.

Sometimes, it can happen that the two models give the same result in terms of LLP and battery lifetime. Instead, if the two models give different results, assuming that the correlations have been calculated correctly, the results of the advanced model are more accurate.

Chapter 3

3 Wind generators modelling

Now that a model to properly simulate battery is available, it is possible to study a micro-grid in order to find the best configuration. In particular, this chapter deals with wind-based micro-grids and studies different wind turbines. The procedure here described is implemented in the *wind micro-grid* module.

3.1 Wind-based micro-grids modelling

The tool object of this thesis is composed by different modules, each of them studies a micro-grid that exploits a different energy source (or more than one together). All these modules study and simulate the micro-grids basing their calculations on simplified configurations.
In the *PV micro-grid* module the analyzed system is constituted by the PV panels and the battery connected to the DC bus which is connected to the AC load by means of an inverter [22]. This means that some elements like the MPPT and the charge controller are neglected in the analysis, so the only considered system loss is the inverter and it is quantified with its efficiency η_{inv}.
In particular, this chapter deals with the *wind micro-grid* module and the chosen configuration is very similar to the one just discussed (Figure 3.1): instead of the PV panels there are the wind turbines and the AC/DC converter is neglected (it has been assumed that the power output given by the power curve of the wind turbines is the DC one, after the converter).

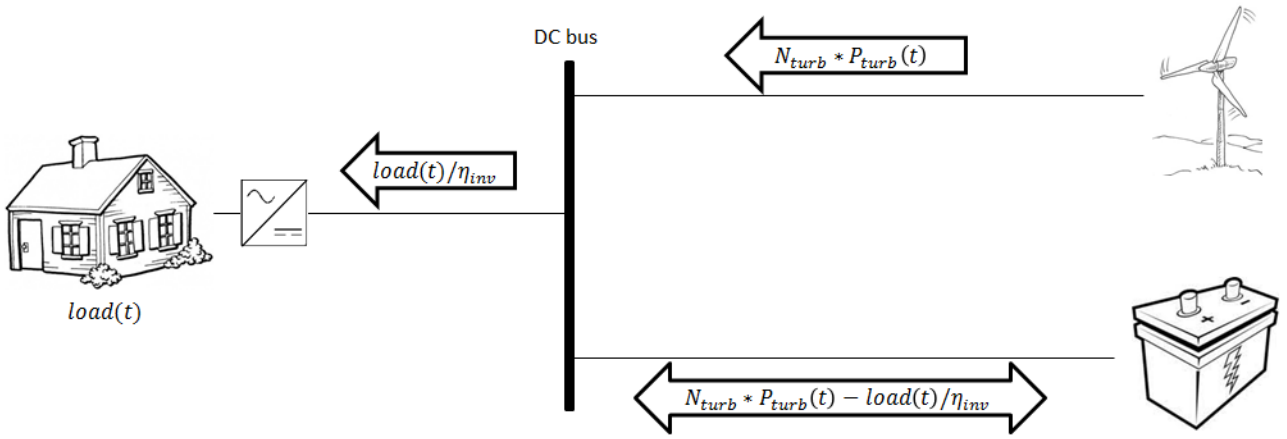

Figure 3.1 *Wind micro-grid* configuration

Once the general configuration is defined, it is possible to implement a procedure to size the components of the system in order optimize the grid in terms of cost and reliability.

In the following paragraphs of this chapter the details of procedure of the *wind micro-grid* module will be explained. The aim is to choose a turbine type from a database and calculate the number of turbines and the size of the batteries that optimize the system. The scheme of the module is the following one:

- The procedure analyzes a database of turbines and discards the ones that are not suitable, in terms of nominal power or working hours.
- The intuitive sizing is calculated: by means of simple equations the starting point for further calculations is evaluated. They are the initial sizes of the wind plant and of the battery.
- The space of analysis is generated: staring from the intuitive sizing, the sizes of the wind plant and of the batteries are modified in order to find many different configurations.
- The best configuration can be found among the ones studied in the space of analysis.

3.2 Turbines database

In order to exploit the wind as an electric power source it is necessary to adopt and model the wind turbines. The main problem that can be faced dealing with wind turbines is that different turbines present different power curves. So, it is not possible to use a generic power curve and calculate the power generated by a generic turbine. Instead, a database of turbines has been implemented in the tool, and the procedure has to be able to choose the best turbine type in the database.

The tool's database was taken from the software HOMER. Among the turbines present in the database of HOMER, only the turbines available in the market with a nominal power lower than 1 MW have been implemented in the tool. So, the database of the tool is composed by 83 turbines and data present in it are: the power curve, the nominal power and the hub height.

The following table represents the tool's database and the nominal power values are reported.

#DB	turbine type	P [kW]	#DB	turbine type	P [kW]	#DB	turbine type	P [kW]
1	Aeolos 18m 50kW	54	29	EWT direct Wind 54m 250kW	250	57	Leitwind 80 1000kW	1000
2	Aircon10S 7.54m 10kW	11	30	EWT direct Wind 52 500kW	500	58	Leitwind 86 1000kW	1000
3	Aria S.R.L Libellula 18m 55kW	55	31	EWT direct Wind 54 500kW	500	59	Leitwind 90 1000kW	1000
4	AWS HC 650 W Wind Turbine	1,13	32	EWT DW 52 [900kW]	900	60	Marlec FM1803-2 1.8m	0,72
5	AWS HC 1,5 Kw Wind Turbine	2,22	33	EWT DW 54 [900kW]	900	61	Northern Power NPS100C-24	95
6	AWS HC 1,8 Kw Wind Turbine	2,66	34	EWT DW 61 [900kW]	900	62	Northern Power NPS 60-24	95
7	AWS HC 3,3 Kw Wind Turbine	4,49	35	Fortis Passaat 3.12m 1.4kW	1,4	63	Northern Power NPS100C-21	100
8	AWS HC 4,2 Kw Wind Turbine	5,68	36	Fortis Montana 5m 5kW	4,48	64	Norvento Ned 22 [100kW]	100
9	AWS HC 5,1 Kw Wind Turbine	6,37	37	Future Energy Airforce10 8m 13kW	13	65	Norvento Ned 24 [100kW]	100
10	Bergey BWCXL1 2.5m 1kw	1,23	38	Gaia Wind 133 - 11kw	11	66	Pinnacle-Tech Caravel 2.5kW 3.5m	2,4
11	Bergey Excel 6	6,66	39	Generic 1kW	1	67	Pinnacle-Tech Frigate 7.5 Kw 6m	7,7
12	Bergey Excel 10	13	40	Generic 3kW	3	68	Pinnacle-Tech Frigate 10kW 7m	10
13	C&F Green Energy CF11 9m 11kW	11	41	Generic 10 Kw	10	69	SkyStream 3.7	2,4
14	C&F Energy CF15e 13.1m 15kW	15	42	Harbon HWT60 19.93m 60kW	59	70	Sonkyo Energy Windspot 1.5kW 4.05m	1,68
15	C&F Green Energy CF15 11.1m 15kW	16	43	Hummer 3.1 m 1kw	2	71	Sonkyo Energy Windspot 3.5kW 4.05m	4,17
16	C&F Green Energy CF20 12.8m 20kW	21	44	Hummer 3.8m 2kw	3,2	72	Tempower Whisper H40 2.1m 0.8kw	0,91
17	C&F Green Energy CF50 2om 50kW	52	45	Hummer 6.4m 5kw	7,75	73	TrueNorthPower Arrow 2m1kw	1,23
18	Electriawind Garbi 150/28 28m 150kw	150	46	Hummer 8m 10kw	15	74	Vergnet GEV MP C 32 m 275kw	275
19	Electriawind Garbi 200/28 28m 200kw	200	47	Kestrel 300i 3m 1kW	1,1	75	Vergnet GEV MP R 32 m 275kw	275
20	Enercon E-48 [800kW]	810	48	Kestrel e230 2.3m 0.8kW	0,82	76	WES 18 [80kW]	83
21	Enercon E-53 [800kW]	810	49	Kestrel 400i 4m 3kW	3,2	77	WES 18 [100kW]	100
22	Enercon E-44 [900kW]	910	50	Kingspan-Proven Kingspan KW3 3.8m 2.5 Kw	2,9	78	WES 18 [250kW]	250
23	Ennera Windera S 4.36m 3,2 Kw	3,16	51	Kingspan-Proven Kingspan KW6 5.6m 6 Kw	6,14	79	Windflow 33 [500kW]	500
24	Eocycle EO20	20	52	Leitwind 77 800kW	800	80	Windflow 45 [500kW]	500
25	Eocycle EO25 Class IIA	25	53	Leitwind 80 800kW	800	81	Windspot 7.5kW 6.3m	8,02
26	Eoltec Scirocco E5.6m-6kw	6	54	Leitwind 77 850kW	850	82	Xzeres Skystream 3.7 [2.4kW]	2,43
27	Ergycon Ely50 20.7m	51	55	Leitwind 80 850kW	850	83	Zephyr Airdolphin 1.8m 1kW	1,52
28	Evance R-9000 5.5m 5kw	5,24	56	Leitwind 77 1000kW	1000			

Table 3.1 Turbines database

A power curve is the curve that relates the wind speed with the power output of the turbine. Each turbine has its own power curve with as specific shape. Here there are two examples.

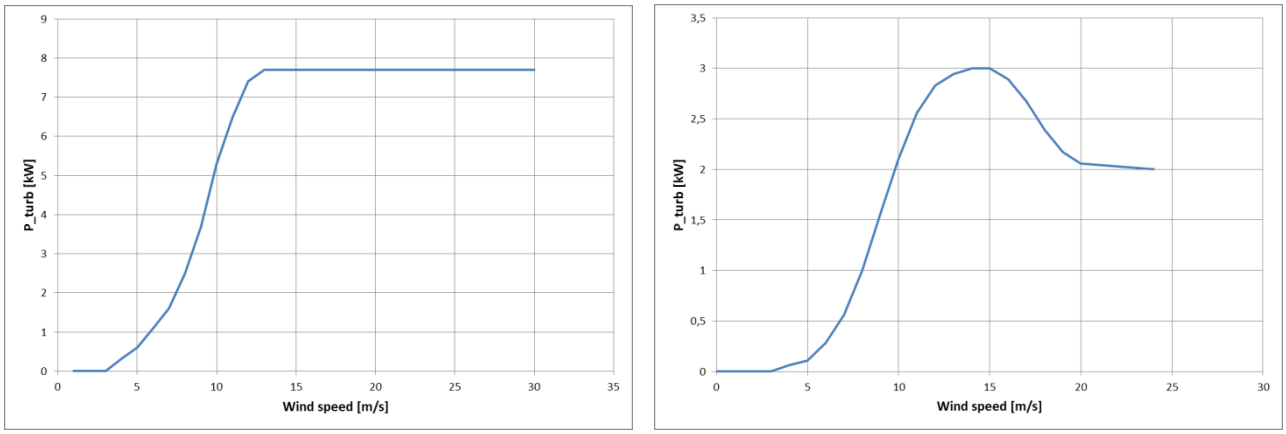

Figure 3.2 Two examples of power curves: turbine 67 (left) and turbine 40 (right)

According to the average wind speed of the studied site, a power curve can be more suitable than another leading to a better exploitation of the wind resource.

3.3 Intuitive sizing for wind resource

The procedure to design the configuration of the system starts calculating an intuitive size. It means that the tool needs a simple equation to evaluate the starting point from which a space of analysis will be created.
The current module deals with wind turbines, so intuitive sizing means to find the number of turbines from which it is possible to start the analysis. In particular, it is necessary to calculate an intuitive number of turbines for each turbine present in the database.
Once the load profile is known, it is necessary to calculate the power generation profile for each turbine in the database. This last profile is calculated interpolating the power curve for each turbine knowing the wind speed at hub height. The tool takes as input the wind speed at anemometer height (10 meters from the soil) so the velocity must be corrected since it increases when the distance from the ground increases (the effect of the friction with the soli decreases) as it shown in the following figure.

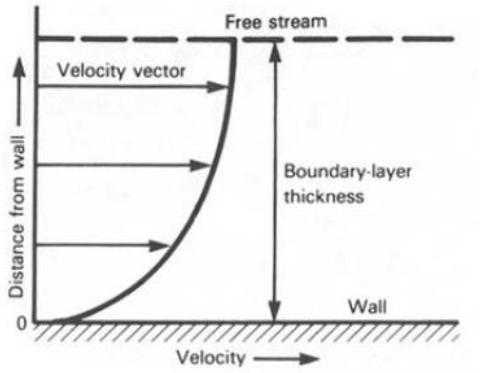

Figure 3.3 Wind velocity increases with distance from the ground

Assuming that the turbines are within the boundary-layer thickness, it is necessary a correction for the wind velocity. The correction implemented in the tool is the logarithmic profile which assumes that the wind speed is proportional to the logarithm of the height above the ground:

$$\frac{U_{hub}}{U_{anem}} = \frac{\ln\left(\frac{z_{hub}}{z_0}\right)}{\ln\left(\frac{z_{anem}}{z_0}\right)}$$

Equation 3.1 Wind speed correction

This equation relates the velocities at hub and at anemometer with their heights, while z_0 is the surface roughness length, a parameter that characterizes the roughness of the surrounding terrain. The z_0 values are listed in Table 3.2 according to the surrounding elements [23].

Terrain Description	z_0
Very smooth, ice or mud	0.00001 m
Calm open sea	0.0002 m
Blown sea	0.0005 m
Snow surface	0.003 m
Lawn grass	0.008 m
Rough pasture	0.010 m
Fallow field	0.03 m
Crops	0.05 m
Few trees	0.10 m
Many trees, few buildings	0.25 m
Forest and woodlands	0.5 m
Suburbs	1.5 m
City center, tall buildings	3.0 m

Table 3.2 Surface roughness length

Therefore, after the tool determines the wind speed at hub height thanks to this correction, it uses all the wind turbines' power curves to calculate the expected power output from each wind turbine. The power curves are given by discrete points. So, for each time step, the wind speed velocity is linearly interpolated between the two closest values in order to get the power generation of the turbine. In the following figure the interpolation is shown.

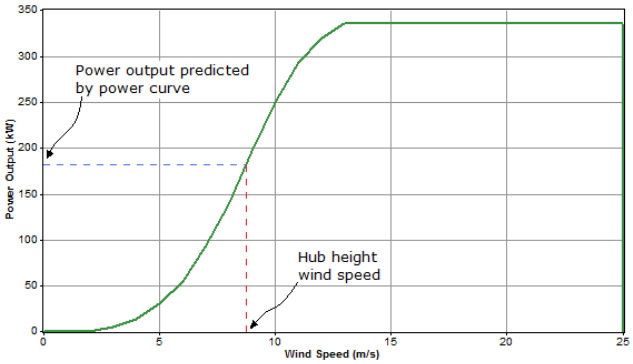

Figure 3.4 Power curve

This curve is based on standard conditions for air temperature and pressure and no density corrections are applied since air density variation is considered negligible. Moreover, in a real case, if more than one turbine is installed in the wind farm, the wind is slowed down because of the interactions among the nearby turbines and so the power generated is reduced. Also this effect is neglected, assuming that all the turbines are far enough from each other to avoid interaction.

If the wind speed at the turbine hub height is not within the range defined in the power curve, the turbine produces no power, following the assumption that wind turbines produce no power at wind speeds below the minimum (cut-in) or above the maximum (cut-out) wind speeds.

Once the power profile generated by each turbine is known, it is possible to calculate the energy generated by each turbine in all the analyzed period. Reminding that the tool works with time steps equal to 1 hour, the energy generated in all the period (in kWh) is equal to the sum of the power profile (in kW) that is equivalent to the hourly average energy profile.

$$E_{tot} = \sum_{t=0}^{T} P_{turb}(t)$$

Equation 3.2 Energy generated in all the analyzed period by a turbine. It is calculated for each turbine in the database.

To carry on with the intuitive sizing, the first consideration that can be made is that the energy generated by the turbines in the analyzed period must be equal or higher than the energy needed by the load in the same period.

$$\sum_{t=0}^{T} load(t) \leq N_{turb} * E_{tot} * \eta_{inv}$$

Equation 3.3 Energy balance for each turbine in the database

Therefore, for each turbine in the database, the intuitive number of turbines that is at least able to satisfy the load in terms of generated energy in the whole period, reminding that a non-integer number of turbines does not make any sense, is:

$$N_{turb} = ceiling\left(\frac{\sum_{t=0}^{T} load(t)}{E_{tot} * \eta_{inv}}\right)$$

Equation 3.4 Intuitive number of turbines for each turbine in the database

This means that the tool is looking for how many turbines of the same type are needed. The possibility to mix different types of turbines is not allowed because otherwise the optimization problem would become too complex since mixing different turbines would increase the degrees of freedom of the problem and the computation effort[1].

[1] Assumptions directly formulated by CESI

Once the intuitive number of turbines is known, it is necessary to look for a strategy to discard from the database all the types of turbines that are not suitable for the specific load. In order to deal with the turbines that are too big, some considerations about the overgeneration can be made.

$$overgen(t) = N_{turb} * P_{turb}(t) * \eta_{inv} - load(t)$$

Equation 3.5 Overgeneration

The following figures show the duration curves of the overgeneration of two different types of turbine. These curves represent on the x-axis the percentage of hours in which the overgeneration is higher or equal to the value reported on the y-axis. The two chosen turbines are "C&F Green Energy CF50" and "Enercon E53".

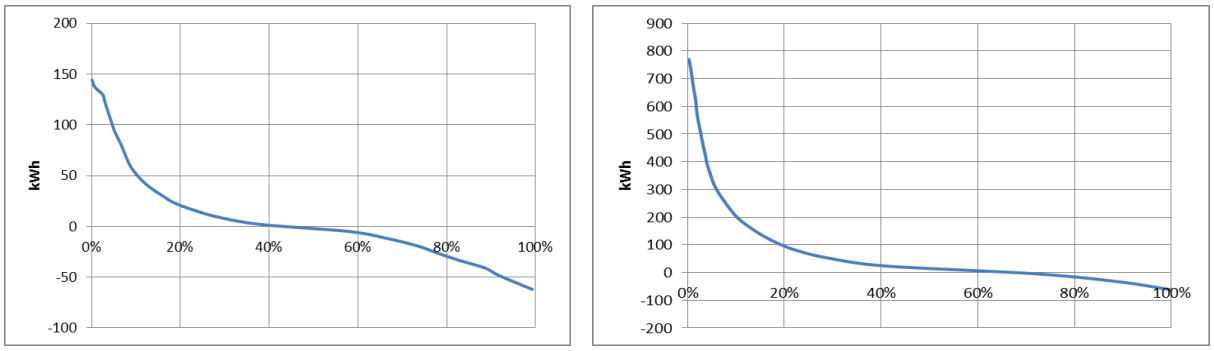

Figure 3.5 Overgeneration duration curve of C&F Green Energy CF50 (left) and Enercon E53 (right)

So, for sake of exemplification, applying the data from the case study (Chapter 5), in the first one the ratio $\frac{\sum_{t=0}^{T} load(t)}{E_{tot} * \eta_{inv}}$ is equal to 2,8 so the closest larger integer number is not very far. Indeed, its duration curve is quite balanced between the positive (actual overgeneration) and the negative (lack of generation) part of the curve.

Instead, with the second turbine the ratio $\frac{\sum_{t=0}^{T} load(t)}{E_{tot} * \eta_{inv}}$ is equal to 0,29 so the closest larger integer number is much higher, leading to a large oversizing. This is evident in Figure 3.5 (right) because in most of the time the system is facing a positive overgeneration with values much higher than the ones given by the previous case.

The final scope of the *wind micro-grid* module is to select a turbine among the ones in the database. So, the considerations just did about the overgeneration duration curves lead to discard the turbines that are too big: if $\frac{\sum_{t=0}^{T} load(t)}{E_{tot} * \eta_{inv}} \leq 0{,}5$ it means that the analyzed turbine gives more than the double of the needed energy so this would be an oversized plant.

As far as the maximum number of turbines is concerned, no considerations can be made about the overgeneration. But, in order to limit cable connection costs, ground occupation and the slowing down of the

wind due to the interaction between the turbines, the maximum number of turbines has been limited to 10. This brings to discard the turbines in the database that are too small.

Another aspect that must be considered, since the wind source can be highly unreliable, is the maximum number of consecutive hours (h_{max}) in which the wind turbines are not producing any power and it can be calculated from the power profile of each turbine. This can happen both when the wind speed is too low and when it is too high. The tool's user can set the maximum number of days ($days_{max}$) without any generation and if a turbine does not fulfill this limit it is discarded. This constraint is meant to limit the battery size since when the turbines are not generating power, the load has to be satisfied by the battery, therefore long periods without generation lead to big and expensive batteries. In order to avoid too large batteries a reasonable value for $days_{max}$ is 1 or 2 days.

To summarize, a type of turbine among the ones in the database is accepted and its intuitive number of turbines is used as a starting point for further calculations if:

- $0{,}5 < \frac{\sum_{t=0}^{T} load(t)}{E_{tot} * \eta_{inv}} \leq 10$
- $h_{max} \leq days_{max} * 24$

Equations 3.6 Constraints for wind turbine selection

So, the other turbines in the database are not suitable for the analyzed case.

The other element that has to be sized is the battery. In principle, increasing the generation size (the number of turbines) the battery size can be reduced but there is not a simple equation to relate the two quantities, so the procedure does not calculate an intuitive size for the battery.

3.4 Space of analysis

Once the intuitive number of turbines is known, it is possible to create a space of analysis. The space of analysis is generated varying the number of turbines and the battery size and this is done only for the turbines that were not discarded applying the constraints seen in the previous paragraph (Equations 3.6).

The aim of the space of analysis is to generate many possible configurations in order to simulate them and to find the optimal one. Each configuration is represented by a type of turbine, a number of turbines and a battery size.

For each type of turbine, the starting point is the intuitive number of turbines. In order to vary the generation size, the number of turbines is increased, always considering integer numbers.

Instead, the battery does not need a discrete sizing and so a specific sizing algorithm has been implemented. Being a very expensive component of the micro-grid, the starting point of the battery is the maximum

acceptable size. This is a free parameter set by the user and, thanks to the experience of CESI, it was chosen to set as default value a battery that is able to cover around 3 days of the load.
Indeed, it is sized setting the number of days (N_{days}) that has to cover.

$$ESS_{max} = N_{days} * \frac{mean\big(load(t)\big) * 24}{\eta_{inv} * (1 - SoC_{min})}$$

Equation 3.7 Maximum battery size

The maximum battery size is somehow equivalent to an intuitive size since it is the value from which a range of sizes is created and simulated. The algorithm that generates the sizes of the batteries modifies the sizes according to how far the configuration is with respect to the optimum.
Once the maximum battery size is calculated, the intuitive number of turbines is set and the configuration can be simulated. In order to modify the battery size, any time a configuration (number of turbine and battery size) is set, it is simulated and once the LLP is evaluated, the battery size for the new configuration is calculated:

$$ESS_{new} = ESS_{old} * LLP/LLP_{max}$$

Equation 3.8 Sizing algorithm for the battery

Where ESS_{new} and ESS_{old} are the batteries sizes of the present and the previous configurations and LLP_{max} is the maximum acceptable LLP (set to 5%).
With this algorithm the battery is reduced by a lager quantity if the system is far from the optimal one. Indeed, the optimal solution is expected to have an LLP close to the maximum one. Indeed, the economic optimization leads to minimize the components sizes increasing the LLP, while the technical optimization imposes a constraint about the system reliability (LLP_{max}). Therefore, the techno-economic optimum is a configuration that gives an LLP close to the maximum allowed value.
In some cases the LLP can result so low that the new battery size becomes too small, or the LLP can be so close to LLP_{max} that the algorithm need too many steps to reach the optimum. So, the dynamic algorithm is limited between $limit_{down}$ and $limit_{up}$ (with $0 < limit_{down} < limit_{up} < 1$).

- $if\ LLP < limit_{down} * LLP_{max}$ $\quad ESS_{new} = ESS_{old} * limit_{down}$
- $if\ limit_{down} * LLP_{max} \leq LLP \leq limit_{up} * LLP_{max}$ $\quad ESS_{new} = ESS_{old} * LLP/LLP_{max}$
- $if\ limit_{up} * LLP_{max} < LLP < LLP_{max}$ $\quad ESS_{new} = ESS_{old} * limit_{up}$

Equations 3.9 Limited sizing algorithm for the battery

This algorithm continues generating new configurations with smaller batteries and fixed number of turbines until the LLP becomes higher than the maximum allowed value. Considering further battery reduction is useless since those configurations would not be considered as acceptable solutions.

Once all the reasonable battery sizes for a specific number of turbines has been simulated, the tool proceeds increasing the number of turbines. There is no need to start from the maximum accepted battery size as it was done for the first intuitive number of turbines. Instead, the last battery that gave an LLP lower than its maximum is a good starting point. After that, the battery is again reduced according to the algorithm of Equations 3.9.

The reason why it is not necessary to start from the maximum battery size is because the battery capacity is expected to decrease. Increasing the number of turbines, the generated energy is increasing, so also the overgeneration is increasing. If the overgeneration increases the turbines are able to provide part of the energy that otherwise would be given by the battery. Therefore, increasing the number of turbines, the optimal battery size decreases.

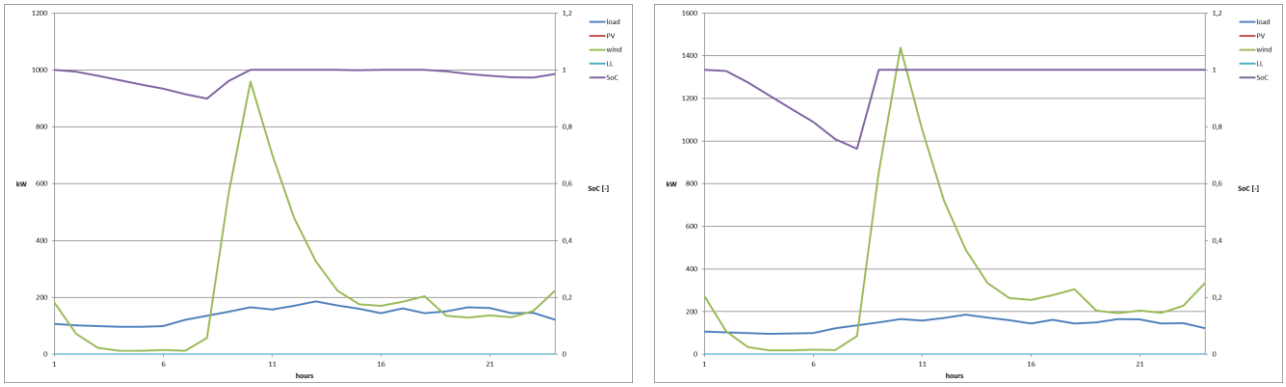

Figure 3.6 Comparison of two different configurations

Figure 3.6 represents the profile of the same day of two different configurations with the same type of turbine (Enercon E53). The figure on the left is performed with 6 turbines and 6418 kWh battery, while the figure on the right with 9 turbines and 1996 kWh battery. The two simulations give the same LLP in the overall simulated period. In the first part of the day simulated it is evident that the smaller battery faces a deeper discharge (Figure 3.6 – right), while in the second part of the day the configuration with more turbines is able to generate enough energy without relying on the battery (Figure 3.6 – right).

The intuitive number of turbines guarantees that in the whole analyzed period it is generated enough energy to cover the load (from integral point of view, the energy balance is satisfied). But when the real time behavior is analyzed, the system may not be able to satisfy the load since some energy may be generated when the battery is fully charged and so it will be dissipated and when the battery is fully discharged there may be loss of load. This means that sometimes the intuitive number of turbines with the maximum accepted battery size may not be enough (the relative LLP exceeds the maximum value). Assuming that the battery is the most expensive component of the micro-grid, in this case the tool does not consider the analyzed number

of turbines and increases it until some acceptable results can be found. It stops when it finds 4 different numbers of turbines that give acceptable results (4 columns in Table 3.3).

For each type of turbine simulated, its space of analysis is constituted by numbers of turbines and batteries (rows). In the following figure it is shown an example where the values of LLP are reported. The red cells are the ones the exceed LLP_{max} and so they are the ones that stop the algorithm for the battery sizing.

		turb 21			kWh/€	0,76
		Enercon E-53 [800kW]			eq h	892
	P turb [kW]	4050	4860	5670	6480	
	#turbines	5	6	7	8	
ESS [kWh]						
	1837,2				5,14%	
	1894,0				5,00%	
	1975,3				4,79%	
	2244,7				4,20%	
	2550,8			5,01%	3,59%	
	2629,7			4,87%	3,45%	
	2988,3			4,34%		
	3395,8			3,82%		
	3858,9		5,05%	3,33%		
	3978,2		4,93%	3,24%		
	4259,6		4,67%			
	4840,5		4,22%			
	5500,6		3,79%			
	6250,6		3,50%			
	7103,0		3,21%			
	8071,6	5,03%	2,98%			
	8321,2	4,96%	2,93%			
	8578,6	4,88%				

Table 3.3 An example of space of analysis for a type of turbine

In this table is evident that when the installed generation power increases, the minimum battery size decreases, as explained before. For this reason, is not possible to understand a priori which configuration is the optimal one, or better which one is the cheapest. Indeed, for each configuration the NPC and the LCoE have to be calculated and the optimal solution is the one with the lowest LCoE which does not exceed the maximum LLP.

So far it was explained the procedure to generate the space of analysis for a type of turbine. Therefore, it should be repeated for all the turbines in the database that respect the constraints of Equations 3.6. This can bring to a procedure that is too time-consuming. Being the computing time a resource that has to be reduced as much as possible, according to requirements given by CESI due to the supposed target of the tool's user, it was decided to limit the calculations to the "best" turbines.

In order to decide which turbines are the "best", a ranking has to be generated. A useful parameter is the equivalent hours:

$$E_{year} = \sum_{t=0}^{8759} P_{turb}(t)$$

Equation 3.10 Energy generated by a turbine in a year

$$h_{eq}\left[\frac{h}{y}\right] = \frac{E_{year}\left[\frac{kWh}{y}\right]}{P_{nom,turb}[kW]}$$

Equation 3.11 Equivalent hours

The best turbines have high equivalent hours because they can generate the same amount of energy with less installed power.

Since in the optimization the economic parameters are important, a second parameter that takes into account the turbines investment cost can be used to generate a ranking. Such a ranking would consider the economies of scale: from the economics point of view, it is better to have few big turbines than lot of small ones. This last parameter is the energy/cost ratio and the higher it is, the lower is the turbines cost with the same generated energy.

$$\left(\frac{E}{c}\right)_{ratio}\left[\frac{kWh}{€ * y}\right] = \frac{E_{year}\left[\frac{kWh}{y}\right]}{C_{turb}[€]}$$

Equation 3.12 Energy/cost ratio. C_{turb} is the investment cost of a turbine.

The two parameters give two different rankings only if the turbines cost is not linear with respect to their power. Indeed, in the following figures the relationship between turbine cost and turbine power is represented [24].

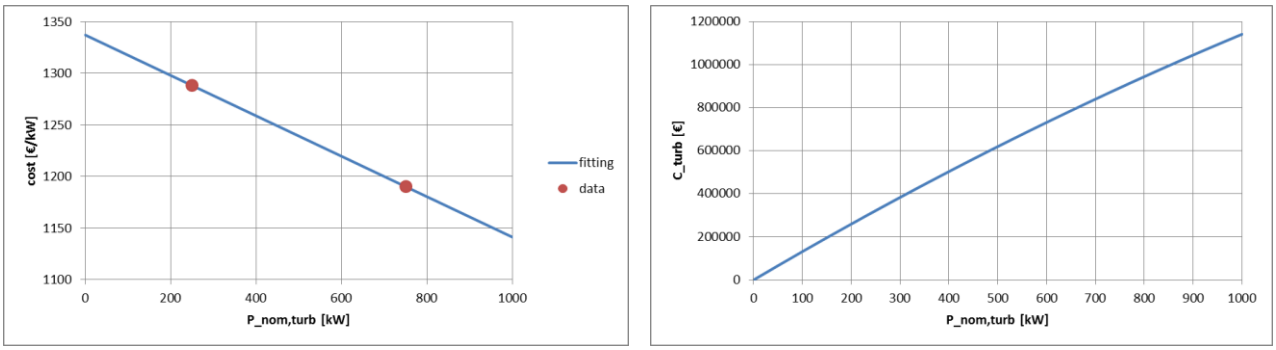

Figure 3.7 Turbine investment cost per kW (left) and total C_{turb} (right)

In the tool the ranking according to the second parameter was implemented, but if the first one had been chosen, there would not have been many differences. This is due to the constraints of Equations 3.6 that limit the power of the acceptable turbines into a narrow interval, so the cost per kW of a turbine does not change so much and two rankings are quite similar.

According to the author's experience validated by the project coordination in CESI, the final result of the module, that is the optimal configuration in the space of analysis, is always within the first 3 best turbines of the ranking also when all the turbines in the database are simulated. To be sure to find the optimum, it was

chosen to select the first 10 turbines. Once the 10 turbines are chosen according to the ranking among the ones that fulfill the constraints of Equations 3.6, a space of analysis composed by only these last turbines can be generated.

3.5 Algorithm implementation

The *wind micro-grid* module aims to find the best configuration for the micro-grid using only wind turbines as energy source. In particular, this module studies the database in order to choose which are the best turbines to be simulated. It selects the best turbine in the database according to technical and economic parameters.

The algorithm implemented in the *wind micro-grid* module is detailed in the flow chart in Figure 3.8. It works in the following way:

- It reads the load profile and the wind speed profile.
- For each turbine in the database, it calculates the power generation profile interpolating the power curve (Figure 3.4) with the wind speed profile.
- Known the wind profile, it is possible to calculate $\frac{\sum_{t=0}^{T} load(t)}{E_{tot}*\eta_{inv}}$ (eq1 in the flow chart) and the maximum consecutive hours without power generation.
- According to the constraints of Equations 3.6 a turbine can be discarded or accepted.
- If a turbine is accepted its intuitive number of turbines (Equation 3.4) can be calculated and its database number can be saved.
- The tool generates a ranking with the saved turbines and 10 best ones according to the energy/cost ratio (Equation 3.12) are selected.
- For each selected turbine the space of analysis is generated and all configurations are simulated: starting from the maximum size of the battery (Equation 3.7) and the intuitive number of turbines the space of analysis is generated reducing the battery size (Equations 3.9) and increasing the number of turbines (reminding that it is not allowed to have more than 10 turbines).
- Once the LLP and the LCoE of all the configurations have been calculated, it is possible to find the optimal solution of the module.

The solution is a techno-economic optimization, meaning that, among the configurations in the space of analysis, the tool chooses the one with the lowest cost (LCoE) with an acceptable reliability ($LLP < LLP_{max}$). Being the space of analysis composed by different types of turbines, the tool is not only able to find an optimal number of turbines and an optimal battery size, but also it finds the best turbine in the database.

The algorithm here described is important to study a procedure to select the best turbine. Once this procedure is defined, it is possible study a way to analyze the turbines database and mix the best turbine with other resources. Indeed, the *wind micro-grid* module is the base for the *PV+wind micro-grid* module where the turbine selection is a fundamental part of the PV and wind mix optimization.

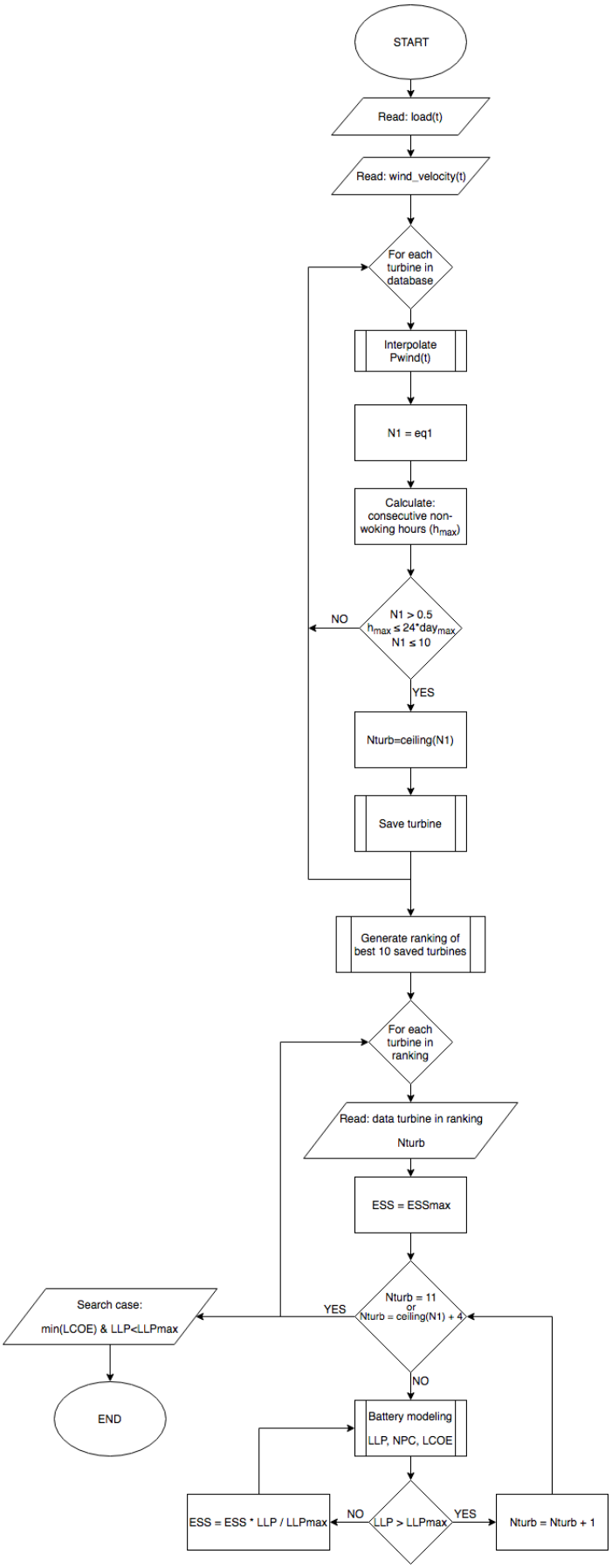

Figure 3.8 Flow chart of the *wind micro-grid* module

Chapter 4

4 Multi-source micro-grid design

This chapter presents the *PV+wind micro-grid* module that aims to optimize the two sources in order to minimize the system cost.

4.1 Review of multi-generation mix approaches

One of the most frequent micro-grids in literature is based on two energy sources: PV and wind. Therefore, it is necessary to find an effective approach to size the components in an optimal way. Optimum component sizing is essential for efficient and economic utilization of the renewable energy sources in integrated systems. Indeed, the optimal design can be evaluated through its lifetime cost.
There are many approaches to provide the optimal configurations, including commercial software tools; anyway, in literature other approaches have been adopted, and some of them are here reported [25] [26] [27].

Artificial intelligence approaches
They are numerical methods and can be differentiated according to the strategy used to reach the optimum [28]. Three examples of artificial intelligence approaches are reported.

1. Genetic algorithm

A genetic algorithm is an optimization method based on genetic processes of biological organisms. In this way, it can provide solutions to complex problems. The input data are the meteorological conditions and the components cost. A genetic algorithm provides an iterative procedure that is implemented until a predefined termination criteria or maximum iteration number are reached. Moreover, an objective function has to be defined as an input.
The algorithm starts with the generation of a random population: for the problem under investigation it corresponds to a random sizing of the system components. Each of the random solutions is evaluated according to the objective function. After that, a defined percentage of the initial population is selected

according to their values of the objective function. Using the selected solutions, new populations are created with the "crossover" operator that aims to provide new possible solutions with higher value of the objective function.

The selection of the best solutions and the "crossover" operator are repeated for each step of the iterative procedure.

During the iterative procedure also a "mutation" operator can be used: it prevents getting stuck at a local minimum by modifying part of the population. Indeed, the main advantage of the genetic algorithm is that it can easily jump out of a local minimum and find the global optimum. Actually, it is relatively hard to code due to its complex structure and, if the number of parameters becomes larger, the computing time increases a lot.

In Figure 4.1 the genetic algorithm is shown in a flow chart.

In [29] a genetic algorithm is used to size a sand-alone plant that exploits PV and wind. Here the variables that have to be optimized are many: number and type of PV modules, wind turbines and battery chargers, the PV modules tilt angle, the installation height of the turbines and the battery type and nominal capacity. The objective function that has to be minimized is the total plant cost in the 20-year simulation.

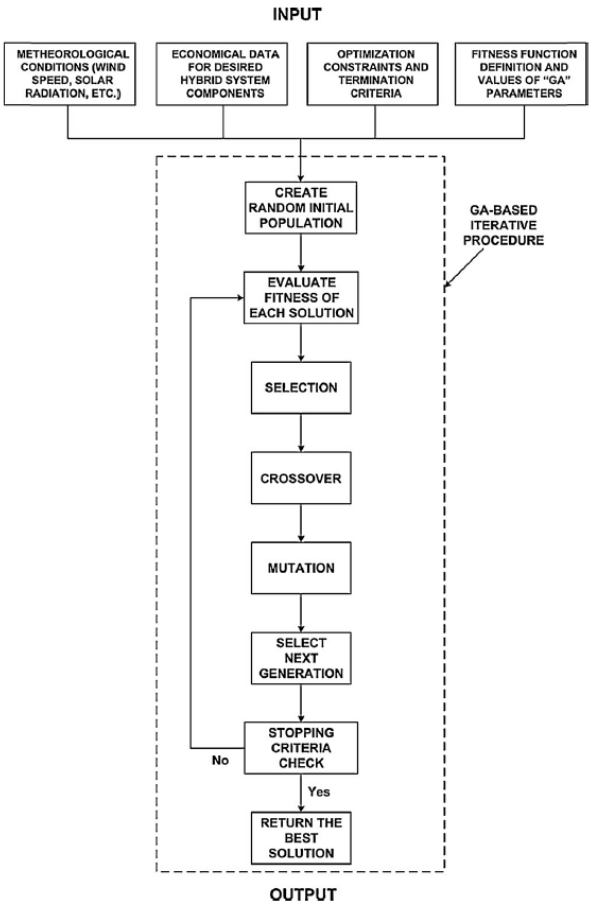

Figure 4.1 Genetic algorithm flow chart

2. Particle swarm optimization

It is an optimization technique based on the movement and the intelligence of swarms. The particle swarm is the social structure of basic creatures which make group to have the same purposes. The input data of this model are the meteorological conditions and the components costs.

The particle swarm optimization is a population-based stochastic procedure. The coordinates of each particle represent a possible solution and to each particle is associated a position and a velocity.

The particles are initialized with a random velocity, and, at each iteration, the particles move towards the optimum with the present velocity. All the particles in the population apply the same procedure at each iteration. Therefore, a group movement is iterated until a predefined termination criterion is reached.

This procedure is based on a simple concept and so involves few equations that are easy to be implemented. So, with respect to the genetic algorithm, it needs less computation time, but it also has less reliability for finding the global optimum.

In Figure 4.2 the flow chart of the particle swarm optimization is shown.

The particle swarm optimization is used in [30] where it is studied a power system adopting PV and wind sources. The objective function consists of the investment of wind turbine, PV, battery and the cost of loss of load which can be calculated by means of the reliability. By transforming the investment cost and the reliability into a comprehensive cost, the presented multi-optimization problem is transformed into a single optimization problem that indicates the direction toward which the particles have to move. Here it is used an improved particle swarm optimization: firstly, a convergence factor is adopted to enhance its search efficiency; secondly, a migration operation is used to improve the algorithm's global optimal searching ability.

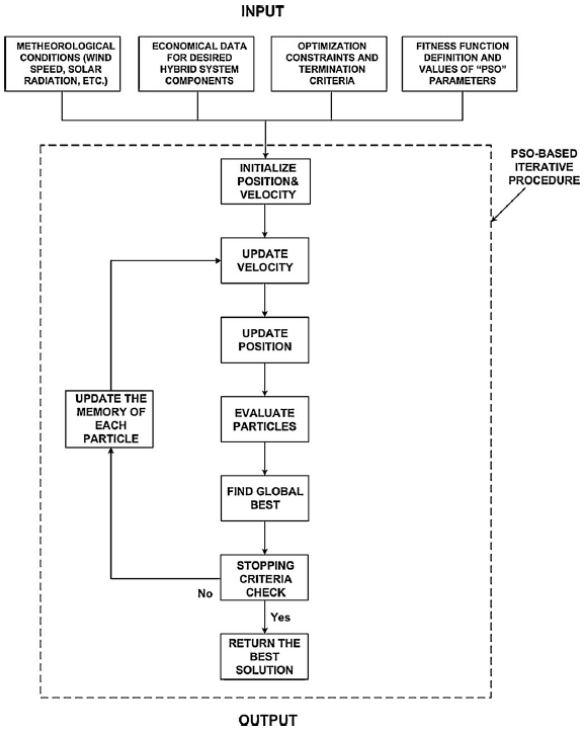

Figure 4.2 Particle swarm optimization flow chart

3. Simulated annealing

The simulated annealing is a general optimization technique for solving combinatorial optimization problems.

In metallurgy, annealing refers to the process that heats up a solid and then it cools it down slowing lowering the temperature.

At each iteration, a candidate move is randomly selected and this move is accepted if it leads to a solution with a better objective function value than the current solution. Otherwise the move is accepted with a probability that depends on the deterioration of the objective function value.

If a new solution has a better value of the objective function than the current best solution in the population, the solution is accepted. If this new solution has a worse value of the objective function may also be considered for the generation of the new population at the following iteration depending on the difference between its value of the objective function and the best value.

The simulated annealing allows for wide area searches at the beginning of the iterative process and local area searches around the best solutions.

In the following figure the algorithm of the simulated annealing is shown.

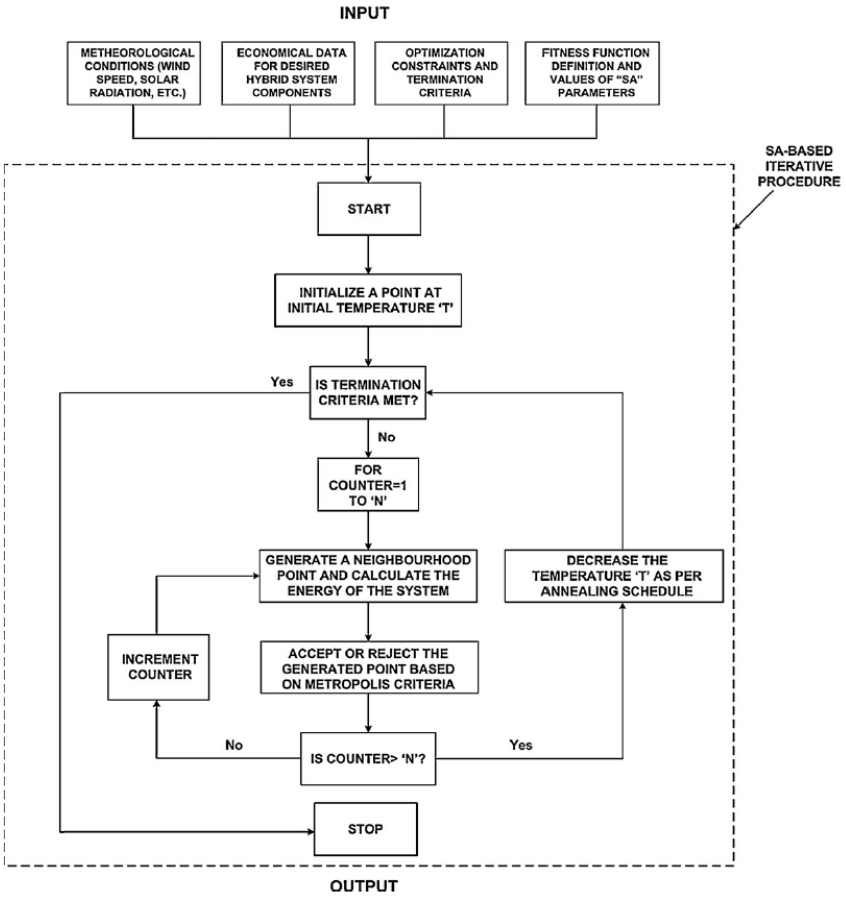

Figure 4.3 Simulated annealing flow chart

In [31] the optimization of PV/wind integrated energy system with battery storage is performed with a simulated annealing algorithm. The non-predictable solar and wind sources are simulated with probability distributions. The decision variables are represented by the sizes of the components while the objective function is their cost. In particular, it is the total cost of: PV, wind turbine rotor, battery and also the battery charger, installation, maintenance, and engineering cost.

Probabilistic approach

It considers the effect of random variability of parameters and enables variation and uncertainty to be quantified, mainly by using distributions instead of fixed values. The main disadvantage is that the probabilistic approach cannot represent the dynamic performances of the system.

In [32] a solar-wind energy conversion system is studied with a probabilistic approach. It is based on the probability distribution of the available solar power and the probability distributions of the wind turbines capacity level due to hardware failure of the solar models and wind turbines. The study is divided in time-frames (1 or 2 hours).

The solar irradiance (r in W/m^2) is assumed to follow a β-distribution, given by the following probability density function:

$$F_r(r) = \frac{\Gamma(\alpha+\beta)}{\Gamma(\alpha)\,\Gamma(\beta)}\left(\frac{r}{r_{max}}\right)^{\alpha-1}\left(1-\frac{r}{r_{max}}\right)^{\beta-1}$$

Equation 4.1 β-distribution for irradiance

So, given the total area of the panes and their efficiency, the power P_m generated by the solar plant composed by M panels follows a new probability density function:

$$F_M(P_M) = \frac{\Gamma(\alpha+\beta)}{\Gamma(\alpha)\,\Gamma(\beta)}\left(\frac{P_M}{P_M(r_{max})}\right)^{\alpha-1}\left(1-\frac{P_M}{P_M(r_{max})}\right)^{\beta-1}$$

Equation 4.2 β-distribution for irradiance for PV generation

In order to account for hardware failure, it is possible to define $P_0(k)$ the capacity level when k out of M modules are operating and q is the unavailability of a module. Applying the Bernoulli distribution:

$$F_0(k) = \binom{M}{k}(1-q)^k\, q^{M-k}$$

Equation 4.3 Bernoulli distribution for PV panels

Therefore, the solar park is modelled by joining the distribution of P_M and P_0 and the power produced becomes:

$$P = \frac{P_M \, P_0(k)}{P_0(M)}$$

Equation 4.4 Power generated by PV

Instead, the wind speed is assumed to have a Weibull distribution:

$$F_v(v) = \frac{k}{c}\left(\frac{v}{c}\right)^{k-1} \exp\left(-\left(\frac{v}{c}\right)^{k}\right)$$

Equation 4.5 Weibull distribution for wind speed

Known the wind speed, the capacity of a wind turbine is:

$$C_t(v) = \begin{cases} 0 & 0 \le v \le cut - in \\ a + b\, v^{\varphi} & cut - in \le v \le rated \\ R & rated \le v \le cut - out \\ 0 & v \ge cut - out \end{cases}$$

Equations 4.6 Wind turbine production

As before, the capacity level $P_t(n)$ when n out of N modules are operating can be defined as a Bernoulli distribution:

$$F_t(n) = \binom{N}{n} (1-q)^n \, q^{N-n}$$

Equation 4.7 Bernoulli distribution for wind turbines

The wind farm power production is modelled joining the wind speed probability and the capacity level. Abd it is obtained by combining the probability distributions of wind turbine capacity levels due hardware failure at the various wind speeds.

Once the probabilities of PV and wind power production are known, their overall probability distribution P_H is obtained by convoluting the distributions of the two sources using the recursive multi-state unit-addition algorithm.

The probability P_H can be calculated for each considered time step and can be compared with the load duration curve of that specific time step. If there is not a battery, the load that will not be supplied is represented in the following figure as E_f^j.

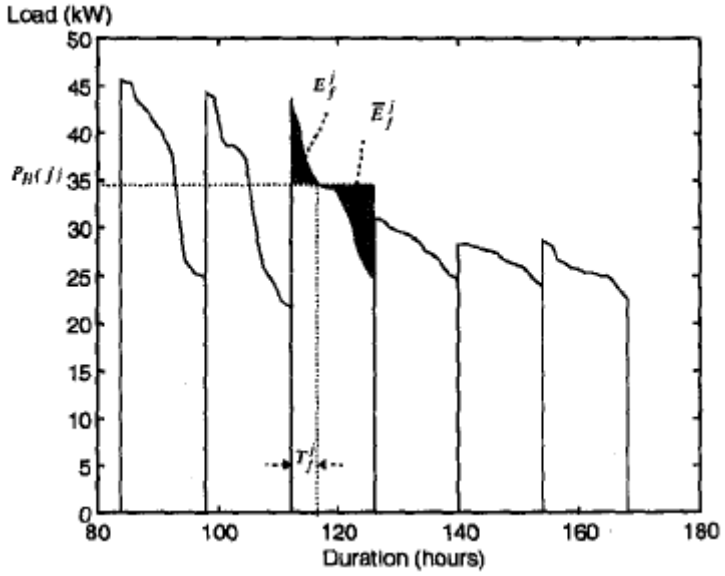

Figure 4.4 Load duration curves

Otherwise, if a battery is present, from the energy not supplied to the load must be subtracted the energy stored in the battery. The maximum size of the battery can be deduced from the energy available for recharge.

Once a model to study a power system has been developed, many configurations can be created varying the number of turbines, the number of PV modules and the battery size. Comparing the different configurations, the best solution can be found.

Graphical construction technique

This is a basic and easily understandable method with no complexity but is not flexible.

It is used in [33] in which the nominal power sizes of PV and wind are defined a_s and a_w. The first one is the power generated per kW of incident radiation, while the second one is the energy generated by a turbine per kW of the kinetic energy of the wind.

Defined the daily averages of the solar irradiation S, the wind kinetic energy W and the load demand d, it can be stated that:

$$d \leq W\, a_w + S\, a_s$$

Equation 4.8 Energy balance constraint

So, the systems that satisfy this condition fill a region of the cartesian plane in the following figure.

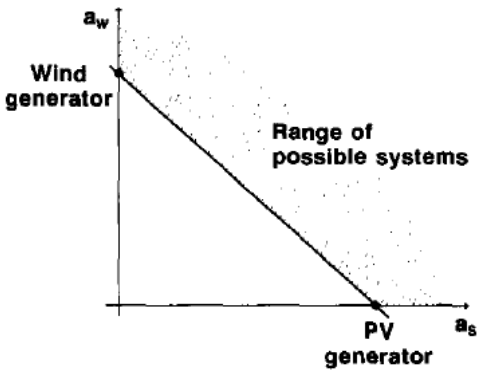

Figure 4.5 Energy balance constraint for an average day

Being Figure 4.5 a straight line and assuming the cost of the two generators linearly dependent on their nominal power, if the cost of PV and wind turbines is minimized it results that the least-cost system will be either the configuration with only PV or the one with only wind.

In order to avoid this issue, Equation 4.8 can be written for each month of the year giving a system of 12 inequations that are represented in the following figure.

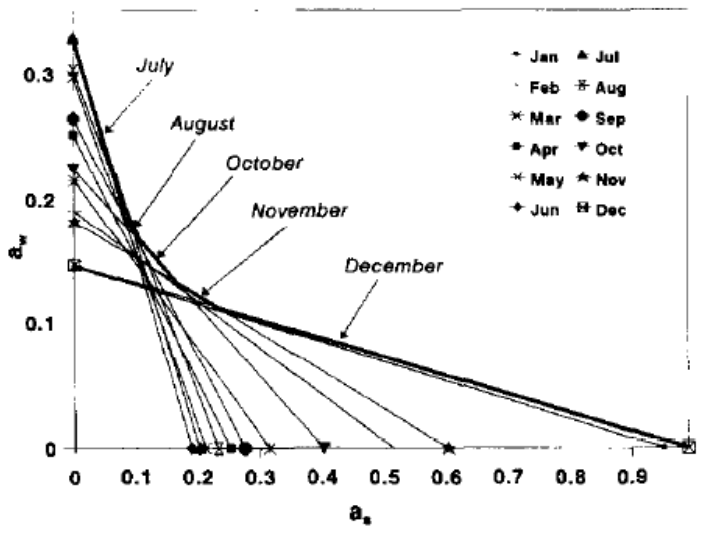

Figure 4.6 Energy balance constraint for each month

It can be easily verified that the optimum system in terms of generation cost will be located at the boundary of the hybrid region, shown in Figure 4.6 by a thick line. The accuracy can be improved reducing the time intervals in which the average is calculated.

Iterative techniques

An iterative method is a mathematical procedure that generates approximate solutions for problems. This is a recursive process which stops when the best configuration is reached.

In [34] an iterative technique is used to design a PV/wind system. Here the objective function that has to be minimized is the total cost, accounting for capital and maintenance costs. The objective function is constrained to minimize the difference between the generated power and the load demand.

$$\Delta P = P_{gen} - P_{dem}$$

Equation 4.9 Difference between generated power and demand

Where the generated power is written as a function of the number of wind turbines K_w and PV panels K_s and the power $P_w(t)$ and $P_s(t)$ generated in each time step t.

$$P_{gen} = K_w\, P_w(t) + K_s\, P_s(t)$$

Equation 4.10 Generated power

Integrating Equation 4.9 it is possible to find the energy curve. On an average day, the battery is required to cycle between the positive and negative peaks of the energy curve. Therefore, the battery should at least have a capacity equal to the difference between the positive and negative peaks of the energy curve.

The algorithm adopted to select the number of turbines and PV modules is the following:

1. Select commercially available wind turbines, PV panels and batteries.
2. Keep constant the number of turbines and increase the number of PV panes until the system is balanced, that is until the average over time of the ΔP curve is zero.
3. Repeat the step 2 for different number of turbines.
4. Calculate the total costs for all configurations that fulfill the target condition explained in step 2.
5. Choose the configuration with lowest cost.

Some of the approaches reported are too complex for the purposes of the tool object of this thesis. Indeed, the author is looking for a procedure that has to be very fast and simple.

The approach adopted in the tool is based on the generation of a space of analysis varying the sizes of wind, PV and battery in a way similar to what is done in example of probabilistic approach just explained [32], but without dealing with the complex statistical study of the performances. Instead, an objective analysis is used to aid the generation of the space of analysis in order to optimize the generation sources from technical point of view.

In the rest of this chapter, this procedure is explained in detail.

4.2 The adopted approach and the micro-grid configuration

The *PV+wind micro-grid* module aims to find the best configuration for a system that exploits both PV and wind sources. As already introduced, the approach adopted is a sub-optimization. It has to choose the best turbine in the database and size the micro-grid components. The choice of the turbine and the definition of a space of analysis is very close to what was developed for the *wind micro-grid* module (first optimization). The innovative part is the optimization of the mix of PV and wind based on an objective function. The approach adopted in the present module is based on the following procedure:

- The objective function is used to find the optimal mix of PV and wind.
- The optimal mix is used to calculate the intuitive sizing of the components.
- Keeping fixed the ratio between PV and wind and starting from the intuitive sizing, the space of analysis is created: many different configurations based on different types of turbines are simulated and compared.
- Among these configurations the best solution is selected, so also the best turbine is chosen (first optimization).
- The solution of the first optimization is the starting point of the second optimization: a new space of analysis based only on the best turbine is created varying the ratio between the two sources.
- The best configuration in the second optimization space of analysis is the solution of the module.

In the following paragraphs this procedure is explained in detail.

The *PV+wind micro-grid* module combines the wind and PV sources, so the system configuration is close to the ones relative to the *PV micro-grid* and the *wind micro-grid* modules. The PV system, the wind turbines and the battery are directly connected to the DC bus and the DC bus is connected to the AC load by means of an inverter [35]. In the following figure the elements implemented in the tool are shown.

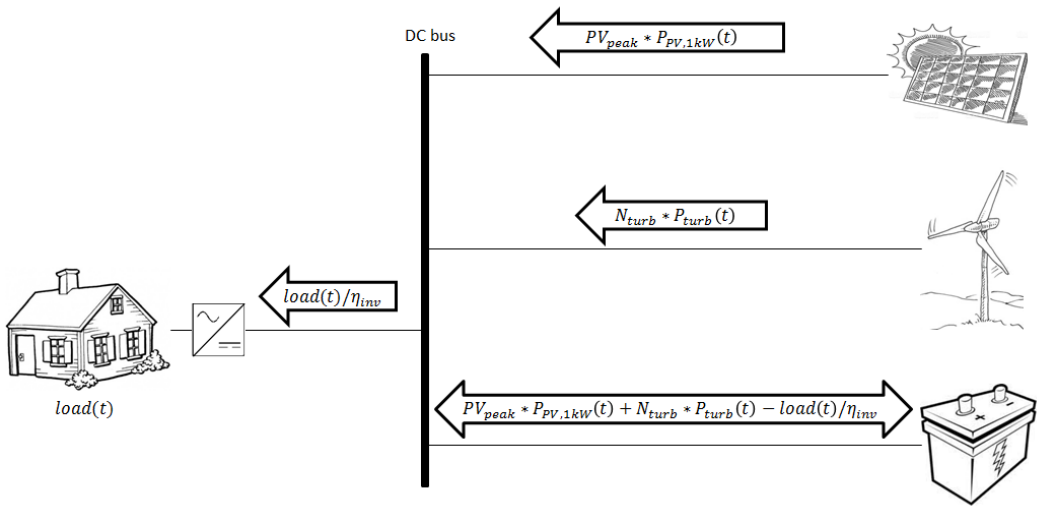

Figure 4.7 *PV+wind micro-grid* configuration

4.3 Objective functions

The present chapter aims to find a procedure to optimize the generations from the PV and from the wind turbines. The tool has to size the components of a micro-grid that exploits both the solar and the wind resources. Therefore, it needs to find a way to choose the share of the two sources in order to optimize the generation from the techno-economic point of view.

The procedure implemented in the tool starts form the study of an objective function that aims to give a first hypothesis about the mix of the PV and wind sources. The scope of the objective function is not to find the real optimum mix, but to suggest an initial share of the two sources from which it is possible to perform further calculation and find the final optimal configuration.

The data necessary for this analysis are the power generation profiles from a 1-kWp PV ($P_{PV,1kW}$) and from all the wind turbines in the database (P_{turb}). From these, the generation profiles result:

$$PV(t) = PV_{peak} * P_{PV,1kW}(t)$$
$$wind(t) = P_{nom,w} * P_{turb,PU}(t)$$

Equations 4.11 Generation profiles

The objective functions that will be presented in this paragraph is devoted to solving the optimal mix, giving the suggested nominal power PV_{peak} and $P_{nom,w}$ that have to be installed. The value of $P_{nom,w}$ is not constrained to be the multiple of the power of a single turbine because otherwise the optimization problem would become much more complicated without gaining much accuracy.

To calculate the profiles of Equations 4.11, it is useful to deal with per unit data. The $P_{PV,1kW}$ profile, being relative to a nominal power of 1 kWp, it is equivalent to its profile in per-unit. Instead, the wind generation profile, for each turbine in the database, has to be transformed in per-unit using the nominal power of each turbine ($P_{nom,turb}$).

$$P_{turb,PU}(t) = \frac{P_{turb}(t)}{P_{nom,turb}}$$

Equation 4.12 Wind generation profile in per-unit for each turbine in the database

Before introducing possible objective functions, it is necessary to set a constraint in order to guarantee that the energy generated is (at least theoretically) enough to cover the load. In other words, it is necessary to impose that the energy balance of the system is satisfied during a whole year. The energy balance is the integral of the power balance for a year, which for discrete time steps of 1 hour becomes:

$$\sum_{t=0}^{8759}\left(PV(t)+wind(t)-\frac{load(t)}{\eta_{inv}}\right)=0$$

Equation 4.13 Energy balance constraint

Dealing with off-grid systems, the battery is always a critical element. It is fundamental to guarantee energy when the renewable energy sources are not working but it is a very expensive component. A way to size the PV and wind mix is to find the share of the two sources that allows to minimize the battery. Therefore, it has to be found an objective function that gives the PV and wind power necessary to be installed in order to have the smallest battery possible.

A way to do so, it is to minimize the energy fluxed to and from the battery. The energy that is given to or required by the battery is represented by the hourly energy balance between generation and load. The sum of the energy balance in both the directions is the total energy flux at the battery and it is the first proposed objective function.

$$OF1=\sum_{t=0}^{8759}\left|PV(t)+wind(t)-\frac{load(t)}{\eta_{inv}}\right|$$

Equation 4.14 Objective function 1

Minimizing the OF1, the energy fluxed by the battery is minimized, so the size of the battery should be minimized.

The objective function OF1 presents a potential issue: being defined with the absolute value operator, it may not be smooth and so there may be problems with the solution of the optimization problem. In order to avoid this issue and in order to keep the argument of the sum positive it is possible to use the square operator:

$$OF2=\sum_{t=0}^{8759}\left(PV(t)+wind(t)-\frac{load(t)}{\eta_{inv}}\right)^2$$

Equation 4.15 Objective function 2

Similarly to the OF1, minimizing the OF2 the energy fluxed by the battery is minimized. The results of the two objective functions should be very close, but the second one should have less problems about resolutions.

The objective functions OF1 and OF2 aims to minimize the energy flux both during the charge and during the discharge. In order to minimize the size of the battery it is important to minimize the flux required by the battery (when $PV(t)+wind(t)-\frac{load(t)}{\eta_{inv}}$ is negative), while the power given to the battery does not need to be limited since the overgeneration is not a problem. Therefore, a new objective function can be defined:

$$f_3 = \begin{cases} 0 & if\ PV(t) + wind(t) - \dfrac{load(t)}{\eta_{inv}} \geq 0 \\ \dfrac{load(t)}{\eta_{inv}} - \left(PV(t) + wind(t)\right) & if\ PV(t) + wind(t) - \dfrac{load(t)}{\eta_{inv}} < 0 \end{cases}$$

$$OF3 = \sum_{t=0}^{8759} f_3$$

Equation 4.16 Objective function 3

Minimizing the OF3, the energy required by the battery is minimized without any consideration about the overgeneration. In this way the battery should be sized to satisfy the load without minimizing the also the overgeneration, differently from the first two objective functions.

Applying a different approach, it can be studied the integral of the power balance.

$$int(h) = \sum_{t=0}^{h} \left(PV(t) + wind(t) - \frac{load(t)}{\eta_{inv}} \right)$$

Equation 4.17 Integral of the power balance

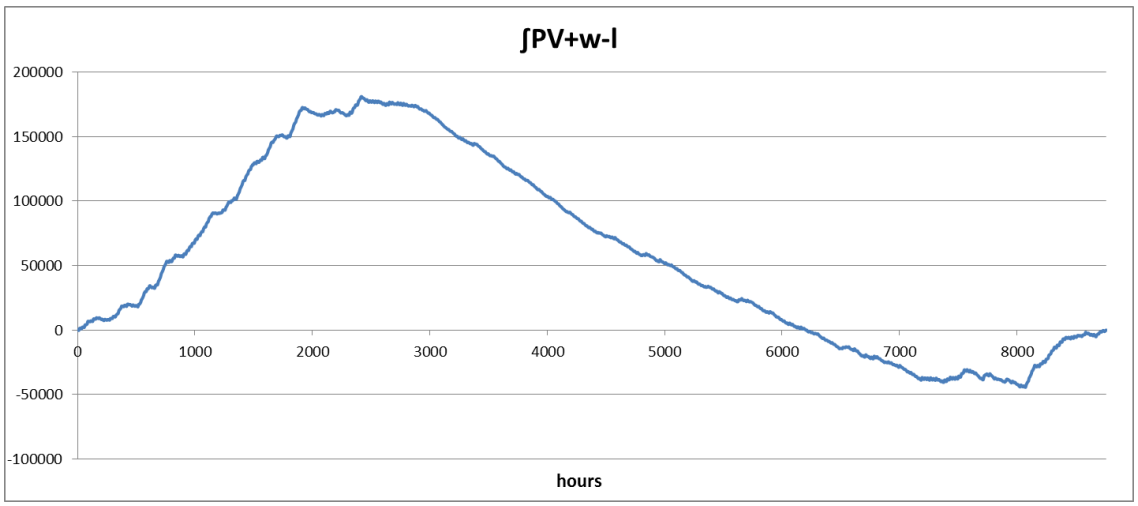

Figure 4.8 Integral of the power balance

Equation 4.17 represents the discretized integral of the power balance until the hour h, and so it is the energy fluxed in or out of the battery from the first hour of the year to the hour h. In the last hour of the year the value of $int(h)$ is zero because of the constraint of Equation 4.13. Therefore, a new objective function can be defined:

$$OF4 = \max(int) - \min(int)$$

Equation 4.18 Objective function 4

Minimizing the OF4 the yearly oscillations of the energy balance should be reduced.
Moreover, the value of the OF4 is the size of the battery that is necessary in order to avoid any loss of load and any overgeneration. From Figure 4.8 is evident that the battery should be able to transfer energy from a period of the year to another, leading to batteries that are at least an order of magnitude bigger than the expected values (the maximum allowed battery has to be able to satisfy around 3 days of the load). Therefore, the OF4 can be useful to find the optimal share of PV and wind, but it cannot be used to find the size of the battery since in the analyzed problem some loss of load is allowed and there are no constraints about the overgeneration, which is different from the hypothesis of the OF4.
Once defined the possible objective functions, they have to be compared in order to find the most suitable to solve the optimization problem.
The first three objective functions aim to minimize the power exchanged by the battery, while the OF4 aims to minimize the energy exchanged in the whole period. Indeed, the main differences are between these two groups.
In general, the optimization problem is defined as:

$$of = \begin{cases} OF1 \\ OF2 \\ OF3 \\ OF4 \end{cases}$$

$\min(of)\ subject\ to$:

- $PV_{peak} \geq 0$
- $P_{nom,w} \geq 0$
- $\sum_{t=0}^{8759} \left(PV(t) + wind(t) - \frac{load(t)}{\eta_{inv}} \right) = 0$

Equation 4.19 General formulation of the optimization problem

4.3.1 Objective functions relationships with generation

The first step to study the four proposed objective functions is to develop a sensitivity analysis, i.e. to plot their behavior varying the two parameters that procedure is looking for: PV_{peak} and $P_{nom,w}$. Observing the shape of these plots it is possible to do some considerations.
In this paragraph will be shown results based on the data of the case study. The wind power generation is based on the power curve of the turbine "EWT 250" while the nominal power of the wind turbines is considered a free parameter, that means that the constraint of integer number of turbines is neglected. This choice was made in order to represent the real behavior of the objective functions.

The following figure represents the shape of the OF1 varying the installed power of PV and wind. Since the energy balance constraint (Equation 4.13) has not been imposed, the objective function is a 3D surface.

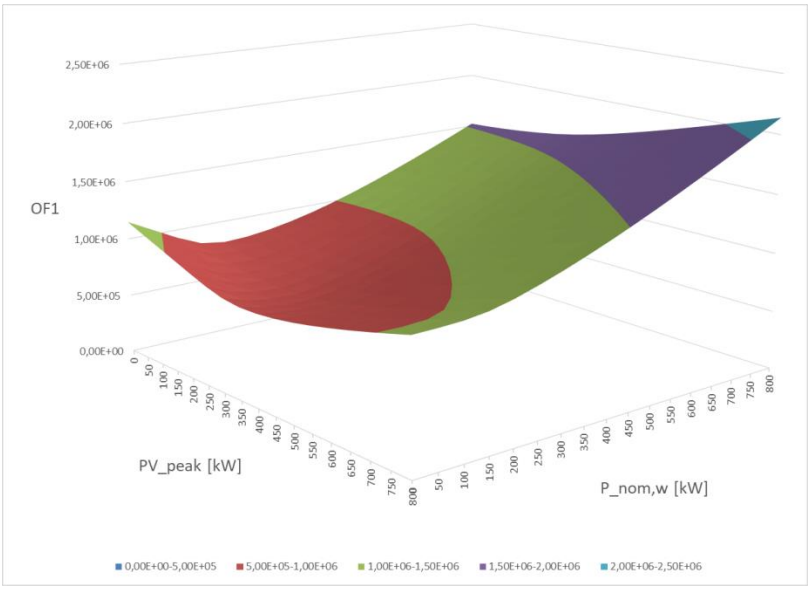

Figure 4.9 Unconstrained OF1

Applying the energy balance constraint, the objective function results is a line on this last surface. Since the energy balance constraint is represented by a linear equation, for each value of PV_{peak} corresponds a unique value of $P_{nom,w}$ and vice versa. Therefore, the OF1 behavior can be plotted as a function of the only wind power size.

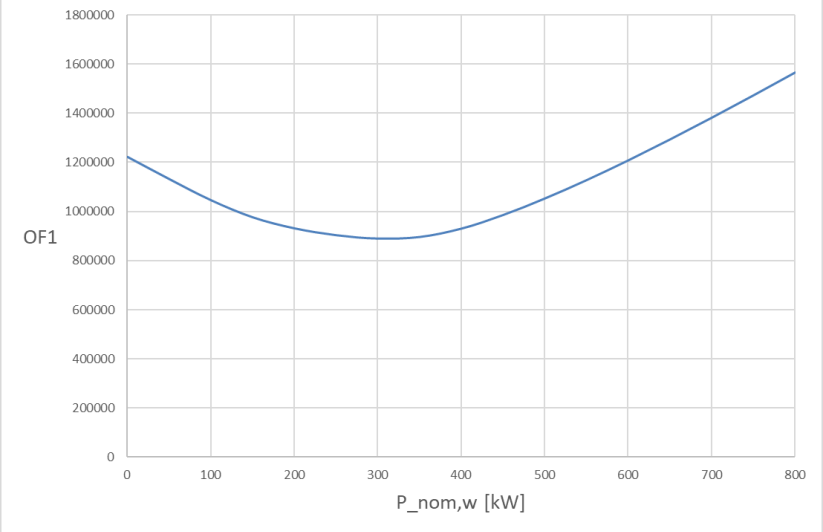

Figure 4.10 Constrained OF1

The optimum wind power size, and consequently the optimum PV size, is where the minimum of the curve of Figure 4.10 is. It is important to notice in this last figure that the curve is smooth despite the absolute value operator present in the definition of the OF1, i.e. there are not sudden variations of its gradient. This is an important condition that has to be verified in order to guaranty the correct convergence of a solution algorithm. Moreover, it is important to highlight that both the surface and curve represented do not show any local minimum that can bring the solution to a result that is not the real optimum.
Similarly to what was done for the OF1, the following figure represents the behavior of the OF2.

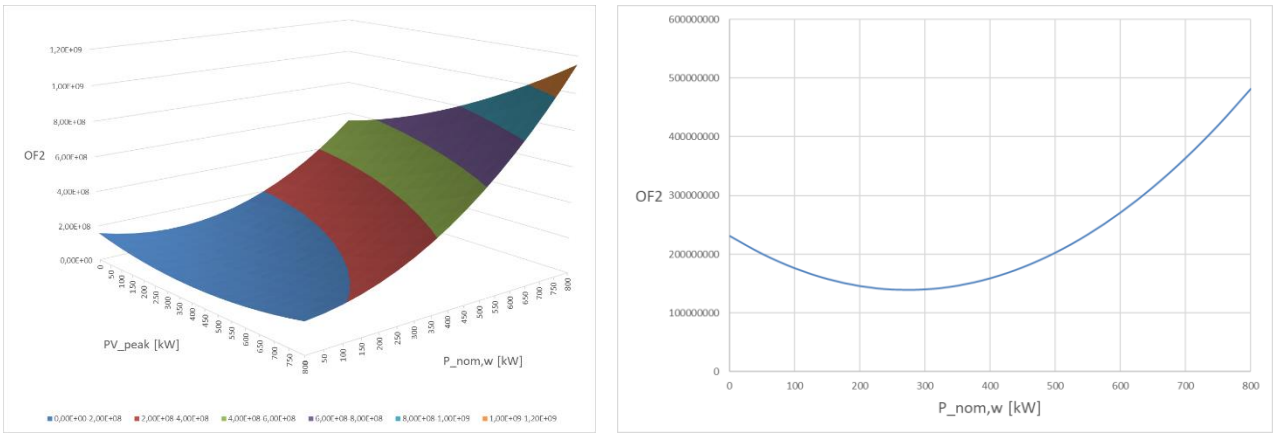

Figure 4.11 Unconstrained OF2 (left) and constrained OF2 (right)

The OF1 and the OF2 are defined in a very similar way. Indeed, the values of the two objective functions are different, but the shapes are very similar. Having very similar behaviors, also the results of the minimization problem of the two objective functions are very similar.
Instead, the behavior of the OF3 is represented in Figure 4.12:

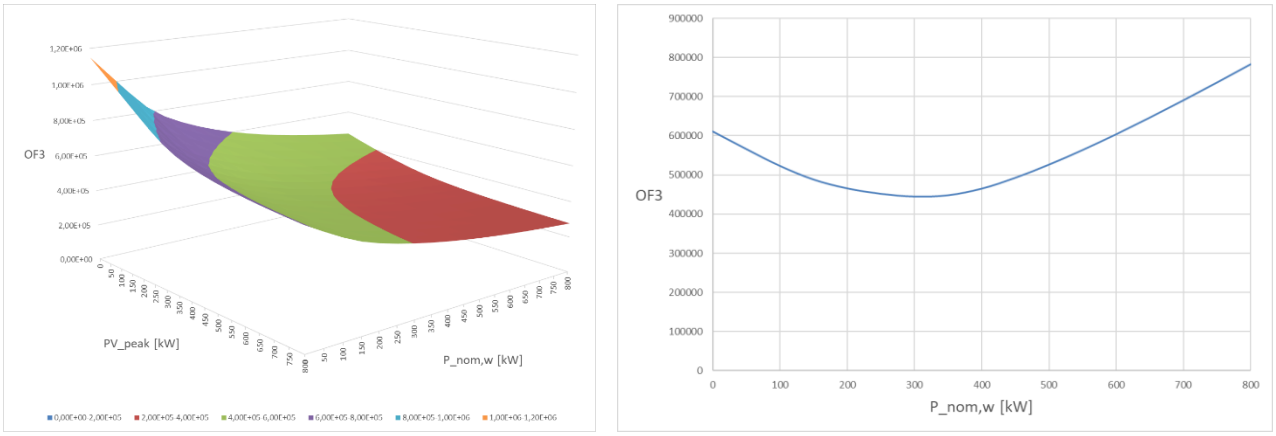

Figure 4.12 Unconstrained OF3 (left) and constrained OF3 (right)

The value of the OF3 is the total energy fluxed by the battery during discharge. Indeed, the OF3 aims to minimize the energy required by the battery. Increasing the installed power of PV and wind the overgeneration increases so less energy is required by the battery. If the generation installed power tends to infinity, the battery size tends to zero. That is why in Figure 4.12 (left) the minimum of the OF3 results at the maximum generation: if the OF3 is minimized without imposing the energy balance constraint (Equation 4.13) the solution will diverge.

Defining the energy that is given to the battery in a year E_{ESS}^{in} (sum of the positive energy balance) and the energy taken from the battery in a year E_{ESS}^{out} (sum of the negative energy balance), the energy balance constraint becomes:

$$E_{ESS}^{in} = |E_{ESS}^{out}|$$

Equation 4.20 Energy balance constraint

And it can be stated that:

$$OF1 = |E_{ESS}^{out}| + E_{ESS}^{in}$$
$$OF3 = |E_{ESS}^{out}|$$

Equations 4.21 General relationships between the OF1 and the OF3

Therefore, when the energy balance constraint is imposed:

$$OF1 = 2 * OF3$$

Equation 4.22 Relationship between the OF1 and the OF3 with energy balance constraint

So, although the unconstrained OF1 and the unconstrained OF3 have completely different shapes, when the energy balance constraint is imposed, the solution of the OF1 and the OF3 is exactly the same.

Finally, the OF4 is represented in the following figure.

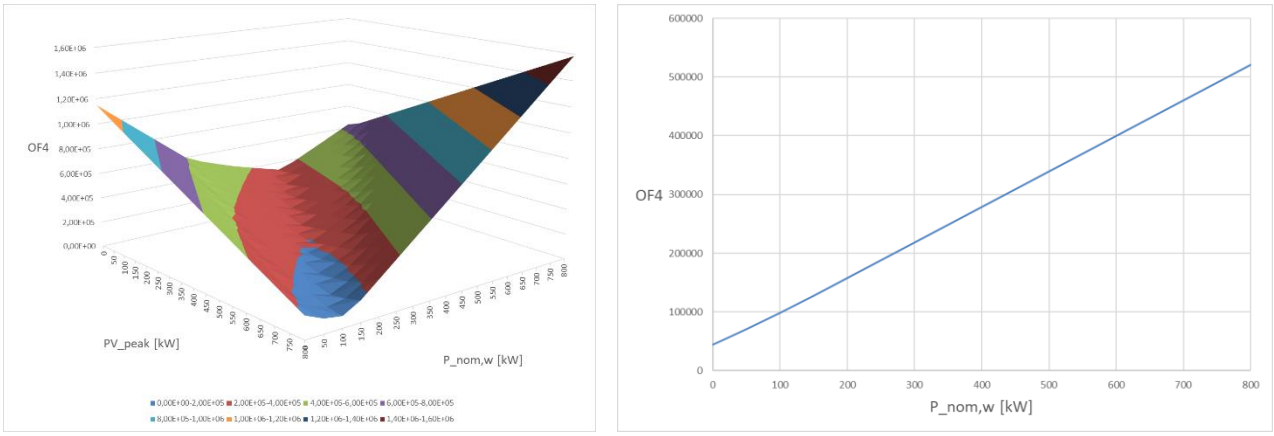

Figure 4.13 Unconstrained OF4 (left) and constrained OF4 (right)

This last objective function presents completely different results. In particular, in Figure 4.13 (right) it can be seen that the OF4 is minimized without wind turbines and so generating energy only from PV.

Once the four objective functions have been studied, it is necessary to compare them in order to choose the most suitable one.

The OF1 and the OF2 presents very similar shapes and very similar results. The OF2 was implemented to avoid eventual issues given by the absolute value operator present in the OF1. Since it was seen that the OF1 is smooth, it can be used freely. Moreover, attempting to minimize the energy fluxed by the battery the OF1 should be more correct, since it is based on absolute values instead of the square of the fluxed energy. For these reasons the OF1 is preferred with respect to OF2.

The OF1 and the OF4 give the same results when the energy balance constraint is imposed. If the unconstrained OF4 is minimized, the solution will diverge, so it is better to use the OF1.

Therefore, the OF2 and the OF3 can be discarded, while a priori nothing can be said about OF1 and OF4. They present very different results, so further analysis is needed to understand which one the most correct objective function is.

4.3.2 Solver

The tool has been implemented in Excel VBA, so the solution of the optimum mix of PV and wind and the minimization of the objective function have to deal with the Excel Solver add-in. In this solver there are three methods or algorithms to choose from [36]:

- GRG Nonlinear
- Evolutionary
- Simplex LP

The GRG Nonlinear method is based on gradient methods. Indeed, GRG means Generalized Reduced Gradient.

This solver method looks at the gradient or slope of the objective function as the input values (or decision variables) change. It determines that it has reached an optimum solution when the partial derivatives equal zero. In order to deal with the gradient, it is necessary that the function is smooth, since any discontinuities in its derivative will cause problems to this algorithm.

The Evolutionary algorithm is more robust than GRG Nonlinear because it is more likely to find a globally optimum solution, indeed it is useful to solve non-smooth problems. However, this solver method is also very slow. The solver starts with a random "population" of sets of input values. These sets of input values are plugged into the model and the results are evaluated respect to the target value. The set of input values that results in a solution that is closer to the target value is selected to create a second population of "offspring". The offspring are a "mutation" of that best set of input values from the first population. The second population is then evaluated, and a winner is chosen to create another population until there is very little change in the objective function from one population to the next.

The Simplex LP method has a limited application because it can be used with problems containing linear functions only. However, it is very robust, because if the problem that is being solved is linear it is sure that the solution obtained by the Simplex LP method is always a globally optimum solution.

Even though the four objective functions are composed by linear elements, according to the Simplex LP solver, the linearity constraint is not satisfied and it is not able to find the solution.

As it was stated in the previous paragraph, and in particular it can be seen in Figure 4.10, the objective functions are smooth despite the presence of the absolute value operator (OF1) and the presence of the if operator (OF3). Therefore, the Evolutionary solver is not the right choice.

The GRG Nonlinear solver may have an issue. If a local minimum is present, the solution that can be obtained with this algorithm is highly dependent on the initial conditions and may not be the global optimum solution. As can be seen in Figure 4.14, the gradient likely brings the solution to the closest local minimum.

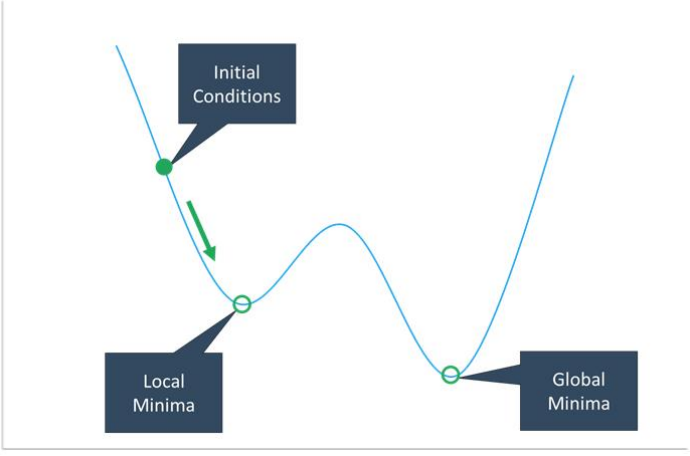

Figure 4.14 GRG Nonlinear solver finds a local minimum

In the previous paragraph, and in particular in Figure 4.10, it is shown that there is no evidence of the presence of local minima in the four analyzed objective functions.
Since it is clear that all the objective functions are smooth and without local minima, it is possible to apply the GRG Nonlinear solver to minimize an objective function, in particular OF1 and OF4, to study which one is the best.

4.3.3 Minimum battery degradation

The first step to study which objective function gives a result that is the closest to the real optimal configuration is the study of the battery degradation.
Once the solver has been chosen, it is possible to solve the optimization problem with the OF1 and the OF4 (the OF2 and the OF3 have been discarded in 4.3.1). The solution of the optimization problem is represented by the power size of the PV panels (PV_{peak}) and the wind turbines ($P_{nom,w}$). In particular it is important to focus on their ratio, since the tool's procedure is based on it.

$$\left(\frac{PV}{wind}\right)_{ratio} = \frac{PV_{peak}}{P_{nom,w}}$$

Equation 4.23 Power generation ratio

For sake of exemplification, using the data from the case study detailed in Chapter 5 and applying the power curve of the wind turbine "EWT 250", the optimization problem results:

	$P_{nom,w}$ [kW]	PV_{peak} [kW]	$\left(\frac{PV}{wind}\right)_{ratio}$
OF1	312	346	1,1
OF4	0	855	#DIV/0!

Table 4.1 Results of the optimization problem solved with the OF1 and the OF4

The validation method proposed to study the battery degradation with respect to the installed power of PV and wind is here explained:

- Generation of an analysis space composed by different sizes of $P_{nom,w}$ and PV_{peak} in order to have different combinations of power generation ratios $\left(\frac{PV}{wind}\right)_{ratio}$ and total nominal installed power ($P_{nom,w} + PV_{peak}$).
- Stress the advanced battery model imposing the replacement of the battery when the SoH reaches 99,9%.

- Calculate the number of battery replacements in the 20 years simulation as a function of the generation nominal power to visualize the battery degradation.

For sake of exemplification, adopting the lithium-ion battery model for a 4000-kWh battery, the degradation results are depicted in Figure 4.15.

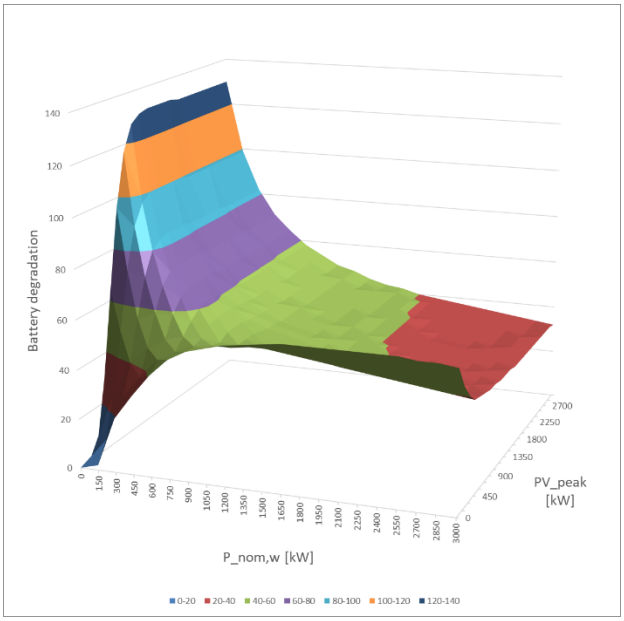

Figure 4.15 Battery degradation as a function of PV and wind nominal power

In Figure 4.15 it is evident that the result of the OF4 (only PV) is far from being the configuration with the smallest battery degradation.

Where both $P_{nom,w}$ and PV_{peak} are close to zero the degradation is very low because the generation is not enough and so the battery is not very used: these configurations are not acceptable because they have very high LLP.

The configuration with the lowest degradation and with an acceptable value of LLP can be found in the red area on the left of Figure 4.15. This area represents the configurations for which the value of $\left(\frac{PV}{wind}\right)_{ratio}$ is not very far from 1,1 given by the OF1.

Therefore, between the two objective functions, the OF1 seems to be the one that allows to reduce the battery degradation.

In a real case, where the battery is replaced when the SoH reaches 80% or when it is used for the maximum number of working hours, very often the limiting parameter is the number of working hours. So, the number of replacements and the relative costs are very similar changing the generation mix. This means that the analysis reported in this paragraph is important to study which configuration reduces the degradation of the battery, but it is not enough to decide which objective function to implement in the tool.

4.3.4 Minimum battery sizing

Another parameter that can be studied in order to compare the results of the OF1 and the OF4 is the battery size. Differently from the battery degradation, the battery size has a clear relationship with the costs of the micro-grid.

In order to validate one of the two objective functions, it is possible to proceed in the following way:

- Set a value for the total power $P_{nom,w} + PV_{peak}$.
- Generate a space of analysis varying the $\left(\frac{PV}{wind}\right)_{ratio}$ and the size of the battery.
- For each $\left(\frac{PV}{wind}\right)_{ratio}$ see which is the minimum battery size that guarantees the LLP constraint.

In this way it is possible to see which $\left(\frac{PV}{wind}\right)_{ratio}$ allows to minimize the size of the battery. This approach is good to validate the tool procedure, since it takes the $\left(\frac{PV}{wind}\right)_{ratio}$ form the optimization solution, and not the power values.

Using the data from the case study, studying the case with a total power equal to 1500 kW and applying the power curve of the wind turbine "EWT 250", the battery minimization algorithm results are depicted in Table 4.2.

		PV/wind																				
		0	0,1	0,2	0,3	0,4	0,5	0,6	0,7	0,8	0,9	1	1,11	1,25	1,43	1,67	2	2,5	3,33	5	10	1000
ESS [kWh]	1105											5,23%	5,20%	5,21%	5,29%							
	1133									5,20%	5,04%	4,95%	4,91%	4,91%	4,96%	5,09%	5,33%					
	1162									4,96%	4,79%	4,69%	4,63%	4,62%	4,65%	4,76%	4,97%	5,33%				
	1190								5,02%	4,74%	4,56%	4,44%	4,37%	4,34%	4,36%	4,44%	4,62%	4,94%				
	1218								4,81%	4,52%	4,33%	4,20%	4,12%	4,07%	4,07%	4,14%	4,29%	4,58%	5,10%			
	1247							5,06%	4,62%	4,32%	4,11%	3,98%	3,88%	3,82%	3,80%	3,85%	3,97%	4,22%	4,70%			
	1275							4,88%	4,43%	4,12%	3,91%	3,76%	3,66%	3,58%	3,55%	3,57%	3,67%	3,89%	4,31%	5,16%		
	1303							4,72%	4,26%	3,94%	3,71%	3,56%	3,44%	3,36%	3,31%	3,31%	3,38%	3,57%	3,95%	4,72%		
	1332							4,56%	4,09%	3,76%	3,52%	3,36%	3,24%	3,14%	3,08%	3,07%	3,12%	3,27%	3,60%	4,30%		
	1360						5,08%	4,41%	3,93%	3,59%	3,35%	3,18%	3,05%	2,94%	2,87%	2,84%	2,86%	2,99%	3,27%	3,90%	5,41%	
	1388						4,94%	4,27%	3,78%	3,43%	3,18%	3,01%	2,87%	2,75%	2,67%	2,62%	2,63%	2,72%	2,97%	3,52%	4,90%	
	1417					5,76%	4,81%	4,13%	3,64%	3,29%	3,03%	2,84%	2,70%	2,58%	2,48%	2,42%	2,41%	2,48%	2,68%	3,17%	4,42%	9,65%
	1700					4,74%	3,80%	3,13%	2,64%	2,28%	2,00%	1,79%	1,62%	1,46%	1,31%	1,19%	1,08%	1,01%	0,98%	1,03%	1,33%	3,24%
	1983				5,28%	4,05%	3,18%	2,55%	2,10%	1,77%	1,52%	1,33%	1,16%	1,02%	0,88%	0,77%	0,66%	0,58%	0,53%	0,51%	0,58%	1,09%
	2266				4,71%	3,55%	2,73%	2,16%	1,75%	1,45%	1,22%	1,05%	0,91%	0,78%	0,66%	0,56%	0,47%	0,40%	0,35%	0,33%	0,35%	0,65%
	2550				4,24%	3,15%	2,39%	1,87%	1,49%	1,22%	1,01%	0,86%	0,73%	0,62%	0,51%	0,43%	0,35%	0,29%	0,24%	0,21%	0,21%	0,40%
	2833			5,33%	3,85%	2,82%	2,12%	1,64%	1,29%	1,04%	0,86%	0,72%	0,61%	0,50%	0,41%	0,33%	0,26%	0,20%	0,16%	0,14%	0,13%	0,24%
	4250		5,65%	3,94%	2,76%	1,95%	1,42%	1,06%	0,81%	0,63%	0,50%	0,40%	0,32%	0,24%	0,17%	0,12%	0,08%	0,05%	0,04%	0,02%	0,02%	0,01%
	5666		4,66%	3,22%	2,21%	1,53%	1,10%	0,82%	0,62%	0,47%	0,36%	0,28%	0,21%	0,15%	0,10%	0,06%	0,03%	0,02%	0,01%	0,01%	0,00%	0,00%
	7083		4,04%	2,79%	1,89%	1,31%	0,94%	0,69%	0,51%	0,38%	0,28%	0,21%	0,15%	0,10%	0,06%	0,03%	0,01%	0,00%	0,00%	0,00%	0,00%	0,00%
	8499	5,32%	3,67%	2,52%	1,68%	1,15%	0,81%	0,58%	0,42%	0,30%	0,22%	0,15%	0,10%	0,06%	0,03%	0,01%	0,00%	0,00%	0,00%	0,00%	0,00%	0,00%

Table 4.2 Battery size minimization study: values of LLP

In the table, the rows represent the battery sizes (ESS) while the columns are the values of $\left(\frac{PV}{wind}\right)_{ratio}$ form zero (only generation from wind turbines) to 1000 (almost only PV). The red cells represent the configurations for which the LLP is higher the 5% and they allow to understand which is the minimum battery size for each $\left(\frac{PV}{wind}\right)_{ratio}$.

Compering Table 4.2 with Table 4.1 it is evident that the OF1 does find a mix of PV and wind generation that allows to minimize the size of the battery, while the OF4 is far from the real optimum.

Varying the total power $P_{nom,w} + PV_{peak}$, the $\left(\frac{PV}{wind}\right)_{ratio}$ that guarantees the minimum battery size may change a bit, but is anyway clear that the objective function that allows to minimize the battery size, and so allows the technical optimization, is the OF1.

Therefore, the OF1 was chosen to be implemented in the tool in order to optimize the generation mix from a technical point of view. Until now, no considerations have been done about the optimal mix from economic point of view, so the result of the OF1 has to be modified in order to satisfy the cost optimization.

4.3.5 Economic optimum

Once it is clear that the OF1 is the right choice to optimize the generation mix from the technical point of view, it is important to solve also the economic optimization problem.

It was chosen to use the battery size as the fundamental parameter to optimize the generation mix because the battery is supposed to be a very expensive component of the off-grid systems. But minimize the battery is usually not enough to minimize the whole micro-grid costs.

Moreover, the cost per kW of nominal power for the PV is usually lower than the one for the wind turbines. So, it is expected that the economic optimum presents a $\left(\frac{PV}{wind}\right)_{ratio}$ higher than the one given by the technical optimum (OF1).

This can be verified applying the cost for the wind turbines given by Figure 3.7 and setting 1200 €/kW for the cost of the PV panels and 200 €/kWh for the battery.

In Table 4.2 the green cell represents the configuration with the lowest LCoE. Indeed, in this case the PV share is higher than the case in which the battery is minimized. The costs can be reduced increasing the installed PV power reducing the wind turbine power, even though the battery size has to be increased a bit. This trend can be verified in the following table, in which are reported the values of the LCoE of each configuration studied in 4.3.4.

		PV/wind																				
		0	0,1	0,2	0,3	0,4	0,5	0,6	0,7	0,8	0,9	1	1,11	1,25	1,43	1,67	2	2,5	3,33	5	10	1000
ESS [kWh]	1105											0,269	0,268	0,267	0,266							
	1133									0,272	0,270	0,269	0,268	0,267	0,266	0,265	0,264					
	1162									0,272	0,271	0,269	0,268	0,267	0,266	0,265	0,265	0,264				
	1190								0,274	0,272	0,271	0,270	0,269	0,268	0,267	0,266	0,265	0,264				
	1218								0,275	0,273	0,272	0,270	0,269	0,268	0,267	0,266	0,265	0,264	0,263			
	1247							0,278	0,275	0,274	0,272	0,271	0,270	0,269	0,267	0,266	0,265	0,264	0,264			
	1275							0,278	0,276	0,274	0,273	0,271	0,270	0,269	0,268	0,267	0,266	0,264	0,264	0,264		
	1303							0,279	0,277	0,275	0,273	0,272	0,271	0,270	0,268	0,267	0,266	0,265	0,264	0,263		
	1332							0,280	0,277	0,275	0,274	0,273	0,271	0,270	0,269	0,268	0,266	0,265	0,264	0,263		
	1360						0,284	0,280	0,278	0,276	0,274	0,273	0,272	0,271	0,269	0,268	0,267	0,265	0,264	0,264	0,265	
	1388						0,284	0,281	0,279	0,277	0,275	0,274	0,273	0,271	0,270	0,269	0,267	0,266	0,265	0,264	0,264	
	1417					0,290	0,285	0,282	0,279	0,277	0,276	0,274	0,273	0,272	0,271	0,269	0,268	0,266	0,265	0,264	0,264	0,275
	1700					0,298	0,294	0,290	0,288	0,286	0,284	0,283	0,282	0,280	0,279	0,277	0,276	0,274	0,272	0,270	0,268	0,269
	1983				0,313	0,307	0,303	0,300	0,297	0,296	0,294	0,293	0,291	0,290	0,289	0,287	0,286	0,284	0,282	0,280	0,277	0,275
	2266				0,322	0,317	0,313	0,310	0,308	0,306	0,304	0,303	0,302	0,300	0,299	0,298	0,296	0,294	0,292	0,290	0,288	0,285
	2550				0,332	0,327	0,323	0,320	0,318	0,316	0,315	0,313	0,312	0,311	0,310	0,308	0,307	0,305	0,303	0,301	0,298	0,296
	2833			0,350	0,342	0,337	0,333	0,330	0,328	0,326	0,325	0,324	0,323	0,321	0,320	0,319	0,317	0,316	0,314	0,312	0,309	0,306
	4250		0,411	0,401	0,394	0,389	0,386	0,383	0,381	0,380	0,378	0,377	0,376	0,375	0,374	0,372	0,371	0,369	0,368	0,365	0,363	0,360
	5666		0,464	0,454	0,447	0,443	0,439	0,437	0,435	0,434	0,432	0,431	0,430	0,429	0,428	0,426	0,425	0,423	0,422	0,419	0,417	0,414
	7083		0,517	0,508	0,501	0,496	0,493	0,491	0,489	0,487	0,486	0,485	0,484	0,483	0,482	0,480	0,479	0,477	0,476	0,474	0,471	0,468
	8499	0,585	0,571	0,562	0,555	0,550	0,547	0,545	0,543	0,541	0,540	0,539	0,538	0,537	0,536	0,534	0,533	0,532	0,530	0,528	0,525	0,522

Table 4.3 Battery size minimization study: values of LCoE

Indeed, considering the same battery size, the cost decreases if the $\left(\frac{PV}{wind}\right)_{ratio}$ increases. While increasing the battery size, the cost does not increase very much. So, the economic optimum is not where the minimum battery size is.

4.4 Intuitive sizing and space of analysis

Once the generation mix optimization problem has been faced, it is necessary to match the objective function optimization algorithm with the turbine selection discussed in Chapter 3.

When the OF1 is minimized, the solver calculates the optimal values of the nominal power for the PV and the wind turbines (PV_{peak} and $P_{nom,w}$). These two values allow to generate enough energy to satisfy the load, without considering the actual state of charge of the battery, which may not be able to store or give the required energy. Therefore, the generation size given by the solver may not be sufficient to get an acceptable LLP. For this reason the tool does not use the power values PV_{peak} and $P_{nom,w}$, but the unique solver output considered is their ratio $\left(\frac{PV}{wind}\right)_{ratio}$ that is used to calculate the intuitive sizes of the two sources.

Similarly to what was done for the *wind micro-grid* module, the tool calculates the intuitive sizes of the energy generation components which will be increased until some configurations that fulfill the constraints are found.

The starting point is again the energy balance in the whole simulated period. When the tool was optimizing the objective function, it dealt with non-dimensional power generation profiles and unconstrained nominal power of the wind turbines. Instead, now that the intuitive sizes have to be found, the energy generated is calculated from the dimensional power profiles and the nominal power of the wind turbines is constrained to be given by an integer number of turbines, adopting an approach similar to what was done in the *wind micro-grid* module. Reminding that the profiles are based on 1-hour steps:

$$E_{tot} = \sum_{t=0}^{T} \left(N_{turb} * P_{turb}(t) + PV_{peak} * P_{PV,1kW}(t) \right)$$

Equation 4.24 Energy generated in all the analyzed period

In the *PV+wind micro-grid* module there have to be found the intuitive sizes of both PV and wind turbines. Therefore, the result of the objective function optimization can be used to relate the two energy sources and transform the two-variable Equation 4.24, in an equation with only one unknown:

$$E_{tot} = \sum_{t=0}^{T} \left(N_{turb} * P_{turb}(t) + \left(\frac{PV}{wind}\right)_{ratio} * N_{turb} * P_{nom,turb} * P_{PV,1kW}(t) \right)$$

Equation 4.25 Energy generated in all the analyzed period as a function of the numbers of the turbines

The energy generated has to be higher or equal to the one necessary to satisfy the load.

$$\sum_{t=0}^{T} load(t) \leq E_{tot} * \eta_{inv}$$

Equation 4.26 Energy balance

So, the minimum number of turbines that is able to satisfy the load can be found applying the upper integer number to this last inequation. This is also the intuitive number of turbines from which the intuitive PV size is calculated.

$$N_{turb} = ceiling \left(\frac{\sum_{t=0}^{T} load(t)}{\sum_{t=0}^{T} \left(P_{turb}(t) + \left(\frac{PV}{wind}\right)_{ratio} * P_{nom,turb} * P_{PV,1kW}(t) \right) * \eta_{inv}} \right)$$

$$PV_{peak} = \left(\frac{PV}{wind}\right)_{ratio} * N_{turb} * P_{nom,turb}$$

Equations 4.27 Intuitive number of turbines and intuitive PV size

The intuitive sizing can be calculated once the objective function is minimized and the optimum generation mix is calculated. So, in principle, the optimum generation mix and the intuitive sizing has to be calculated for each turbine in the database.

Implementing the *PV+wind micro-grid* module is particularly important to pay attention on the time needed by the algorithm and to reduce the turbines that have to be taken into account during the calculations. This is because the optimization of the mix by means of the GRG Nonlinear solver is a very time-consuming operation.

So, a way to discard a type of turbine in the database before the objective function minimization has to be found. It can be said that if a turbine is too big with respect to the load that has to satisfy when the PV is not present, it is for sure too big when the PV is present. Setting $\left(\frac{PV}{wind}\right)_{ratio}$ to zero in the intuitive number of turbines of Equations 4.27, it becomes:

$$N_{turb,0} = ceiling\left(\frac{\sum_{t=0}^{T} load(t)}{\sum_{t=0}^{T} P_{turb}(t) * \eta_{inv}}\right)$$

Equation 4.28 Intuitive number of turbines without PV

Reminding the considerations about the duration curves of the overgeneration that were made in Chapter 3 and that can be seen in Figure 3.5, the turbines that not fulfill the following constraint have to be discarded before the objective function optimization:

$$\frac{\sum_{t=0}^{T} load(t)}{\sum_{t=0}^{T} P_{turb}(t) * \eta_{inv}} \leq 0{,}5$$

Equation 4.29 Constraint without PV

This means that the turbines that generate more than the double of the energy needed by the load without considering the one generated by the PV are too big.

The remaining turbines can be used to solve the generation mix optimization and once the $\left(\frac{PV}{wind}\right)_{ratio}$ is known, it is possible to eliminate the turbines that are too big (like in Equation 4.29) or too small (for reasons based on costs, land occupation and wind speed slowing down, the number of turbines is limited to 10).

Therefore, a turbine is good to be used in the simulation if:

$$0{,}5 < \frac{\sum_{t=0}^{T} load(t)}{\sum_{t=0}^{T}\left(P_{turb}(t) + \left(\frac{PV}{wind}\right)_{ratio} * P_{nom,turb} * P_{PV,1kW}(t)\right) * \eta_{inv}} \leq 10$$

Equation 4.30 Constraint for wind turbine selection

The central term in Equation 4.30 decreases passing from the case without PV to the optimal case since the $\left(\frac{PV}{wind}\right)_{ratio}$ increases. For this reason, before the mix optimization is not possible to do any consideration about the small turbines. Adopting the opposite strategy, that is starting from a configuration with only generation from PV and make the $\left(\frac{PV}{wind}\right)_{ratio}$ decrease would not make any sense since in this way all the turbines would be discarded.

Differently from the *wind micro-grid* module, there is no need to calculate the number of consecutive hours in which the turbines are not working. If there is the generation from the PV, it can be considered that at least part of the generation is always present, so the consecutive working hours are not used to eliminate turbines from the database.

In order to limit the calculation time, it is necessary to reduce the number of cases calculated, that means to reduce the types of turbines in the database that have to be taken into account during the analysis. This can

be done with the creation of a ranking. The parameter chosen to generate the ranking of the turbines is the energy/cost ratio.

$$\left(\frac{E}{c}\right)_{ratio}\left[\frac{kWh}{€ * y}\right] = \frac{\sum_{t=0}^{8759} P_{turb}(t)}{c_{turb}}$$

Equation 4.31 Energy/cost ratio

In this way the turbines in the database can be ordered according to a techno-economic parameter. The turbines with the highest energy/cost ratio, with the same installed power, can generate more energy and present lower investment cost. Therefore, the generation of a turbine ranking is the first step: the objective function optimization can be made with the best turbines in the ranking.

The tool deals with different turbines, i.e. with different power curves, leading to very different energy generation performances (h_{eq}). Instead, it is not taken into account a database of PV panels assuming that the performances of different PV panels (if the same technology is used) are very similar. That is why all this work is carefully based on the study of the different turbines while the size of the PV is just a consequence without taking into account different PV curves.

Moreover, the number of the turbines is constrained to be integer, while the PV_{peak} is free to take any value. In a real case, a PV plant nominal power is constrained to be a multiple of the size of a panel, which is a quantity that is quite low with respect to the total power of a PV plant, so in the tool the discretization of the PV size can be neglected.

Once the turbine ranking is defined and the intuitive sizes for the PV and the wind turbines are calculated, it is possible to generate the space of analysis.

The starting point for the two generation sources is the intuitive sizes (Equations 4.27) while the battery is starting from its maximum accepted value:

$$ESS_{max} = N_{days} * \frac{mean\big(load(t)\big) * 24}{\eta_{inv} * (1 - SoC_{min})}$$

Equation 4.32 Maximum battery size

From this configuration, the battery is reduced with a dynamic algorithm based on the results of the previous simulated configuration.

- $if\ LLP < limit_{down} * LLP_{max}$ $\quad ESS_{new} = ESS_{old} * limit_{down}$
- $if\ limit_{down} * LLP_{max} \leq LLP \leq limit_{up} * LLP_{max}$ $\quad ESS_{new} = ESS_{old} * LLP/LLP_{max}$
- $if\ limit_{up} * LLP_{max} < LLP < LLP_{max}$ $\quad ESS_{new} = ESS_{old} * limit_{up}$

Equations 4.33 Limited dynamic algorithm for the battery sizing

This algorithm generates configurations with smaller batteries fixing the number of turbines and the PV size until the LLP becomes higher than the maximum value that is accepted (5%). Once the minimum battery size for a specific generation size is reached, the power generation sizes is increased and the battery is set to the last value that was able to give $LLP < LLP_{max}$. From here, the algorithm of Equations 4.33 is started again.
The algorithm just described is the same explained in 0 for the *wind micro-grid* module. The difference is in the way in which the generation size is increased.
Since the number of turbines has to be integer, it is increased by 1. The generation mix is constrained to have the $\left(\frac{PV}{wind}\right)_{ratio}$ calculated with the objective function. Therefore, once the number of turbines is increased, the PV size has to be calculated as before.

$$PV_{peak} = \left(\frac{PV}{wind}\right)_{ratio} * N_{turb} * P_{nom,turb}$$

Equation 4.34 Relationship between the PV and the number of wind turbines

The number of turbines (and the PV size as a consequence) is increased until the four columns of the space of analysis of a type of turbine are completed or until the number of turbines reaches 10 (maximum allowed quantity).
In order to show how a space of analysis is constituted, in the following table it is reported an example of space of analysis of the turbine EWT 250 applying the data of the case study (Chapter 5). The four columns represent the four generation sizes considered, indeed on the top of each column is reported the number of turbines and the relative PV sizes. The rows represent the different battery sizes considered fixing the generation size. For sake of exemplification, in the table are reported the values of LLP for each case simulated.

PV [kW]		668	1002	1336	1670
#turbines		2	3	4	5
ESS [kWh]	574				5,15%
	591				4,94%
	672			5,18%	4,05%
	764		5,68%	4,09%	3,14%
	859		4,44%	3,08%	
	976	5,68%	3,05%		
	1110	3,91%	1,80%		
	1261	2,37%			
	1433	1,25%			
	1628	0,68%			
	1850	0,43%			
	2102	0,27%			
	2389	0,12%			
	2715	0,01%			
	3085	0,00%			
	3506	0,00%			
	3984	0,00%			
	4527	0,00%			
	5145	0,00%			
	5846	0,00%			
	6643	0,00%			
	7549	0,00%			
	8579	0,00%			

Table 4.4 Example of space of analysis of a type of turbine in the first optimization. Values of LLP.

It is possible to notice that increasing the generation size, the optimal battery decreases. The red cells represent the configurations that stopped the battery reduction algorithm since LLP>$LLP_{max.}$

This space of analysis has to be repeated for the first 10 types of turbines in the ranking that fulfill the constraints about the turbines too big or too small (Equation 4.30). Among all those configurations the tool has to find the one with the lowest LCoE with an LLP that is lower than the maximum.

This configuration is the result of what will be here called "first optimization".

The first optimization is based on technical parameters because its generation mix is constrained by the $\left(\frac{PV}{wind}\right)_{ratio}$. This ratio is given by the optimization of OF1 which aims to minimize the battery size. The first optimization finds the best configuration in which the battery size is minimized.

It was already explained that minimize the battery size is not a sufficient condition to minimize the costs, so, in order to find the real economic optimum, it is necessary a second optimization.

The result of the first optimization is composed by:

- A type of turbine.
- A number of turbines.
- A PV size.
- A battery size.

The most important aim of the first optimization is the selection of the type of turbine from the database, since the second optimization works only with the turbine selected by the first optimization. Instead, the values of wind, PV and battery are used as starting points (intuitive sizing) for the second optimization.

The aim of the second optimization is to remove the $\left(\frac{PV}{wind}\right)_{ratio}$ constraint and modify the generation mix.

Since the calculations are based on a unique type of turbine it is possible to generate different sub-spaces of analysis, each of them is based on a different number of turbines. The tool considers sub-spaces of analysis in which the numbers of turbines are both increased and decreased with respect to the result of the first optimization. It considers five sub-spaces of analysis based on the number of turbines that varies from -2 to +2 with respect to the result of the first optimization.

In each sub-space of analysis the size of PV is centered on a total power generation equal to the one given by the first optimization. Defining $PV_{peak,0}$ as the central PV size of a space of analysis and the variables with the subscript "subopt" as the solutions of the first optimization, it results:

$$PV_{peak,0} = PV_{peak,subopt} + \left(N_{turb,subopt} - N_{turb}\right) * P_{nom,turb}$$

Equation 4.35 Central PV size

From this, the columns of the space of analysis are generated increasing and decreasing the value of $PV_{peak,0}$ by a fixed percentage.

Applying this procedure, the $\left(\frac{PV}{wind}\right)_{ratio}$ is both increased and decreased. According to the current values of cost of the system's elements is expected that the optimal ratio has to increase with respect to the result of the first optimization, but the tool is implemented to face also different behaviors and different costs that there may be in the future.

The battery (rows of the space of analysis) is sized with the dynamic algorithm of Equations 4.33. But it was chosen to take a maximum value closer to the result of the first optimization: the maximum battery size of the second optimization is the average between the maximum of the first optimization and the result of the first optimization.

$$ESS_{max,1} = \frac{ESS_{max} + ESS_{subopt}}{2}$$

Equation 4.36 Maximum battery size for the second optimization

Applying these rules, the space of analysis for the second optimization results as it is shown in Tables 4.5. They are 5 different tables and in each of them the columns represent different sizes of PV while the rows represent the battery sizes. So, each table is a space of analysis with fixed number of turbines and different tables are necessary to simulate different number of turbines. For sake of exemplifications, in the following tables are reported the values of LLP based on the data of the case study.

# turbines	1						
PV [kW]	856	1014	1172	1331	1489	1647	1805
ESS [kWh]							
1268					5,48%	5,25%	5,08%
1307		6,35%	5,60%	5,18%	4,87%	4,64%	4,47%
1485	5,66%	4,16%	3,34%	2,85%	2,57%		
1688	4,16%	2,53%					
1918	3,32%						
2180	2,83%						
2477	2,45%						
2815	2,13%						
3199	1,87%						
3635	1,68%						
4130	1,53%						
4694	1,42%						
5334	1,33%						

	2						
	606	764	922	1081	1239	1397	1555
1119					5,50%	5,25%	5,09%
1179			5,67%	5,11%	4,74%	4,50%	4,32%
1340		5,06%	3,88%	3,26%	2,90%		
1523		3,74%	2,43%				
1731		2,85%					
1967	5,02%	2,32%					
2027	4,90%	2,23%					
2180	4,65%						
2477	4,25%						
2815	3,89%						
3199	3,57%						
3635	3,29%						
4130	3,06%						
4694	2,86%						
5334	2,69%						

	3						
	356	514	672	831	989	1147	1305
1021						5,27%	5,06%
1052				5,75%	5,21%	4,88%	4,68%
1196			5,43%	4,27%	3,68%	3,34%	
1359			4,21%	2,94%			
1544			3,21%				
1755		5,13%	2,53%				
1809		4,98%	2,40%				
1918		4,72%					
2180		4,22%					
2477		3,81%					
2815		3,45%					
3199		3,13%					
3635		2,84%					
4130		2,58%					
4694		2,36%					
5334	5,49%	2,17%					

	4						
	106	264	422	581	739	897	1055
952						5,36%	5,03%
1016					5,29%	4,69%	4,35%
1047					4,99%	4,37%	
1190				5,12%	3,77%		
1229				4,84%	3,47%		
1397				3,85%			
1587				3,06%			
1804			5,14%	2,47%			
1860			4,99%	2,35%			
1918			4,85%				
2180			4,31%				
2477			3,84%				
2815			3,41%				
3199			3,05%				
3635			2,74%				
4130			2,47%				
4694			2,23%				
5334	9,81%	5,04%	2,03%				

	5						
	0	14	172	331	489	647	805
881							5,43%
971						5,24%	4,53%
1034						4,70%	3,97%
1175					5,23%	3,64%	
1336					4,33%	2,69%	
1518					3,53%		
1725					2,87%		
1960				5,12%	2,37%		
2021				4,98%	2,26%		
2114				4,78%			
2403				4,24%			
2730				3,75%			
3103				3,30%			
3526				2,92%			
4006				2,62%			
4553				2,36%			
5174			5,06%	2,13%			
5334	9,91%	9,43%	4,95%	2,07%			

Tables 4.5 Example of space of analysis for the second optimization

The result of the first optimization was 3 turbines (250 kW each) and 831 kW of PV. Indeed, the space of analysis is centered in the configuration with 3 turbines and 831 kW of PV. Again, the battery size reduction algorithm stops in the red cells where LLP is higher than the maximum value.
Once this new space of analysis is generated, it is possible to look for the configuration with the lowest LCoE that fulfills the constraint about the maximum LLP.
Since there are no more technical constraints that fix a specific power generation mix, the solution is the real techno-economic optimum.
The solution is also the most cost-effective solution in which PV and wind are used as power sources. Since this module has to find the best configuration using any mix between only PV and only wind, the result of the cost the *PV+wind micro-grid* module has to be lower of the ones of the *PV micro-grid* and *wind micro-grid* modules. Otherwise, the result of the *PV+wind micro-grid* module will coincide with one of the other two.

4.5 Algorithm implementation

Finally, the *PV+wind micro-grid* module aims to find the best configuration for a micro-grid that exploits two different renewables resources: PV and wind. It has to find the optimal generation mix of the PV panels and the wind turbines and it has to size all the main components of the grid: it has to find the battery and the PV size and it has to choose how many and which turbines to use.
The module proceeds in two steps.
At first it studies all the turbines in the database and it calculates the ratio between the PV and wind nominal power that guarantees the minimum battery size. For this reason, this first part is a technical optimization. Freezing the ratio between the two sources, a space of analysis is created varying the battery and the generation sizes. The best configuration is chosen looking at cost and reliability of the system. This is the first optimization, in which the best turbine type is selected.
In the second optimization the analysis is based only on the best turbine type just selected. The study is not anymore constrained to fix the ratio between the two energy sources, so the space of analysis is generated varying battery, PV and wind sizes independently. Once the best configuration in terms of cost and reliability is found, it is the real techno-economic optimum.
The algorithm, shown in the flow chart of Figure 4.16, for simplicity can be divided in four parts.

First part: ranking.

- The tool reads the load profile, the wind speed profile and the PV power generation profile.
- For each turbine in the database, the wind power generation profile is calculated interpolating the power curves (Figure 3.4) with the wind speed profile.
- The tool calculates the energy/cost ratio and generate the ranking of the turbines (Equation 4.31).

Second part: objective function. The turbines are considered following the order given by the ranking.

- A turbine is discarded if it is too big when there is no generation from PV (Equation 4.29).
- If it passes the first check, the OF1 is minimized and the $\left(\frac{PV}{wind}\right)_{ratio}$ is calculated.
- Once the generation mix is known, a turbine is discarded if it is too big or too small (Equation 4.30).
- If a turbine is discarded the tool starts again the second part of the algorithm with a new turbine, otherwise it calculates the intuitive sizes (Equations 4.27) and the maximum battery (Equation 4.32) and proceeds with the third part.

Third part: first optimization.

- The space of analysis is created reducing the battery size (Equations 4.33) and increasing the generation nominal power staring from the intuitive sizes.
- To increase the generation the number of turbines is increased and the $\left(\frac{PV}{wind}\right)_{ratio}$ is kept constant.
- The number of turbines is increased until four acceptable generation sizes are found or the number of turbines reaches 10.

The second and the third part of the algorithm are repeated until the space of analysis is composed by 10 acceptable turbines. After that, the best configuration in terms of LLP and LCoE is found.

Fourth part: second optimization. Based only on the turbine type given by the solution of the first optimization.

- The space of analysis is composed by 5 sub-spaces in which the number of turbines is increased or decreased with respect to the result of the first optimization (from -2 to +2).
- In each sub-space, the PV size is centered with Equation 4.35 and then increased and decreased.
- The battery starts with the new maximum size (Equation 4.36) and then is reduced with the dynamic algorithm (Equations 4.33).
- Finally, the result of the module can be found looking at the values of LLP and LCoE of the various configurations.

Both the first and the second optimization look for the configuration in which the cost (LCoE) is minimum and the reliability is acceptable ($LLP<LLP_{max}$). So, both are techno-economic optimizations. But, in order to reduce the degrees of freedom when the best turbine has not been selected yet, the first optimization needs an additional constraint to link the PV and the wind power sizes. For this reason, the first optimization is more a technical optimization. This is the starting point for the second optimization which result is the real optimal configuration.

The algorithm and its four parts are summarized in the following figure with a flow chart, where some equations have been replaced with a symbol:

- $eq1 = \frac{\sum_{t=0}^{T} load(t)}{\sum_{t=0}^{T} P_{turb}(t) * \eta_{inv}}$
- $eq2 = \frac{\sum_{t=0}^{T} load(t)}{\sum_{t=0}^{T} \left(P_{turb}(t) + \left(\frac{PV}{wind}\right)_{ratio} * P_{nom,turb} * P_{PV,1kW}(t) \right) * \eta_{inv}}$
- $eq3 = P_{tot,sobopt} * (1 + z * 0{,}1) - N_{turb} * P_{nom,turb}$ therefore:

  $eq3 = PV_{peak,subopt} + \left(N_{turb,subopt} - N_{turb}\right) * P_{nom,turb} + z * 0.1 * \left(N_{turb,subopt} * P_{nom,turb} + PV_{peak,subopt}\right)$

Where the subscript "subopt" refers to the solution of the first optimization and $P_{tot} = N_{turb} * P_{nom,turb} + PV_{peak}$

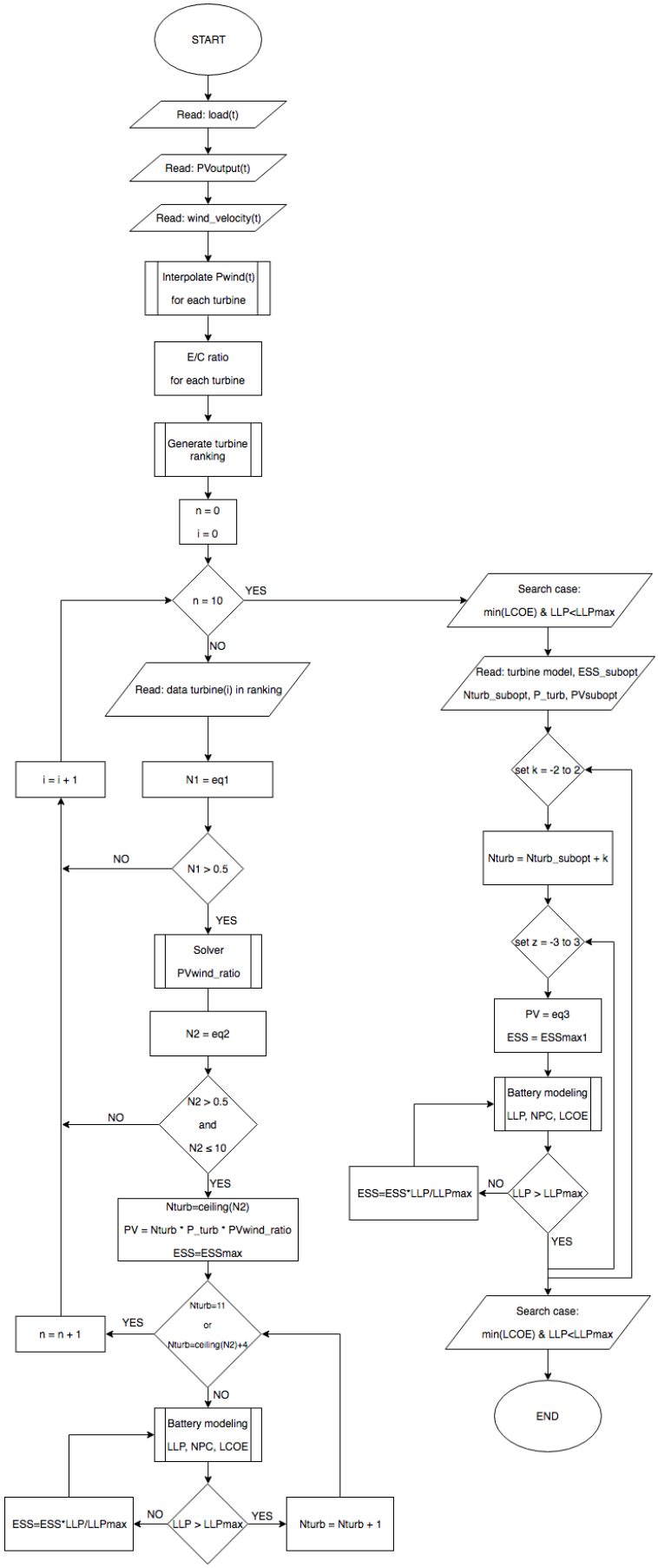

Figure 4.16 Flow chart for the *PV+wind micro-grid* module

Chapter 5

5 Case study

So far, the procedure to study and optimize a micro-grid was presented. It is now interesting to apply this procedure to a real case in order to validate the tool. The data necessary for the simulation are the weather conditions, the load and the components cost.

The target of this tool is a rural village without access to electricity far from the national electric grid. The data about the load of such a village are hardly available. For this reason, it was decided to simulate the load of a hospital in Uganda, instead of a village. Indeed, the author has the access to these data thanks to the collaboration between Politecnico di Milano and some associations such as the St. Mary's Lacor Hospital, the Fondazione Piero e Lucille Corti and the UNESCO Chair in Energy for Sustainable Development. In particular, the data have been measured for a Mater thesis held by Politecnico [37].

5.1 St. Mary's Lacor Hospital

The data chosen for the case study concern Uganda. It is one of the poorest countries in the world. Even though in the last years its income per capita has improved a lot, the 34% of the population still lives on less than $1,90 per day. Uganda occupies the last places in the world rankings in terms of economic and energy development.

The most important sector of the economy is agriculture, employing over 70% of the work force, however it exhibits one of the lowest productivity levels in the world due to the high agriculture employment per hectare of arable land and to the lack of appropriate tools. The industrial sector is improving but is still marginal.

Uganda has plenty of energy sources both renewable (hydropower, solar, wind) and fossil. But only 20% of the population has access to the electricity, which is even lower in rural areas. This poor service is also not efficient: the transmission system presents 19% of energy losses, while the distribution system 4%.

Moreover, the energy consumption per capita is one of the lowest in the world.

St. Mary's Lacor Hospital is the largest private non-profit catholic based institution in Uganda. It is located in Lacor, a small village about six kilometers west of Gulu, the main town in the Northern part of the

country. It was founded in 1959 as a small hospital with only 30 beds, while now it is a complex compound made of: outpatients department, two medicine wards, two Surgery wards, an Intensive Care Unit, six operating theatres, a radiology ward, a maternity ward, a children ward, a laboratory, an isolation unit, a pharmacy, staff quarters, foundation residences (Corti's House, Bruno's House, Red Villa, White Villa, Comboni's House and Guest House) and a university.

For such a complex structure, it is necessary to have a technical department inside it that has so manage the system.

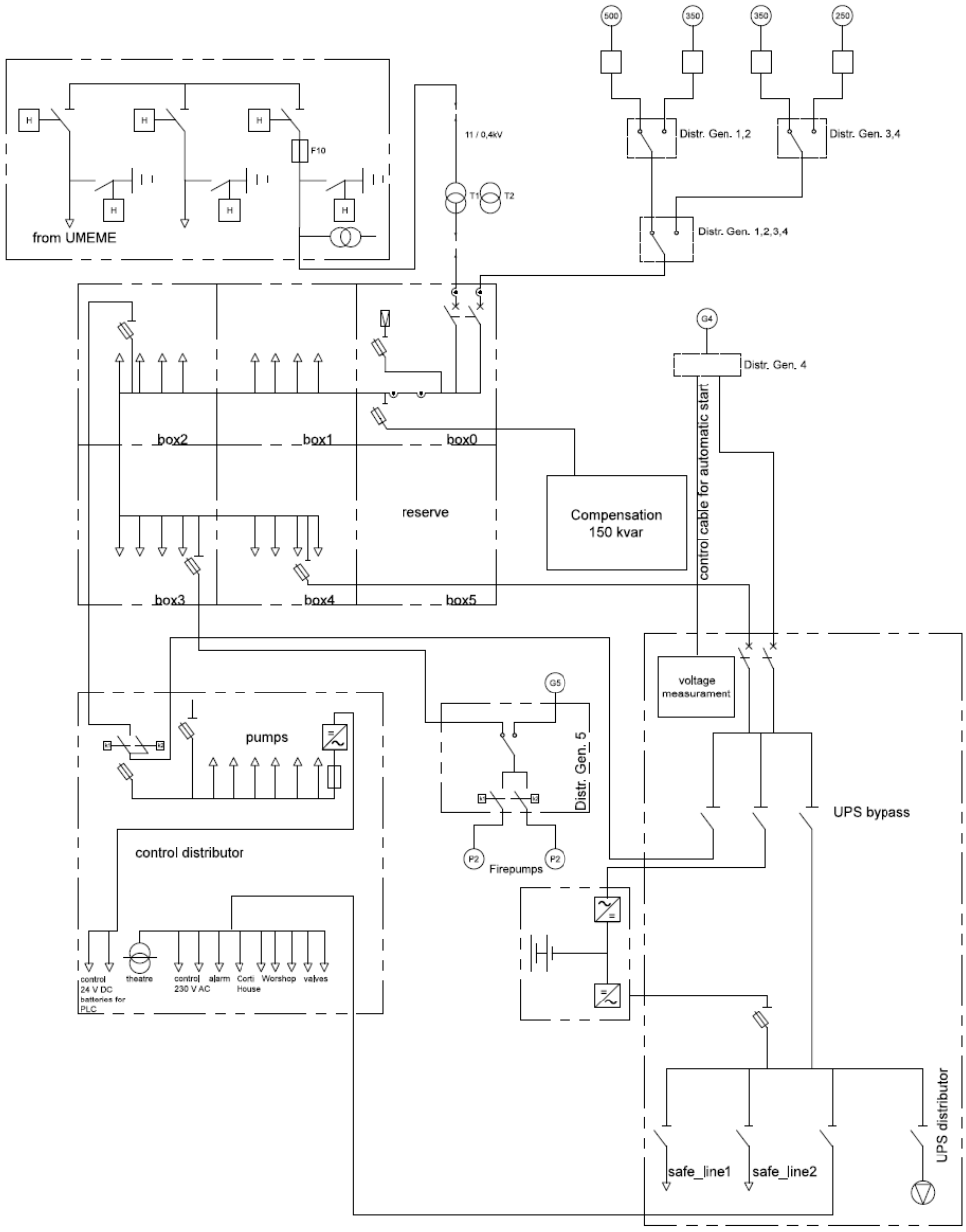

Figure 5.1 Distribution system at St. Mary's Lacor Hospital

The Ugandan national grid is not reliable, therefore to satisfy the electric load, the hospital is equipped with:

- Some diesel generators that are turned on just in case of power outages of the national grid.
- Solar thermal for water heating.
- Photovoltaic power system provided by different donors, for a total installed power of 186 kW_p.
- Battery energy storage system that has to satisfy the load in the case in which the fuel is not available or during the stat-up time of diesel generator.

In Figure 5.1 it is shown the schematic of the distribution system of the hospital, in which can be seen the main switchboard (box 0) where the main busbar, the circuit breakers to choose either to use the national grid or the diesel generator and the main meters are placed.

5.2 Data, simulations and results

The procedure implemented in the tool object of this thesis was applied to study the case of the St. Mary's Lacor Hospital. In particular, the author is not interested in its actual configuration and in the installed energy sources. Instead, it was considered to study the best system configuration to fulfill the hospital load, implementing PV panels, wind turbines and batteries in an off-grid system. Indeed, the author is not proposing a stand-alone micro-grid to be implemented by the hospital, but its load is simply used as an example to show how the presented procedure works. Moreover, the case study was used to validate the optimization algorithm for the *PV+wind micro-grid* module. Indeed, the results of the procedure are compared with further analysis that made possible the validation of the algorithm.

To perform such analysis the procedure needs several inputs: the load profile, the weather data and the components costs.

The authors of [37] monitored the load of the St. Mary's Lacor Hospital and they were able to provide the load profile for a year. Once this profile has been transformed in hourly data, it can be used by the procedure under validation. The load profile is repeated for the 20-year simulated lifespan and the data are summarized in the following table.

Peak load	170 kW
Average daily load	2573 kWh
Day with maximum load (323rd)	2889 kWh
Day with minimum load (321st)	2223 kWh
Yearly load	939 MWh

Table 5.1 Load

For sake of exemplification, it can be calculated the load of the average day:

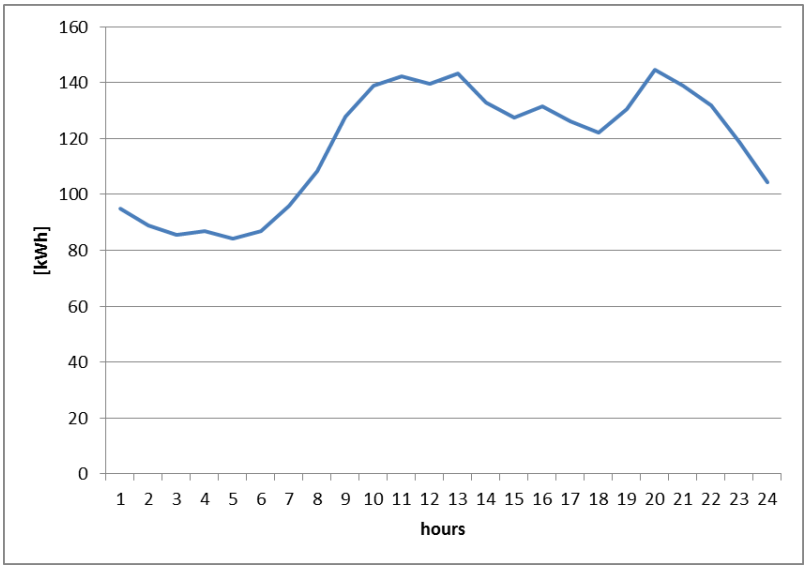

Figure 5.2 Load of the average day

The meteorological data, and in particular the data concerning the generation from the PV panels and the wind speed, have been taken from the online database Renewables.ninja knowing the coordinates of the hospital. In the following figure the interface of the Renewables.ninja website is presented and it can be seen the St. Mary's Lacor Hospital in the map.

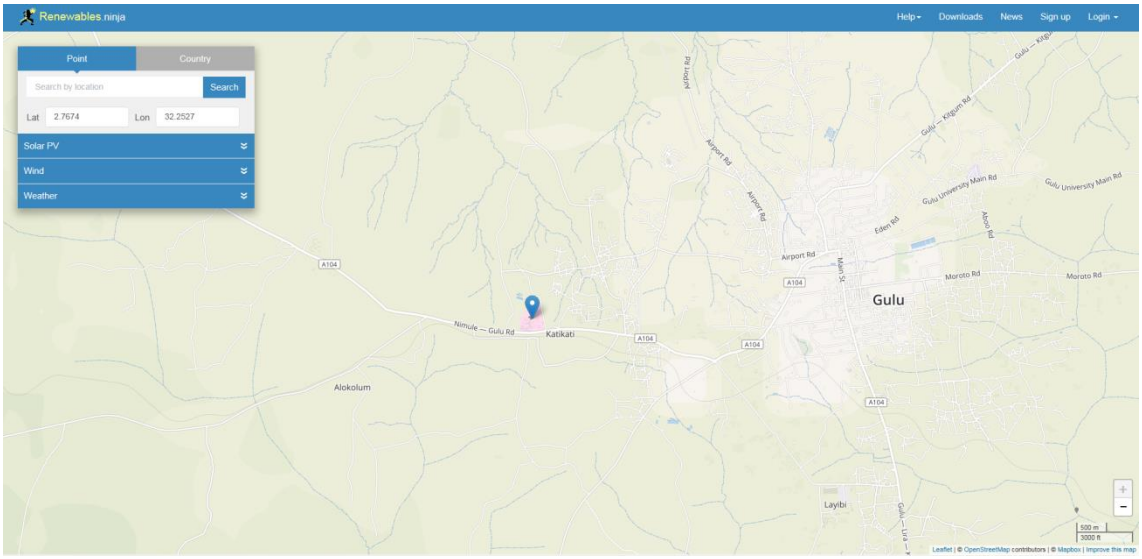

Figure 5.3 Renewables.ninja interface

The meteorological data can be summarized as follows.

Irradiation peak	0,78 kW/kW_p
Average irradiation	0,18 kW/kW_p
Day with maximum generation from PV (270^{th})	5,85 kWh/kW_p
Day with minimum generation from PV (170^{th})	1,76 kWh/kW_p
Annual generation from PV	1617 kWh/kW_p
Minimum wind speed	0 m/s
Average wind speed	4 m/s
Maximum wind speed	15 m/s

Table 5.2 Meteorological data

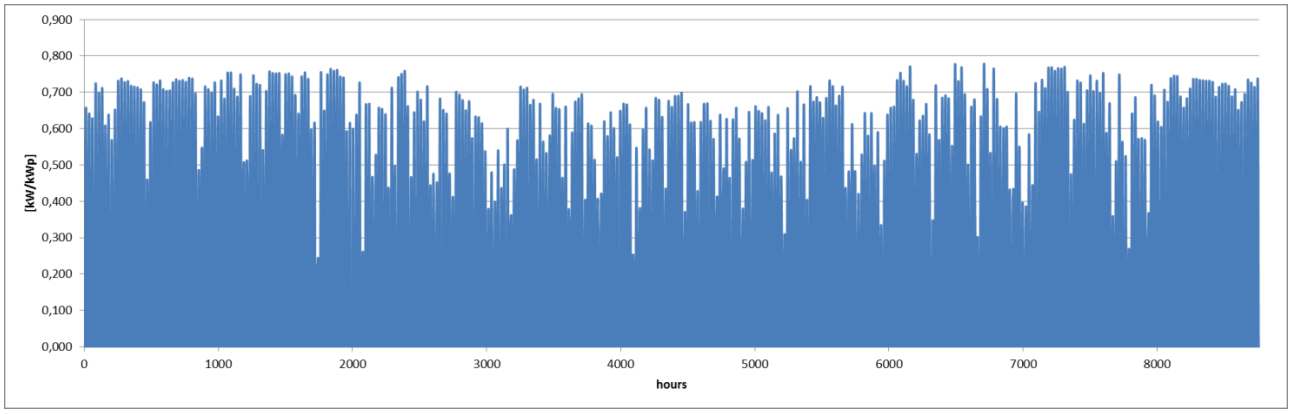

Figure 5.4 power generated per kW_p of PV for each hour in the year

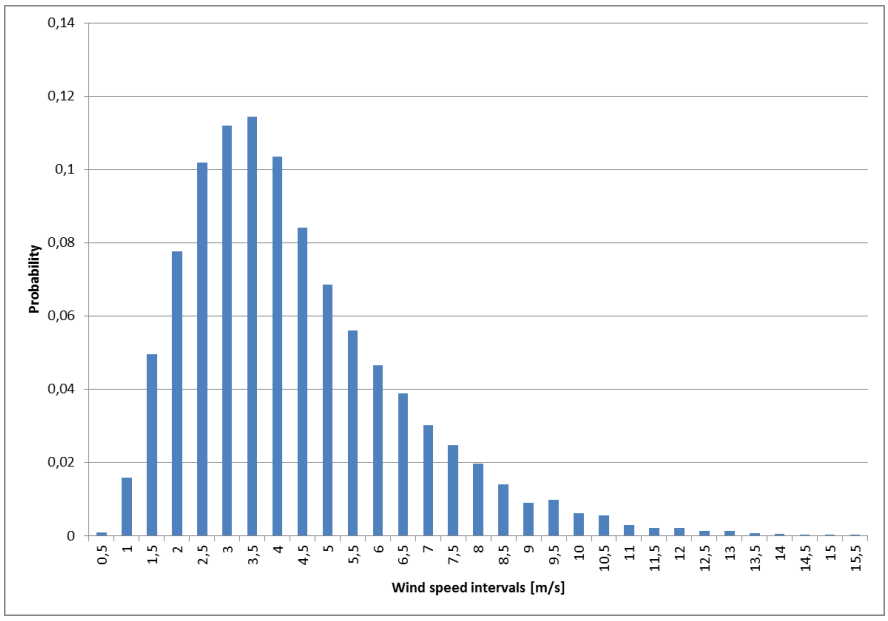

Figure 5.5 Probability density of wind speed

Other important parameters needed by the procedure are the costs. The current costs of some components are given in [37] together with the yearly load of the hospital and are reported in the following table.

Component	Cost
Inverter	300 €/kW
PV panels (investment)	1200 €/kW_p
PV O&M	1,5% of the investment per year
Pb-acid battery	200 €/kWh
Li-ion battery [38]	500 €/kWh
Battery O&M	1% of the investment per year
r (discount rate)	6%

Table 5.3 Components cost

Instead, the costs of the turbines are calculated according to the correlation reported in 3.4 and taken from [24]. The O&M costs related to the wind turbines are assumed to be 3% of the investment per year [39].
The technical parameters assumed in the simulation are:

Technical parameter	Value
Inverter efficiency (η_{inv})	90%
Battery maximum SoC	100%
Battery minimum SoC (Pb-acid)	40%
Battery minimum SoC (Li-ion)	0%
Battery maximum power/energy ratio (Pb-acid)	0,5 kW/kWh
Battery maximum power/energy ratio (Li-ion)	1 kW/kWh
Battery maximum working time (Pb-acid)	5 years
Battery maximum working time (Li-ion)	15 years
Maximum acceptable LLP	5%

Table 5.4 Components parameters

Once the input data are defined, it is possible to perform the simulations considering the three configurations discussed in the thesis: PV, wind and PV+wind with battery storage. Firstly, the results of the simulations adopting Li-ion battery are presented and detailed. Then, the results of the Pb-acid battery are briefly reported.

5.2.1 The PV+Li-ion battery configuration

Firstly, the optimization of a micro-grid composed by PV and Li-ion battery storage is performed. In the following table is presented the space of analysis generated varying the sizes of PV and battery. The red cells are the ones that do not fulfill the constraint about the maximum LLP, while the green cell is the optimal solution for the configuration with PV and battery.

		PV [kW]						
		478	547	615	683	752	820	888
ESS [kWh]	1425	27,47%	19,76%	15,24%	12,41%	10,54%	9,30%	8,43%
	1628	27,18%	18,06%	12,25%	8,70%	6,39%	4,88%	3,91%
	1832	27,07%	17,40%	10,86%	7,02%	4,58%	3,14%	2,26%
	2035	27,00%	17,07%	10,17%	6,15%	3,73%	2,45%	1,65%
	2239	26,94%	16,87%	9,65%	5,54%	3,08%	1,90%	1,17%
	2443	26,89%	16,75%	9,25%	5,05%	2,54%	1,42%	0,79%
	2646	26,85%	16,66%	8,95%	4,62%	2,05%	1,02%	0,52%

Table 5.5 LLP of the configuration PV+battery

		PV [kW]						
		478	547	615	683	752	820	888
ESS [kWh]	1425	0,232	0,220	0,221	0,226	0,233	0,240	0,247
	1628	0,251	0,234	0,228	0,231	0,237	0,243	0,252
	1832	0,270	0,249	0,241	0,241	0,246	0,252	0,259
	2035	0,290	0,266	0,255	0,254	0,257	0,263	0,270
	2239	0,309	0,283	0,270	0,268	0,270	0,276	0,283
	2443	0,329	0,300	0,285	0,281	0,283	0,289	0,296
	2646	0,349	0,317	0,300	0,295	0,297	0,303	0,310

Table 5.6 LCoE of the configuration PV+battery

Here the space of analysis is generated starting from the intuitive PV and ESS sizes (central values of the previous tables) and increasing and decreasing these values by fixed steps that corresponds to 10% of the intuitive sizes.

It is interesting to plot some simulated power profiles in specific days. In the following figures are reported the load profile (dark blue), the power profile generated by PV (red), the profile of the loss of load (light blue) and the behavior of the SoC (violet).

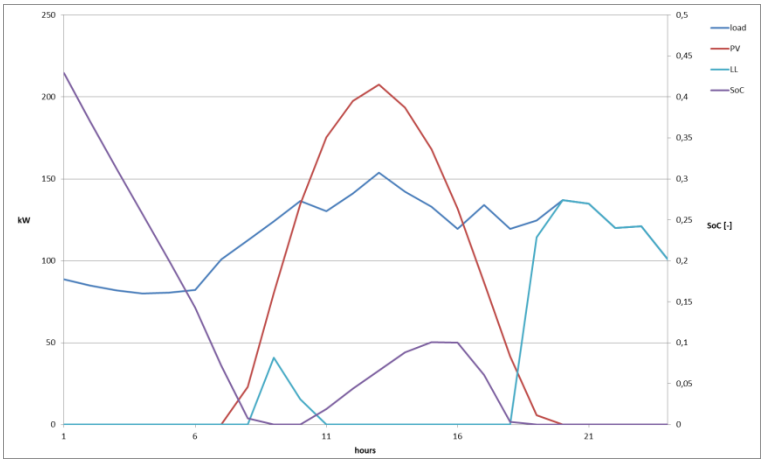

Figure 5.6 Profiles of the day with the lowest irradiation (170)

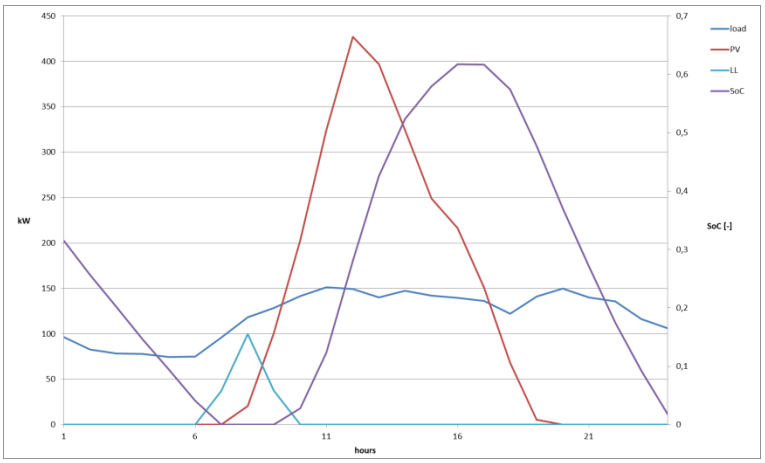

Figure 5.7 Profiles of the day with the highest load (323)

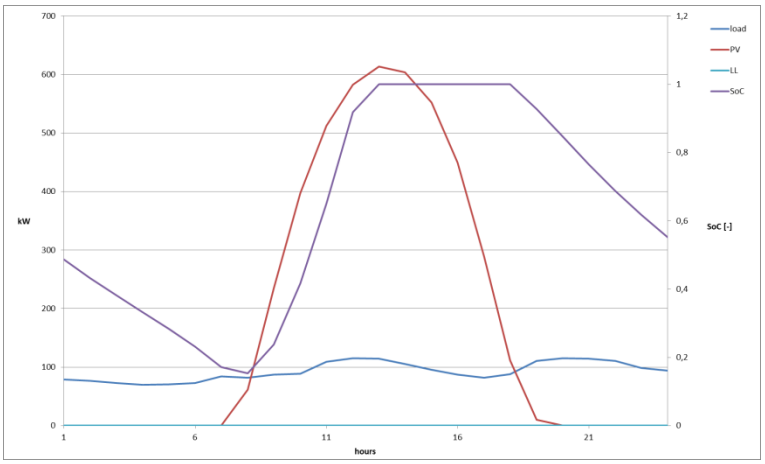

Figure 5.8 Profiles of the day with the lowest load (321)

As can be seen it the previous figures, when the irradiation is minimum there is a lot of loss of load, while when the load is minimum it is always fulfilled.

5.2.2 The wind+Li-ion battery configuration

It is now considered the configuration composed by wind turbines and battery. In order to clarify the algorithm explained in Chapter 3, in the following all the steps of the procedure are reported.

Study of the power profile of the turbines

It is known the hourly load profile for the analyzed period of time. It is also known the hourly velocity of the wind for a year (8760 values). Once the velocity has been corrected for the hub height, it is possible to calculate the power profile generated by each turbine in the database applying their power curve.

#DB	turbine type	ratio	h_max	#DB	turbine type	ratio	h_max
1	Aeolos 18m 50kW	20,3	54	43	Hummer 3.1 m 1kw	631,9	54
2	Aircon10S 7.54m 10kW	106,8	54	44	Hummer 3.8m 2kw	323,7	54
3	Aria S.R.L Libellula 18m 55kW	22,1	54	45	Hummer 6.4m 5kw	149,0	17
4	AWS HC 650 W Wind Turbine	1190,0	21	46	Hummer 8m 10kw	102,2	54
5	AWS HC 1,5 Kw Wind Turbine	513,5	21	47	Kestrel 300i 3m 1kW	783,9	17
6	AWS HC 1,8 Kw Wind Turbine	427,9	21	48	Kestrel e230 2.3m 0.8kW	1302,6	17
7	AWS HC 3,3 Kw Wind Turbine	263,0	21	49	Kestrel 400i 4m 3kW	444,4	54
8	AWS HC 4,2 Kw Wind Turbine	211,9	21	50	Kingspan-Proven Kingspan KW3 3.8m 2.5 Kw	485,9	54
9	AWS HC 5,1 Kw Wind Turbine	176,6	21	51	Kingspan-Proven Kingspan KW6 5.6m 6 Kw	215,2	54
10	Bergey BWCXL1 2.5m 1kw	925,8	17	52	Leitwind 77 800kW	0,9	54
11	Bergey Excel 6	177,3	17	53	Leitwind 80 800kW	0,8	54
12	Bergey Excel 10	133,8	17	54	Leitwind 77 850kW	0,9	54
13	C&F Green Energy CF11 9m 11kW	85,7	17	55	Leitwind 80 850kW	0,8	54
14	C&F Energy CF15e 13.1m 15kW	34,6	17	56	Leitwind 77 1000kW	0,8	54
15	C&F Green Energy CF15 11.1m 15kW	61,3	17	57	Leitwind 80 1000kW	0,8	54
16	C&F Green Energy CF20 12.8m 20kW	40,7	17	58	Leitwind 86 1000kW	0,7	54
17	C&F Green Energy CF50 2om 50kW	14,0	17	59	Leitwind 90 1000kW	0,6	54
18	Electriawind Garbi 150/28 28m 150kw	6,1	17	60	Marlec FM1803-2 1.8m	3022,1	54
19	Electriawind Garbi 200/28 28m 200kw	5,7	17	61	Northern Power NPS100C-24	9,0	17
20	Enercon E-48 [800kW]	1,8	17	62	Northern Power NPS 60-24	9,0	17
21	Enercon E-53 [800kW]	1,4	5	63	Northern Power NPS100C-21	12,3	17
22	Enercon E-44 [900kW]	2,1	17	64	Norvento Ned 22 [100kW]	10,2	54
23	Ennera Windera S 4.36m 3,2 Kw	298,7	54	65	Norvento Ned 24 [100kW]	9,2	54
24	Eocycle EO20	27,0	43	66	Pinnacle-Tech Caravel 2.5kW 3.5m	478,2	54
25	Eocycle EO25 Class IIA	41,5	76	67	Pinnacle-Tech Frigate 7.5 Kw 6m	191,4	54
26	Eoltec Scirocco E5.6m-6kw	178,7	17	68	Pinnacle-Tech Frigate 10kW 7m	154,2	180
27	Ergycon Ely50 20.7m	12,4	17	69	SkyStream 3.7	543,2	54
28	Evance R-9000 5.5m 5kw	212,1	54	70	Sonkyo Energy Windspot 1.5kW 4.05m	747,8	54
29	EWT direct Wind 54m 250kW	1,9	17	71	Sonkyo Energy Windspot 3.5kW 4.05m	399,3	54
30	EWT direct Wind 52 500kW	1,7	17	72	Tempower Whisper H40 2.1m 0.8kw	1978,6	54
31	EWT direct Wind 54 500kW	1,5	17	73	TrueNorthPower Arrow 2m1kw	1382,0	17
32	EWT DW 52 [900kW]	1,6	17	74	Vergnet GEV MP C 32 m 275kw	5,8	54
33	EWT DW 54 [900kW]	1,5	17	75	Vergnet GEV MP R 32 m 275kw	5,8	54
34	EWT DW 61 [900kW]	1,2	17	76	WES 18 [80kW]	18,7	54
35	Fortis Passaat 3.12m 1.4kW	1095,1	54	77	WES 18 [100kW]	18,1	54
36	Fortis Montana 5m 5kW	302,3	17	78	WES 18 [250kW]	6,8	54
37	Future Energy Airforce10 8m 13kW	86,5	17	79	Windflow 33 [500kW]	6,7	616
38	Gaia Wind 133 - 11kw	63,9	54	80	Windflow 45 [500kW]	3,3	180
39	Generic 1kW	1954,5	0	81	Windspot 7.5kW 6.3m	147,6	54
40	Generic 3kW	652,6	0	82	Xzeres Skystream 3.7 [2.4kW]	555,7	30
41	Generic 10 Kw	195,8	0	83	Zephyr Airdolphin 1.8m 1kW	1841,2	54
42	Harbon HWT60 19.93m 60kW	22,0	54				

Table 5.7 Database of the turbines

Once the power profile is known, it is possible to calculate the total energy E_{tot} generated by each turbine and so also the parameter $\frac{\sum_{t=0}^{T} load(t)}{E_{tot}*\eta_{inv}}$ can be evaluated (reported in Table 5.7 under "ratio").

From the power profile, it is also possible to understand when the turbine is not generating any power because the velocity is lower than the cut-in speed or higher than the cut-out speed. Therefore, the maximum consecutive non-working hours can be calculated (reported in Table 5.7 under "h_max").

Selection of the turbines and ranking generation

The turbines highlighted in yellow in Table 5.7 are the ones that fulfill the constraints of Equations 3.6 about the acceptable range of the ratio $\frac{\sum_{t=0}^{T} load(t)}{E_{tot}*\eta_{inv}}$ and the maximum non-operative hours (set to 24).

Only the turbines highlighted are used to generate the ranking. In the next table the ranking is reported showing the values of the energy/cost ratio and the equivalent hours.

#DB	E/C ratio	h_eq
29	1,70	2193
31	1,09	1356
30	0,97	1198
61	0,92	1213
62	0,92	1213
18	0,88	1150
34	0,83	961
19	0,70	911
21	0,76	892
33	0,68	791
32	0,61	704
20	0,60	703
22	0,46	538

Table 5.8 Ranking

The ranking is based on the energy/cost ratio, but it is evident that the equivalent hours would have led to a very similar ranking.

Intuitive sizing

Only the first 10 turbines of this ranking are considered for the space of analysis.

To generate the space of analysis is necessary to set the maximum size of the battery. It was chosen to take a battery that can cover 3 days of load and so the maximum accepted battery has a capacity of 8579 kWh.

From the value of $\frac{\sum_{t=0}^{T} load(t)}{E_{tot}*\eta_{inv}}$ the intuitive number of turbines is calculated. Any time a configuration is set, it is simulated and its LLP is calculated. The configuration with the maximum battery and the intuitive number of turbines may not be enough to fulfill the constraint about the maximum LLP, so the number of turbines is

increased until the LLP becomes lower than 5%. Indeed, in the following table the ratio $\frac{\sum_{t=0}^{T} load(t)}{E_{tot} * \eta_{inv}}$, the intuitive number of turbines and the minimum acceptable number of turbines that fulfills the maximum LLP are reported.

With the intuitive number of turbines it is sure that the energy generated is higher than the energy needed by the load. But the energy may not be generated when it is needed, resulting in a loss of load. Increasing the number of turbines more energy is generated, so the load can be satisfied but some energy is wasted. In the following table it is reported the energy wasted per year implementing the minimum acceptable number of turbines and the LLP given with the maximum allowed battery.

#DB	ratio	Intuitive N_{turb}	Minimum N_{turb}	Energy wasted with minimum N_{turb}	LLP with maximum battery and minimum N_{turb}
29	1,9	2	6	2246 MWh	3,92 %
31	1,5	2	6	3025 MWh	3,59 %
30	1,7	2	8	3747 MWh	3,78 %
61	9,03	10	>10 => non-acceptable turbine		
62	9,03	10	>10 => non-acceptable turbine		
18	6,1	7	>10 => non-acceptable turbine		
34	1,2	2	5	3282 MWh	3,69 %
19	5,7	6	>10 => non-acceptable turbine		
21	1,4	2	5	2568 MWh	4,88 %
33	1,5	2	6	3225 MWh	3,80 %

Table 5.9 Intuitive and minimum number of turbines for the space of analysis

It may occur that increasing the number of turbines looking for the minimum number that allows to have an LLP lower than its maximum, the turbines become more than 10, that is the maximum value accepted in order to limit land occupation and turbines interference. In this case, the turbine type is not suitable for the analyzed scenario.

Space of analysis

All the other turbines can be used to generate the space of analysis of Tables 5.10. It is therefore constituted by 6 tables, each of them relative to a different turbine type. In each table, the columns represent different generation sizes, so different number of turbines, while the rows represent different battery sizes. In the following tables are reported the values of LLP, but similar tables could be shown reporting the values of NPC or LCoE.

turb 29
EWT direct Wind 54m 250kW

P turb [kW]	1500	1750	2000	2250
#turbines	6	7	8	9
ESS [kWh]				
2314				5,03%
2520				4,59%
2864			5,02%	3,90%
3254			4,33%	3,21%
3698		5,14%	3,73%	
3812		5,00%	3,59%	
3955		4,82%		
4494		4,24%		
5107		3,80%		
5804	5,04%	3,42%		
5983	4,91%	3,35%		
6643	4,50%			
7549	4,17%			
8579	3,92%			

turb 31
EWT direct Wind 54 500kW

	3000	3500	4000	4500
	6	7	8	9
2168				5,02%
2330				4,65%
2647			5,09%	3,99%
3008			4,37%	3,32%
3419		5,13%	3,71%	
3524		4,99%	3,57%	
4005		4,40%		
4551		3,86%		
5172	5,08%	3,46%		
5332	4,95%	3,37%		
5846	4,56%			
6643	4,16%			
7549	3,81%			
8579	3,59%			

turb 30
EWT direct Wind 52 500kW

	4000	4500	5000	
	8	9	10	
3491			5,14%	
3599			4,99%	
3834			4,69%	
4356		5,12%	4,09%	
4491		4,97%	3,94%	
5104		4,39%		
5799	5,08%	3,91%		
5979	4,94%	3,81%		
6643	4,50%			
7549	4,14%			
8579	3,78%			

turb 34
EWT DW 61 [900kW]

P turb [kW]	4500	5400	6300	7200
#turbines	5	6	7	8
ESS [kWh]				
1931				5,09%
2170				4,45%
2466			5,02%	3,82%
2543			4,85%	3,67%
2889			4,16%	
3283		5,11%	3,48%	
3385		4,97%	3,33%	
3643		4,65%		
4140		4,07%		
4704		3,59%		
5346	5,10%	3,19%		
5511	4,97%	3,10%		
5846	4,71%			
6643	4,28%			
7549	3,93%			
8579	3,69%			

turb 21
Enercon E-53 [800kW]

	4050	4860	5670	6480
	5	6	7	8
1837				5,14%
1894				5,00%
1975				4,79%
2245				4,20%
2551			5,01%	3,59%
2630			4,87%	3,45%
2988			4,34%	
3396			3,82%	
3859		5,05%	3,33%	
3978		4,93%	3,24%	
4260		4,67%		
4840		4,22%		
5501		3,79%		
6251		3,50%		
7103		3,21%		
8072	5,03%	2,98%		
8321	4,96%	2,93%		
8579	4,88%			

turb 33
EWT DW 54 [900kW]

	5400	6300	7200	8100
	6	7	8	9
2205				5,02%
2388				4,62%
2714			5,07%	3,95%
2798			4,90%	3,79%
3180			4,21%	
3613		5,03%	3,62%	
3725		4,90%	3,48%	
4233		4,31%		
4810		3,82%		
5466	5,11%	3,44%		
5635	4,98%	3,35%		
5846	4,82%			
6643	4,36%			
7549	4,04%			
8579	3,80%			

Tables 5.10 Space of analysis – values of LLP

It is worth reminding that the battery is reduced from the maximum acceptable one using the algorithm explained in Equations 3.9. The number of turbines is only increased and not reduced otherwise it would be necessary a battery bigger than the maximum.

Selection of the optimal configuration

Once the space of analysis has been generated, it is necessary to compare all the simulated cases. The optimal configuration is the one with the lowest LCoE with an LLP lower than 5%. So, the turbine type associated to the optimal configuration is the best turbine in the database and its space of analysis is detailed in the following tables, highlighting the values of LLP and LCoE.

turb 29
EWT direct Wind 54m 250kW

P turb [kW]		1500	1750	2000	2250
#turbines		6	7	8	9
ESS [kWh]					
	2314				5,03%
	2520				4,59%
	2864			5,02%	3,90%
	3254			4,33%	3,21%
	3698		5,14%	3,73%	
	3812		5,00%	3,59%	
	3955		4,82%		
	4494		4,24%		
	5107		3,80%		
	5804	5,04%	3,42%		
	5983	4,91%	3,35%		
	6643	4,50%			
	7549	4,17%			
	8579	3,92%			

	1500	1750	2000	2250
	6	7	8	9
2314				0,559
2520				0,571
2864			0,557	0,593
3254			0,582	0,617
3698		0,578	0,612	
3812		0,586	0,619	
3955		0,596		
4494		0,632		
5107		0,674		
5804	0,693	0,723		
5983	0,706	0,736		
6643	0,752			
7549	0,816			
8579	0,890			

Table 5.11 Space of analysis of the best turbine – Values of LLP (left) and LCoE in €/kWh (right)

The cells in red do not fulfill the constraint about the maximum LLP while the cells highlighted in green represent the best configuration for a micro-grid adopting wind turbines and battery, that is the result of the *wind micro-grid* module.

This result can be used to plot the power profiles in specific days of the simulation. In Figures 5.9 there are plotted the load profile (dark blue), the power generated by wind turbines (green), the loss of load (light blue) and the SoC behavior (violet).

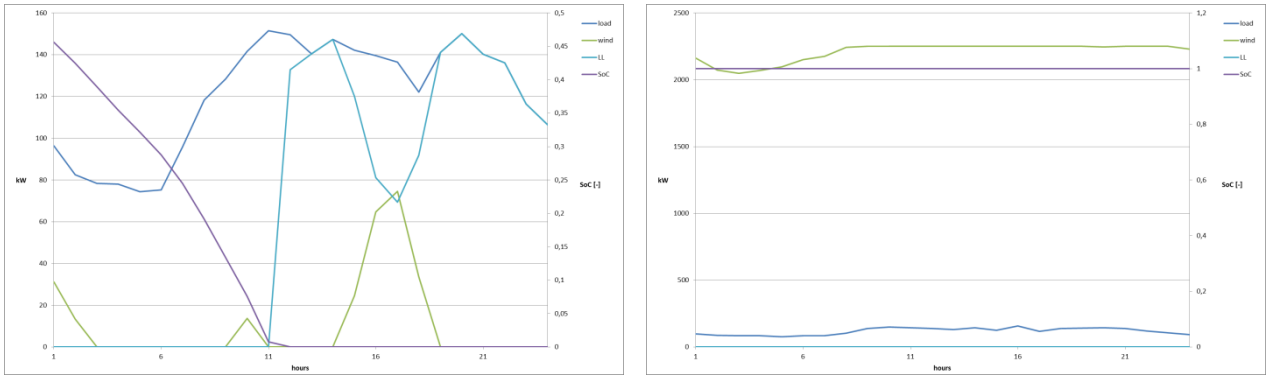

Figures 5.9 Profiles of the day with the lowest generation from wind (162) (left) and with the highest (57) (right)

To guarantee an acceptable loss of load during the whole analyzed period it is necessary to have a generation size highly oversized with a lot of energy wasted. Indeed, when the power from wind turbines is maximum, the power generation is far too much and the system is facing an overgeneration. Instead, when the power generation is minimum the system is facing a loss of load.

5.2.3 The PV+wind+Li-ion battery configuration

Finally, it is performed the analysis of a micro-grid that exploits PV panels, wind turbines and a Li-ion battery storage. To clarify the algorithm of the *PV+wind micro-grid* module presented in Chapter 4, the procedure is detailed in the following. After that, it is presented a way to validate the algorithm.
Here the procedure is detailed.

Ranking

Once the load profile, the PV generation profile and the power generation from all the turbines in the database are known, it is possible to generate the ranking of the turbines according to the energy/cost ratio. The turbine ranking is shown in the following table, where also the values of the equivalent hours are reported.

#DB	E/C ratio	h_eq	#DB	E/C ratio	h_eq	#DB	E/C ratio	h_eq
29	1,70	2193	21	0,76	892	51	0,59	790
14	1,49	1983	44	0,75	1008	4	0,58	776
59	1,46	1662	48	0,74	983	82	0,58	774
24	1,45	1930	26	0,73	974	36	0,58	771
53	1,30	1540	1	0,72	956	50	0,55	741
55	1,26	1470	28	0,70	939	49	0,55	734
27	1,25	1663	19	0,70	911	67	0,53	708
52	1,25	1478	37	0,70	928	80	0,52	642
58	1,22	1395	9	0,69	928	46	0,51	686
54	1,21	1415	6	0,69	917	74	0,51	655
57	1,14	1300	5	0,69	917	75	0,51	655
38	1,12	1494	10	0,68	914	35	0,51	681
31	1,09	1356	33	0,68	791	76	0,51	669
56	1,09	1243	66	0,68	909	68	0,49	651
17	1,08	1436	45	0,68	904	78	0,48	614
30	0,97	1198	2	0,67	889	71	0,47	627
61	0,92	1213	11	0,66	884	12	0,47	622
62	0,92	1213	7	0,66	884	22	0,46	538
47	0,91	1210	81	0,66	882	73	0,46	614
16	0,90	1203	8	0,65	867	77	0,44	577
18	0,88	1150	3	0,65	859	72	0,43	577
65	0,86	1132	63	0,64	849	39	0,40	534
34	0,83	961	70	0,62	831	41	0,40	533
23	0,83	1106	43	0,62	826	40	0,40	533
13	0,82	1098	42	0,61	810	60	0,36	480
15	0,78	1044	32	0,61	704	83	0,28	372
64	0,78	1025	69	0,60	800	79	0,25	311
25	0,76	1009	20	0,60	703			

Table 5.12 Turbine ranking based on E/C ratio

Turbine selection and intuitive sizing

Following the order given by the ranking, every turbine is considered to perform the following calculations:

- First constraint:

$$\frac{\sum_{t=0}^{T} load(t)}{\sum_{t=0}^{T} P_{turb}(t) * \eta_{inv}} \leq 0{,}5$$

Equation 5.1 Constraint without PV

- If the first constraint is fulfilled, the objective function OF1 can be minimized and the $\left(\frac{PV}{wind}\right)_{ratio}$ is calculated.
- Second constraint:

$$0{,}5 < \frac{\sum_{t=0}^{T} load(t)}{\sum_{t=0}^{T}\left(P_{turb}(t) + \left(\frac{PV}{wind}\right)_{ratio} * P_{nom,turb} * P_{PV,1kW}(t)\right) * \eta_{inv}} \leq 10$$

Equation 5.2 Constraint for wind turbine selection

- If the second constraint is fulfilled, the turbine can be used to generate a space of analysis.

This is represented in the following table.

#DB	First constraint	PV/wind ratio	Second constraint	Intuitive N_{turb}	Minimum N_{turb}
29	OK	0,92	OK	2	2
14	OK	0,76	NO		
59	OK	0,78	NO		
24	OK	1,02	NO		
53	OK	0,80	NO		
55	OK	0,77	NO		
27	OK	0,71	OK	8	>10 (not acceptable)
52	OK	0,74	NO		
58	OK	0,77	NO		
54	OK	0,71	NO		
57	OK	0,70	NO		
38	OK	0,93	NO		
31	OK	0,62	OK	1	2
56	OK	0,64	NO		
17	OK	0,62	OK	9	>10 (not acceptable)
30	OK	0,62	OK	1	2
61	OK	0,58	OK	6	8
62	OK	0,58	OK	6	8
47	OK	0,58	NO		
16	OK	0,57	NO		
18	OK	0,48	OK	4	6
65	OK	0,68	OK	5	7
34	OK	0,46	OK	1	2
23	OK	0,71	NO		
13	OK	0,66	NO		
15	OK	0,48	NO		
64	Ok	0,59	OK	6	8
25	OK	0,72	OK		
21	OK	0,41	OK	1	2

Table 5.13 Turbines selection

This procedure is continued until 10 types of turbines that fulfill the second constraint are selected.
If the second constraint is fulfilled, the intuitive number of turbines can be calculated. This number may not be enough to have an LLP higher than 5%. So, the number of turbines is increased until an acceptable configuration is reached with the biggest allowed battery. This number is reported in the last column of Table 5.13. But if this number is higher than 10, the turbine is discarded.

Space of analysis of the first optimization

From the turbines chosen in Table 5.13 the space of analysis is generated. Indeed, in the following tables is reported the space of analysis of the first optimization. The starting point of each sub-space of analysis is the minimum number of turbines just calculated and the maximum battery size, here set to 3 days of load that corresponds to 8579 kWh. Each of the 10 tables corresponds to a type of turbine, the columns represent the generation sizes, keeping fixed the $\left(\frac{PV}{wind}\right)_{ratio}$ optimized for that specific turbine and the rows represent the battery sizes. The values of LLP are reported for each case simulated.

turb 29
EWT direct Wind 54m 250kW

PV [kW]		460	690	920	1150
#turbines		2	3	4	5
ESS [kWh]					
	703				5,26%
	799			5,16%	4,16%
	824			4,85%	3,90%
	936		5,08%	3,55%	
	1064		3,59%	2,37%	
	1209		2,24%		
	1373	5,11%	1,16%		
	1433	4,79%	0,88%		
	1628	4,04%			
	1850	3,48%			
	2102	3,06%			
	2389	2,71%			
	2715	2,39%			
	3085	2,13%			
	3506	1,95%			
	3984	1,81%			
	4527	1,69%			
	5145	1,57%			
	5846	1,43%			
	6643	1,32%			
	7549	1,23%			
	8579	1,12%			

turb 31
EWT direct Wind 54 500kW

	622	932	1243	1554
	2	3	4	5
670				5,24%
726			5,59%	4,62%
825		5,79%	4,39%	3,58%
937		4,34%	3,18%	
1065	5,36%	2,88%		
1110	4,80%	2,45%		
1261	3,19%			
1433	1,93%			
1628	1,17%			
1850	0,79%			
2102	0,57%			
2389	0,40%			
2715	0,24%			
3085	0,12%			
3506	0,03%			
3984	0,00%			
4527	0,00%			
5145	0,00%			
5846	0,00%			
6643	0,00%			
7549	0,00%			
8579	0,00%			

turb 30
EWT direct Wind 52 500kW

	618	928	1237	1546
	2	3	4	5
773				5,68%
879			5,28%	4,39%
998		5,06%	3,81%	3,06%
1135	6,10%	3,31%	2,33%	
1261	4,50%	1,98%		
1433	2,90%			
1628	1,89%			
1850	1,41%			
2102	1,09%			
2389	0,81%			
2715	0,57%			
3085	0,40%			
3506	0,28%			
3984	0,18%			
4527	0,13%			
5145	0,07%			
5846	0,00%			
6643	0,00%			
7549	0,00%			
8579	0,00%			

turb 61
Northern Power NPS100C-24

PV [kW]		443	499	554	
#turbines		8	9	10	
ESS [kWh]					
	1249			5,26%	
	1288			4,88%	
	1464		5,23%	3,51%	
	1663		4,37%	2,64%	
	1890		3,77%		
	2148		3,30%		
	2441		2,93%		
	2774	5,06%	2,60%		
	2859	4,98%	2,53%		
	2948	4,90%			
	3091	4,77%			
	3506	4,41%			
	3984	4,08%			
	4527	3,83%			
	5145	3,67%			
	5846	3,53%			
	6643	3,45%			
	7549	3,36%			
	8579	3,25%			

turb 62
Northern Power NPS 60-24

	443	499	554	
	8	9	10	
1249			5,26%	
1288			4,88%	
1464		5,23%	3,51%	
1663		4,37%	2,64%	
1890		3,77%		
2148		3,30%		
2441		2,93%		
2774	5,06%	2,60%		
2859	4,98%	2,53%		
2948	4,90%			
3091	4,77%			
3506	4,41%			
3984	4,08%			
4527	3,83%			
5145	3,67%			
5846	3,53%			
6643	3,45%			
7549	3,36%			
8579	3,25%			

turb 18
Electriawind Garbi 150/28 28m 150kw

	433	505	577	650
	6	7	8	9
888				5,53%
955			5,74%	4,65%
1085		5,74%	4,17%	3,21%
1233		4,35%	2,82%	
1401		3,27%		
1592		2,55%		
1809	5,08%	2,11%		
1865	4,97%	2,02%		
1923	4,86%			
2102	4,57%			
2389	4,19%			
2715	3,84%			
3085	3,47%			
3506	3,10%			
3984	2,87%			
4527	2,72%			
5145	2,59%			
5846	2,50%			
6643	2,42%			
7549	2,33%			
8579	2,23%			

turb 65
Norvento Ned 24 [100kW]

PV [kW]		475	543	611	679
#turbines		7	8	9	10
ESS [kWh]					
	1254				5,46%
	1293			6,02%	4,94%
	1426			4,53%	3,40%
	1620		5,19%	3,16%	
	1819		4,45%	2,47%	
	2067		3,85%		
	2349		3,38%		
	2669		2,99%		
	3033		2,61%		
	3447		2,27%		
	3917		2,10%		
	4451		1,94%		
	5058	5,05%	1,76%		
	5214	5,00%	1,72%		
	5376	4,95%			
	5542	4,90%			
	5713	4,87%			
	5907	4,84%			
	6140	4,81%			
	6425	4,78%			
	6778	4,74%			
	7225	4,69%			
	7803	4,63%			
	8579	4,55%			

turb 34
EWT DW 61 [900kW]

	825	1237	1649	2062
	2	3	4	5
601				5,15%
683			5,13%	4,28%
776		5,35%	4,09%	3,35%
833		4,65%	3,50%	
947	5,31%	3,33%		
976	4,92%	3,03%		
1110	3,25%			
1261	1,79%			
1433	0,73%			
1628	0,25%			
1850	0,10%			
2102	0,03%			
2389	0,00%			
2715	0,00%			
3085	0,00%			
3506	0,00%			
3984	0,00%			
4527	0,00%			
5145	0,00%			
5846	0,00%			
6643	0,00%			
7549	0,00%			
8579	0,00%			

turb 64
Norvento Ned 22 [100kW]

	471	530	589	
	8	9	10	
1301			5,97%	
1478			4,27%	
1680		5,09%	3,17%	
1847		4,55%	2,68%	
2099		3,99%		
2385		3,55%		
2711		3,17%		
3080		2,78%		
3500		2,43%		
3977		2,23%		
4520	5,03%	2,07%		
4660	4,98%	2,03%		
4804	4,94%			
4952	4,89%			
5118	4,84%			
5378	4,76%			
5739	4,69%			
6192	4,63%			
6774	4,57%			
7549	4,49%			
8579	4,38%			

turb 21
Enercon E-53 [800kW]

PV [kW]		668	1002	1336	1670
#turbines		2	3	4	5
ESS [kWh]					
	574				5,15%
	591				4,94%
	672			5,18%	4,05%
	764		5,68%	4,09%	3,14%
	859		4,44%	3,08%	
	976	5,68%	3,05%		
	1110	3,91%	1,80%		
	1261	2,37%			
	1433	1,25%			
	1628	0,68%			
	1850	0,43%			
	2102	0,27%			
	2389	0,12%			
	2715	0,01%			
	3085	0,00%			
	3506	0,00%			
	3984	0,00%			
	4527	0,00%			
	5145	0,00%			
	5846	0,00%			
	6643	0,00%			
	7549	0,00%			
	8579	0,00%			

Tables 5.14 Space of analysis of the first optimization – values of LLP

Second optimization

The green cell of Tables 5.14 is the optimal configuration in terms of LLP and LCoE. So, the turbine EWT 250 is select as the best turbine and it is chosen to perform the second optimization, where the PV size and the number of turbines can vary independently. The maximum battery size is set to the average between the 3-day battery and the result of the first optimization (Equation 4.36). Indeed, Tables 5.15 are composed by 5 tables, each of them is relative a different number of turbines. The columns represent different PV sizes and the rows represent the battery sizes.

# turbines		0						
PV [kW]		672	768	864	960	1056	1152	1248
ESS [kWh]								
	1438			8,32%	7,36%	6,68%	6,19%	5,85%
	1635		5,87%	4,12%	3,10%	2,40%	1,94%	1,63%
	1858		4,02%	2,43%				
	2111		3,09%					
	2399		2,29%					
	2726	5,02%	1,56%					
	3002	4,54%	1,10%					
	3411	4,02%						
	3876	3,57%						
	4405	3,21%						
	5006	2,94%						

	1						
	422	518	614	710	806	902	998
1146						5,63%	5,29%
1181					5,43%	5,00%	4,69%
1218				5,49%	4,86%	4,42%	
1263			6,07%	4,82%	4,19%		
1397			4,52%	3,22%			
1588			3,17%				
1804		5,12%	2,44%				
1860		4,98%	2,31%				
2046		4,55%					
2325		4,06%					
2642		3,67%					
3002		3,29%					
3411		2,97%					
3876		2,81%					
4405		2,69%					
5006	8,27%	2,56%					

	2						
	172	268	364	460	556	652	748
1018						5,97%	5,50%
1127					5,38%	4,52%	4,03%
1185					4,75%	3,84%	
1346				5,27%	3,34%		
1530				4,37%	2,33%		
1739				3,74%			
1976				3,25%			
2245				2,88%			
2551				2,54%			
2899				2,26%			
3294			5,03%	2,02%			
3396			4,93%	1,99%			
3517			4,83%				
3876			4,54%				
4405			4,22%				
5006	15,62%	9,04%	3,93%				

	3						
	0	18	114	210	306	402	498
987							5,70%
1115							4,43%
1267						5,13%	3,26%
1440						4,28%	2,32%
1636						3,59%	
1859						3,04%	
2113						2,57%	
2401					5,05%	2,25%	
2475					4,93%	2,18%	
2642					4,69%		
3002					4,26%		
3411					3,87%		
3876					3,56%		
4405					3,31%		
5006	18,31%	17,09%	11,12%	6,20%	3,07%		

	4						
	0	0	0	0	56	152	248
2155							5,12%
2221							4,98%
2325							4,78%
2642							4,22%
3002							3,82%
3411							3,42%
3876							3,10%
4405							2,84%
5006	11,91%	11,91%	11,91%	11,91%	9,17%	5,29%	2,61%

Tables 5.15 Space of analysis of the second optimization – values of LLP

The green cell is the optimal configuration, so it is the case with minimum LCoE among the configurations with LLP < LLP_{max}, as can be seen in the following table that is the LCoE values in the sub-space of analysis relative to the cases with 1 turbine.

# turbines		1						
PV [kW]		422	518	614	710	806	902	998
ESS [kWh]								
	1146						0,261	0,273
	1181					0,249	0,261	0,274
	1218				0,238	0,250	0,262	
	1263			0,228	0,238	0,251		
	1397			0,235	0,244			
	1588			0,245				
	1804		0,254	0,259				
	1860		0,257	0,263				
	2046		0,270					
	2325		0,289					
	2642		0,312					
	3002		0,337					
	3411		0,366					
	3876		0,399					
	4405		0,437					
	5006	0,497	0,480					

Table 5.16 Space of analysis of the second optimization – values of LCoE for 1 turbine

Minimizing the objective function applying the power curve of the turbine EWT 250 (the best turbine), the $\left(\frac{PV}{wind}\right)_{ratio}$ resulted 0,92. The result of the second optimization (1 turbine and 593 kW of PV) have a $\left(\frac{PV}{wind}\right)_{ratio}$ of 2,46. This confirms that in the economic optimum the share of PV has to increase with respect to the wind since the investment cost of PV is lower than the wind turbines one.

Validation

Once the procedure has been explained, it is important to verify if the procedure proposed finds the real techno-economic optimum. The validation procedure here proposed is a sensitivity analysis on the generation sizes:

- The number of turbines is varied between 0 and 10.
- The PV sizes are varied between 0 and 2500 kW with fixed steps of 125 kW.
- For each couple of PV and wind values, the battery size is firstly set to 5500 kWh, then it is reduced until the LLP becomes equal (or close) to 5%.
- Once a matrix of PV and wind sizes is generated and a battery size is associated to every PV/wind couple, it is possible to calculate the LCoE for each case.

Applying the validation procedure to the turbine EWT 250 that is the best turbine resulted from the first optimization, and so it is the turbine on which the second optimization is based, the following table is calculated. It shows the LCoE values for each configuration, so the minimum (green cell) is the real optimal configuration for the micro-grid.

		wind										
#turb		0	1	2	3	4	5	6	7	8	9	10
P turb [kW]		0	250	500	750	1000	1250	1500	1750	2000	2250	2500
PV [kW]	0	930,918	0,893	0,685	0,633	0,631	0,650	0,675	0,591	0,567	0,568	0,585
	125	2,137	0,713	0,612	0,596	0,612	0,504	0,456	0,460	0,477	0,507	0,539
	250	1,114	0,614	0,568	0,512	0,375	0,368	0,389	0,421	0,452	0,490	0,526
	375	0,775	0,553	0,363	0,300	0,316	0,346	0,378	0,416	0,453	0,492	0,530
	500	0,605	0,288	0,258	0,283	0,316	0,352	0,388	0,427	0,465	0,504	0,543
	625	0,513	0,238	0,262	0,295	0,328	0,365	0,402	0,441	0,479	0,519	0,559
	750	0,246	0,247	0,275	0,308	0,343	0,380	0,417	0,456	0,496	0,535	0,574
	875	0,253	0,262	0,291	0,323	0,358	0,396	0,434	0,473	0,511	0,551	0,591
	1000	0,266	0,278	0,305	0,339	0,375	0,412	0,450	0,489	0,528	0,568	0,607
	1125	0,281	0,294	0,322	0,356	0,392	0,429	0,467	0,506	0,545	0,584	0,624
	1250	0,297	0,310	0,340	0,373	0,408	0,445	0,483	0,522	0,562	0,601	0,641
	1375	0,313	0,327	0,356	0,388	0,424	0,462	0,500	0,539	0,578	0,618	0,658
	1500	0,352	0,344	0,373	0,405	0,441	0,479	0,517	0,556	0,595	0,635	0,674
	1625	0,369	0,361	0,390	0,422	0,458	0,495	0,534	0,573	0,612	0,651	0,691
	1750	0,385	0,378	0,406	0,439	0,475	0,512	0,551	0,589	0,629	0,668	0,708
	1875	0,402	0,395	0,423	0,457	0,492	0,529	0,568	0,606	0,646	0,685	0,725
	2000	0,419	0,411	0,441	0,474	0,509	0,546	0,584	0,623	0,663	0,702	0,743
	2125	0,435	0,428	0,458	0,491	0,526	0,563	0,602	0,640	0,679	0,720	0,760
	2250	0,451	0,445	0,474	0,507	0,543	0,581	0,619	0,658	0,696	0,737	0,777
	2375	0,472	0,462	0,491	0,524	0,560	0,597	0,636	0,675	0,713	0,754	0,794
	2500	0,488	0,478	0,508	0,541	0,577	0,614	0,653	0,692	0,731	0,771	0,810

Table 5.17 Validation matrix – values of LCoE

The optimum results to be the configuration with 1 turbine and 625 kW of PV to which corresponds a battery of 1377 kWh and a $\left(\frac{PV}{wind}\right)_{ratio}$ of 2,5. The number of turbines is the same given by the optimization algorithm implemented in the tool, while the PV size is slightly different because the discrete steps considered are different. The implemented optimization algorithm and the validation process give two values of LCoE that are very close, so it can be stated that the procedure implemented in the tool finds the real optimal configuration for a micro-grid exploiting PV and wind sources.

The validation process presented in Table 5.17 is clearly much more robust than the procedure implemented since it is sure to find the real optimum within a specified range, but it is very slow. The optimization explained in Chapter 4 takes around 5 minutes to reach the result starting from all the turbines in the database, while the validation process takes almost an hour to find the optimal configuration with only one type of turbine. Therefore, the validation cannot be used as standard optimization algorithm.

Profiles

In order to understand the behaviour of the micro-grid, in the following figures there are reported the working profiles in particular days. They represent the load (dark blue), the power generated by PV (red), the power generated by wind turbines (green), the loss of load (light blue) and the SoC (violet).

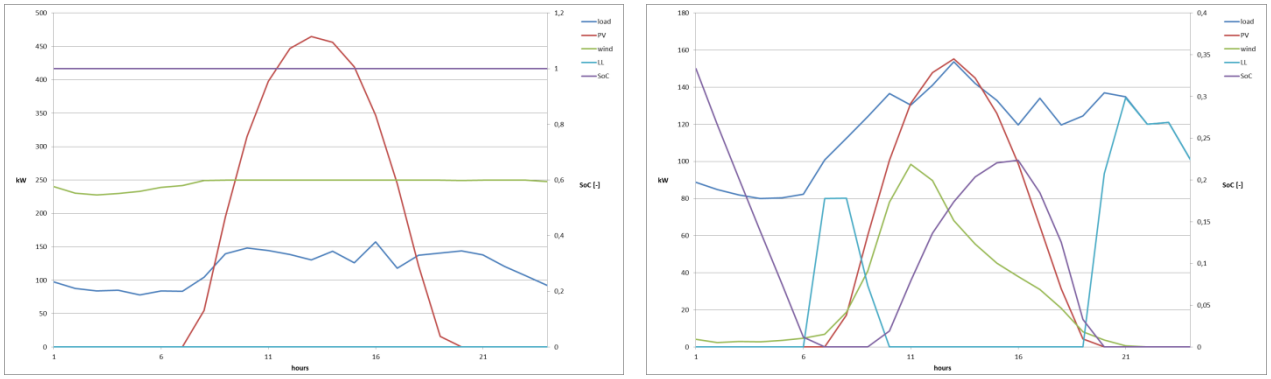

Figures 5.10 Profiles of the day with the highest generation from wind and PV together (left) and with the lowest from PV (right)

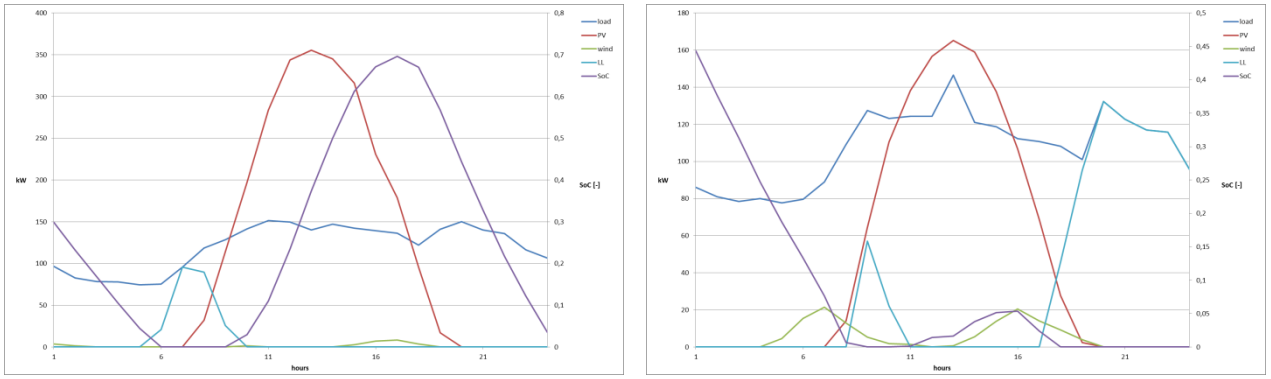

Figures 5.11 Profiles of the day with the lowest generation from wind (left) and with the lowest from PV and wind together (right)

In Figures 5.10 (left) both the PV and the wind power production are higher than the load and the battery is charged, so the system is facing an overgeneration.

In Figures 5.10 (right) the PV has its lower generation, but also the wind is not generating much, therefore there is a loss of load.

In Figures 5.11 (left) there is no generation from the wind turbine, so all the load is up to the PV and the battery.

In Figures 5.11 (right) there is the minimum generation form both the sources, therefore there is a loss of load.

5.2.4 Costs of Li-ion battery configurations

To summarize, the results of the 3 configurations are:

Configuration	PV [kW]	Wind [kW]	Battery [kWh]	Wasted energy [MWh]	LCoE [€/kWh]
PV+battery	820		1628	282	0,243
Wind+battery		2250	2520	3891	0,571
PV+wind+battery	614	250	1397	498	0,235

Table 5.18 Summary results with Li-ion battery

In Table 5.18 the values of the energy wasted per year are reported and it is evident that the high variability of the wind resources leads to install a plant very oversized: in order to have an acceptable LLP it is necessary to have a high number of turbines and waste a lot of energy. For this reason and because the cost of turbines is higher than the cost of PV, the LCoE of wind+bettery configuration is much higher than the PV+battery one. But the adoption of the multi-generation (PV+wind+battery configuration) allows to minimize the costs of the micro-grid, because the optimal usage of different sources make it possible to minimize the battery. Therefore, it may be the right way that has to be followed to minimize the costs of the rural electrification.

This procedure that optimize the configuration with PV, wind and battery is able to find the optimum using PV and wind turbines, so also the configurations with only PV and only wind are considered. Therefore, the result of the *PV+wind micro-grid* module has to be better in terms of LCoE with respect to the modules that consider only one source.

The PV+wind+battery configuration presents the lowest cost. So, it is interesting to see the different composition of the costs. In the following figures are presented the composition of the costs as percentages of the NPC (pie charts) and the cash flow in the 20-year simulation (histograms).

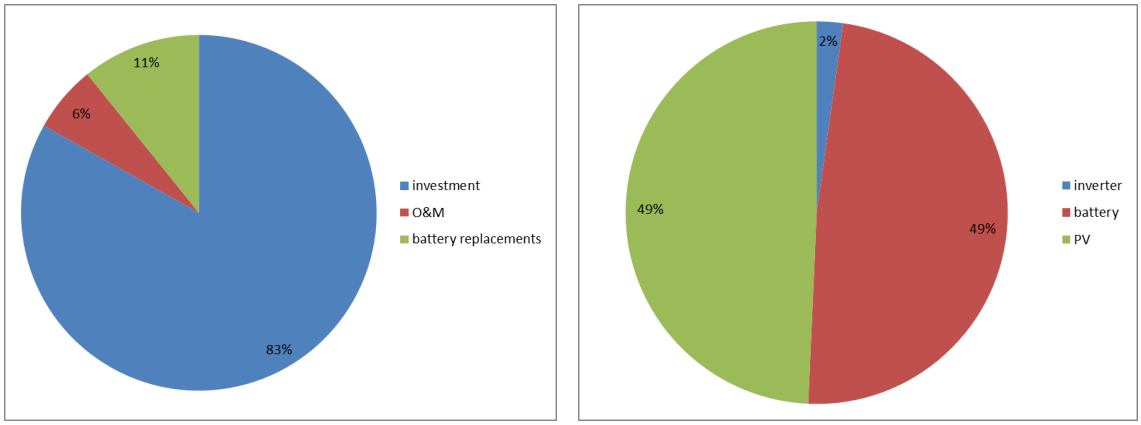

Figures 5.12 NPC percentages of PV+Li-ion battery optimal configuration

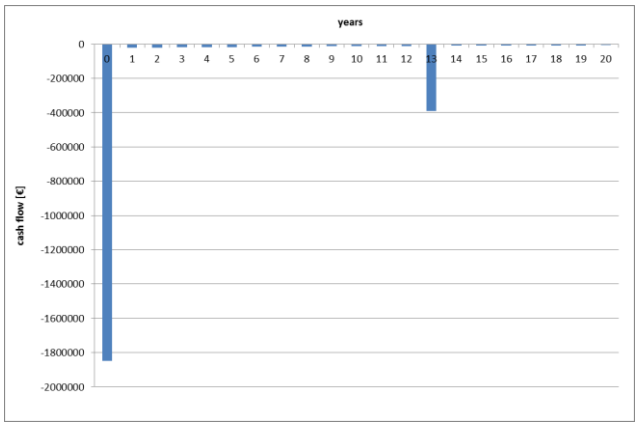

Figure 5.13 Cash flow of PV+Li-ion battery optimal configuration

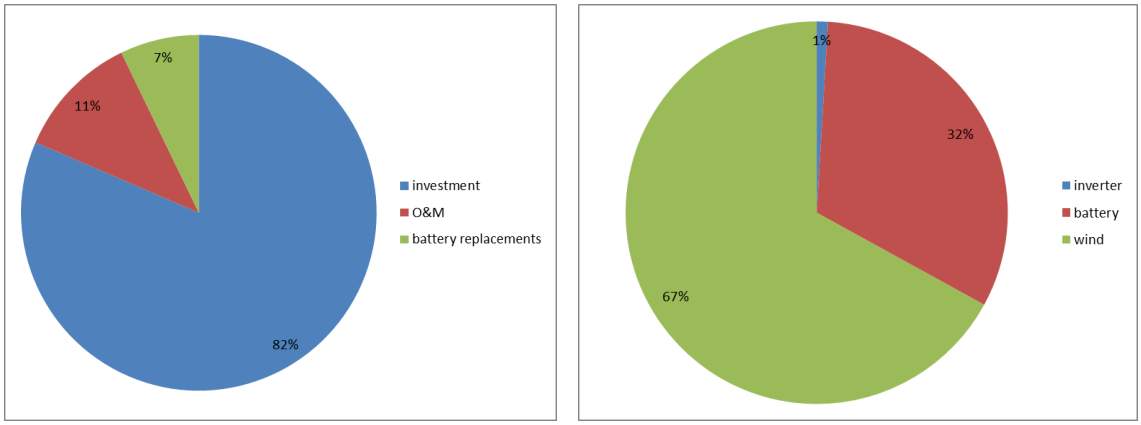

Figures 5.14 NPC percentages of wind+Li-ion battery optimal configuration

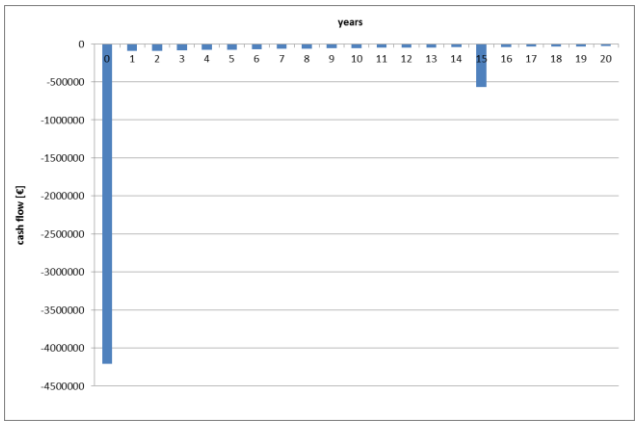

Figure 5.15 Cash flow of PV+Li-ion battery optimal configuration

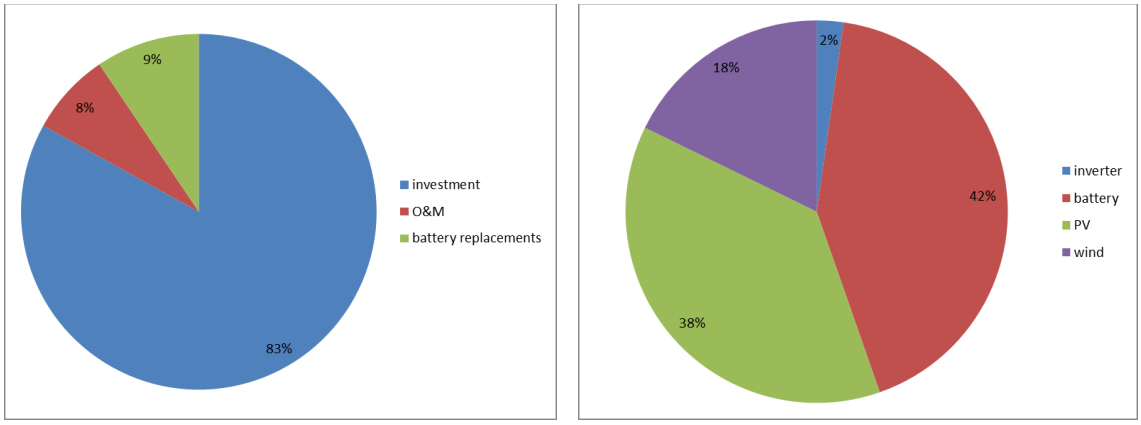

Figures 5.16 NPC percentages of PV+wind+Li-ion battery optimal configuration

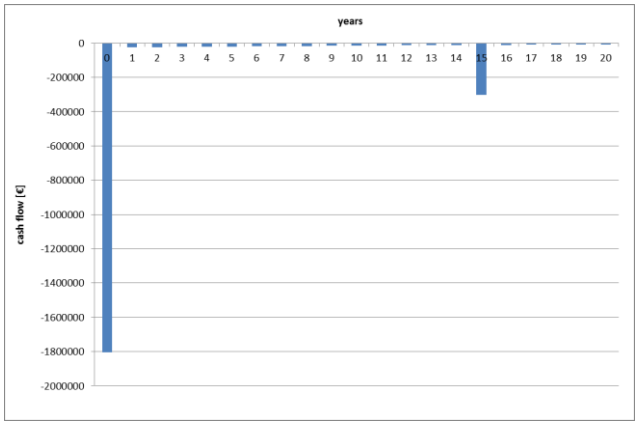

Figure 5.17 Cash flow of PV+wind+Li-ion battery optimal configuration

Dealing with renewable energies, it is evident that the large part of the cost is relative to the investment, while the operation and maintenance costs and the battery replacement costs are less than 20% of the total. The costs of the power generation components and the costs of the batteries are equally important.

The replacement of the batteries can be seen in the cash flows on the 13th or 15th year (the maximum lifetime due to calendar aging is 15 years) since the effect of the SoH reduction is not very important because the

analysed batteries are not very small. In the following figure the SoH trend is reported comparing the PV+battery configuration that reaches the minimum SoH with the wind+battery configurations that does not.

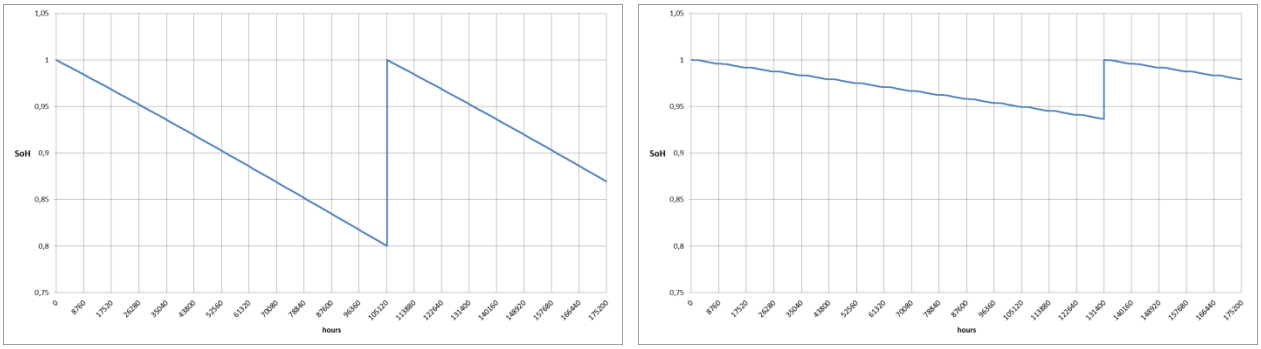

Figures 5.18 SoH for PV+battery optimal configuration (left) and wind+battey optimal configuration (right)

The PV+battery configuration deals with a smaller battery and the solar source presents a high daily variability, therefore the battery faces higher degradation and in Figures 5.18 (left) the minimum SoH (80%) is reached. The opposite happens to the wind+battey configuration, where the battery is replaced for calendar aging (15 years).

5.2.5 The Pb-acid battery configurations

Applying the same procedure to the same profiles of PV, wind and load but adopting Pb-acid batteries, the results are summarized in:

Configuration	PV [kW]	Wind [kW]	Battery [kWh]	Wasted energy [MWh]	LCoE [€/kWh]
PV+battery	820		2714	282	0,281
Wind+battery		2250	4009	3891	0,630
PV+wind+battery	710	250	1983	653	0,266

Table 5.19 Summary results with Pb-acid battery

Also in this case the configuration that mixes the solar and the wind sources is the best solution, and the configuration that adopts only wind turbines presents lot of energy wasted and the highest cost. The installed power of PV and wind turbines is very close to the result given by the configurations with Li-ion battery. But, for all the Pb-acid configurations, the costs are higher with respect to the solutions that adopt Li-ion batteries.

The Pb-acid battery has to work with a lower depth of discharge, therefore to guarantee the same available energy storage it is necessary to have a bigger battery size. Even though the cost per kWh is lower with Pb-

acid batteries, the final cost of the micro-grid is higher because the battery is bigger but also because the lifetime due to calendar aging is shorter, therefore more replacements are necessary.

The costs compositions and the cash flows relative to these configurations are presented in the following charts.

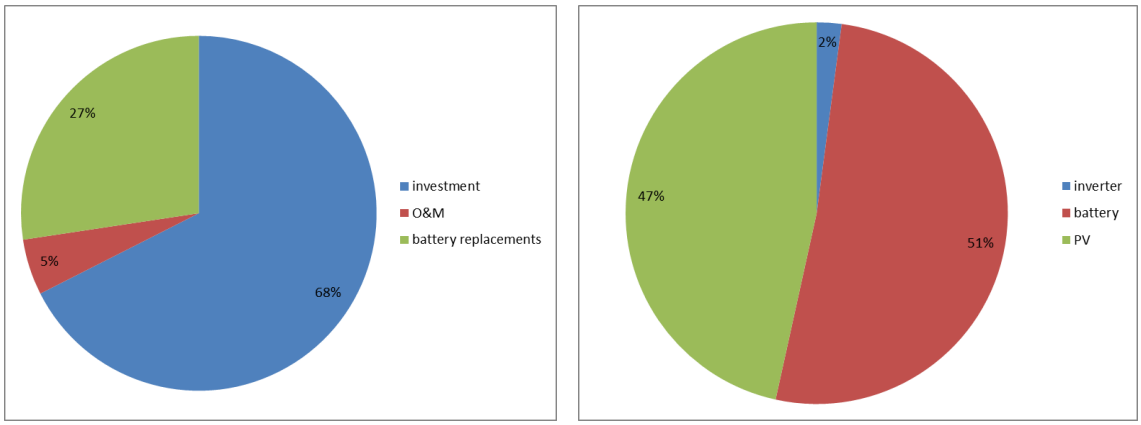

Figures 5.19 NPC percentages of PV+Pb-acid battery optimal configuration

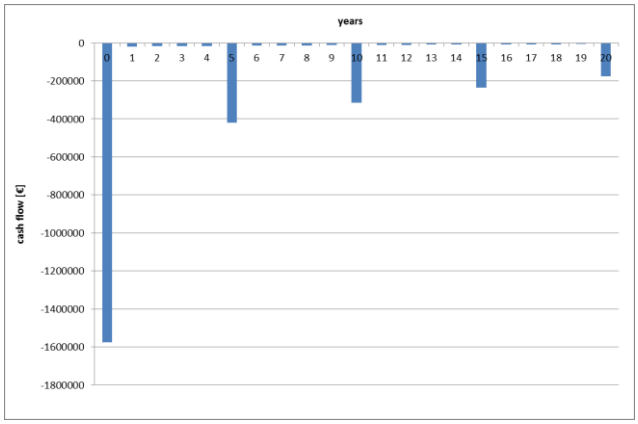

Figure 5.20 Cash flow of PV+Pb-acid battery optimal configuration

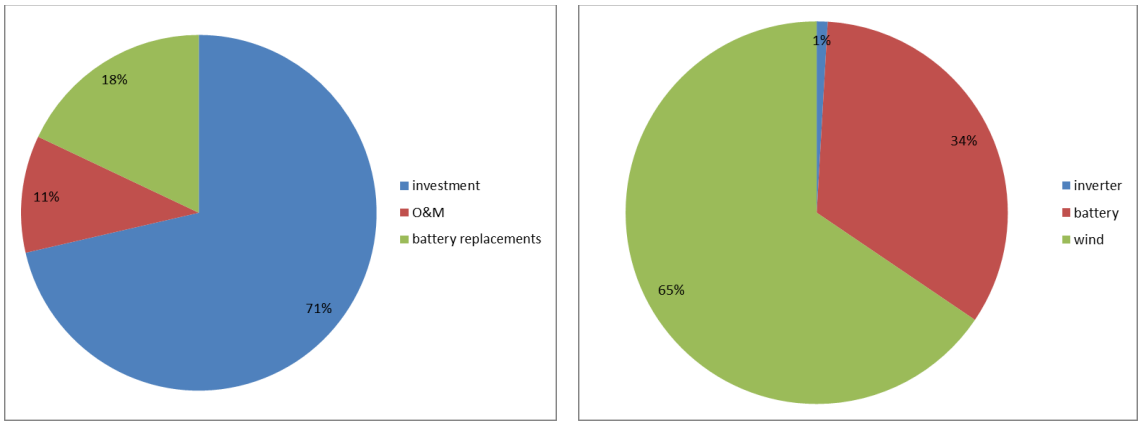

Figures 5.21 NPC percentages of wind+Pb-acid battery optimal configuration

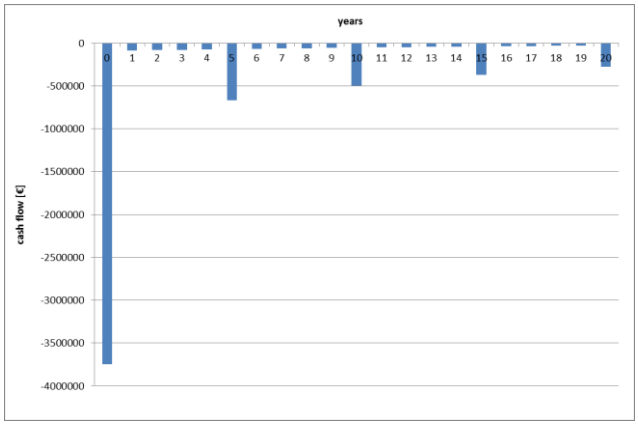

Figure 5.22 Cash flow of wind+Pb-acid battery optimal configuration

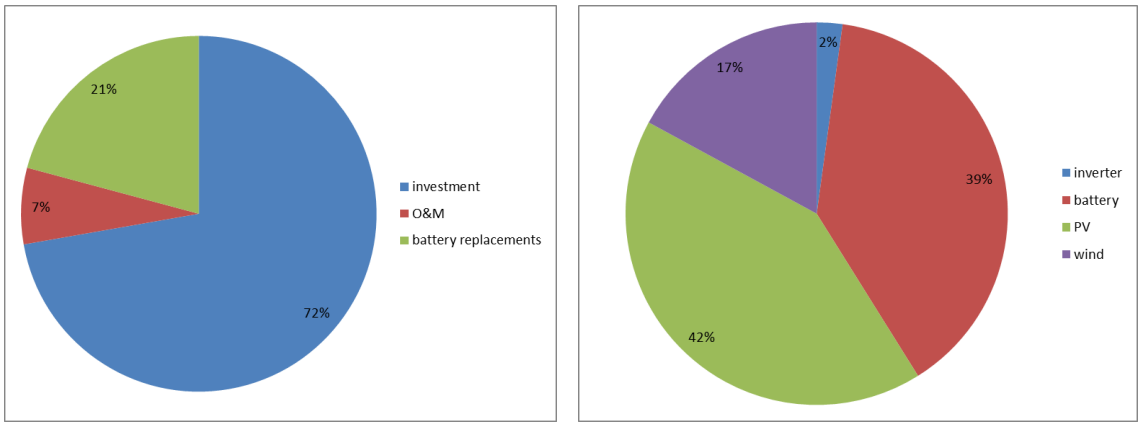

Figures 5.23 NPC percentages of PV+wind+Pb-acid battery optimal configuration

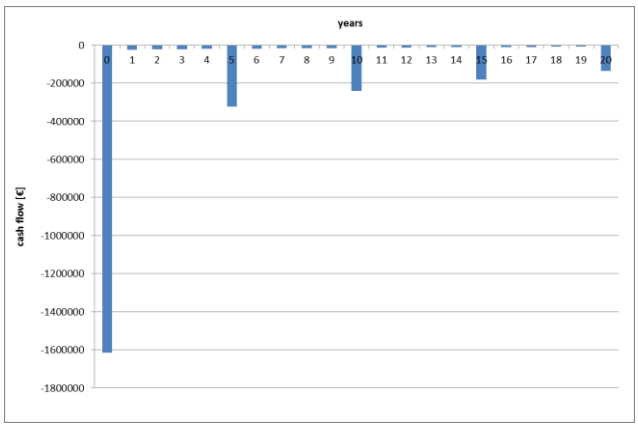

Figure 5.24 Cash flow of wind+Pb-acid battery optimal configuration

In these graphs it is evident that the battery replacements costs are much more important with respect to the results of Li-ion batteries, even though the investment costs are still predominant. As can be seen in the cash flows, the battery replacements are only due to calendar aging (5 years) and the limit on the SoH is never reached. As can be seen in Figure 5.25 where the trend of the SoH for the optimal PV+wind+battery

configuration is reported, since Pb-acid batteries has quite short calendar aging (5 years) the minimum SoH (80%) can be hardy reached.

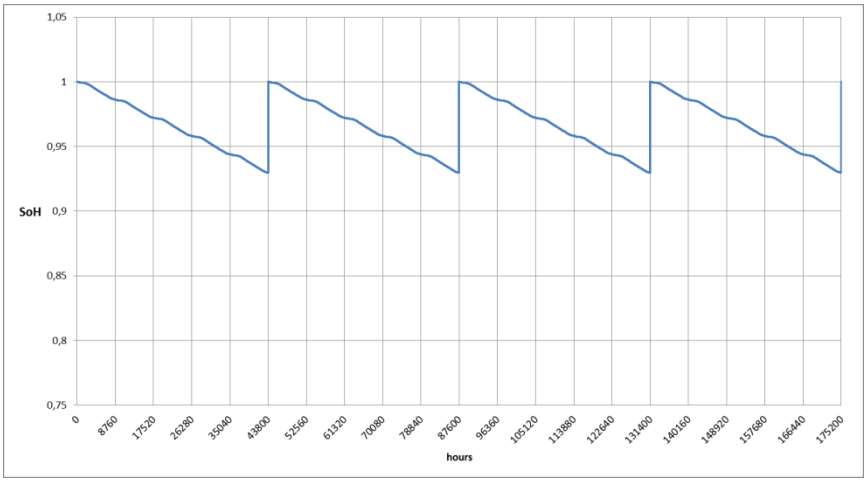

Figure 5.25 SoH for PV+wind+battery optimal configuration

The cost of the battery is an important part of the total cost of the micro-grid; since the Pb-acid battery resulted to be the most expensive, it is not the right solution to minimize the costs of the plant.

5.2.6 Comparison between Li-ion and Pb-acid battery configurations

For sake of exemplification, the working profiles of the system components are shown in the following figures, comparing the solutions with Li-ion and Pb-acid batteries. They represent the power profiles (load in dark blue, power generated by PV in red, power generated by wind turbines in green and loss of load in light blue) and the SoC trend (in violet) in a random day of the simulation.

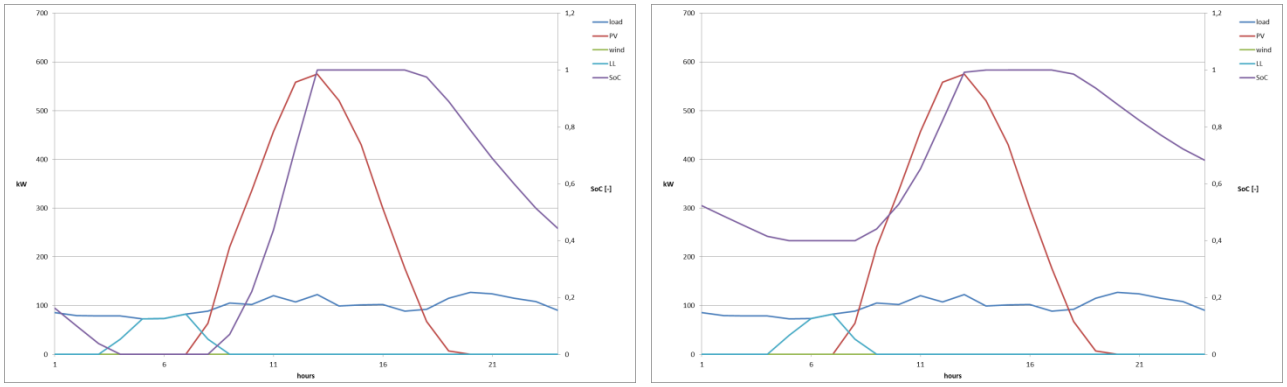

Figures 5.26 Profiles for PV+battery optimal configuration with Li-ion battery (left) and Pb-acid battery (right)

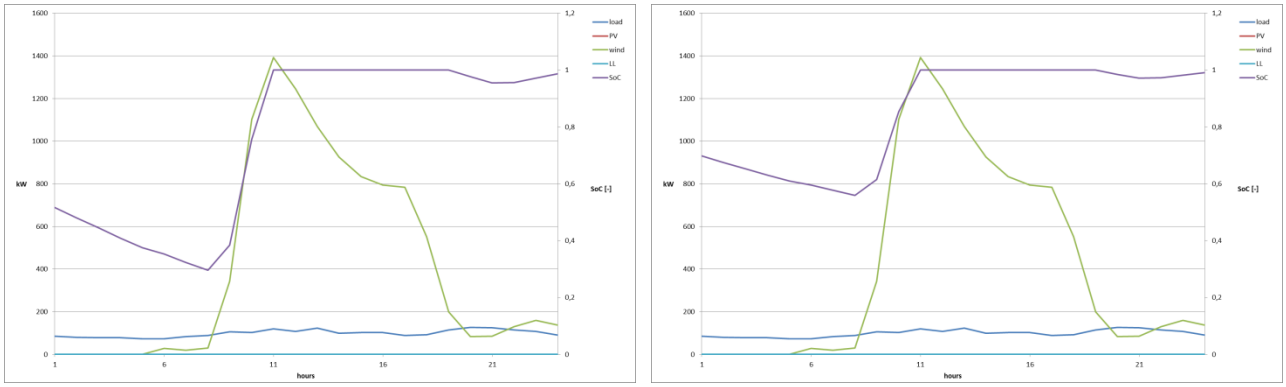

Figures 5.27 Profiles for wind+battery optimal configuration with Li-ion battery (left) and Pb-acid battery (right)

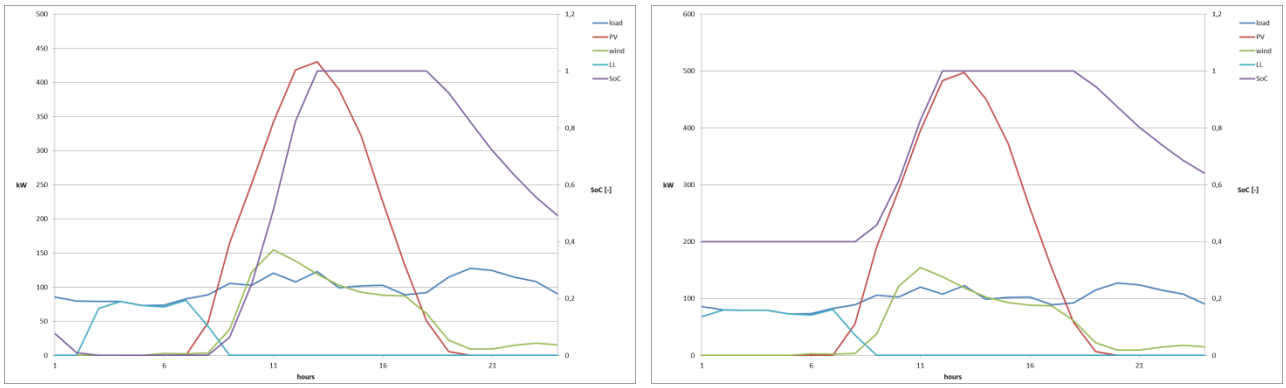

Figures 5.28 Profiles for PV+wind+battery optimal configuration with Li-ion battery (left) and Pb-acid battery (right)

Changing battery technology there are no evident differences about the energy exchanged and the power profiles. The only difference regards the different depth of discharge allowed by the batteries. But adopting different power sources the power exchanged and the loss of load for the same day are completely different.

5.2.7 PV degradation and load increase

So far, the simulations performed are based on load and generation data that are repeated identically from year to year. It is now interesting to consider the possibility that the load will increase during time, while the performances of the PV will decay. Therefore, starting from the 939260-kWh load of the first year (value adopted in all the years in the previous analyses), it is increased by 1% each year of the 20-year simulation. While, to account for decay, the PV generation is reduced by 2% per year. The trends are reported in the following figures.

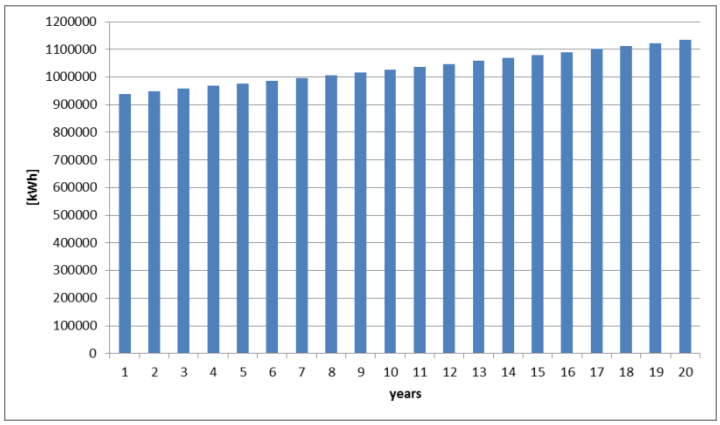

Figure 5.29 Trend of the annual load

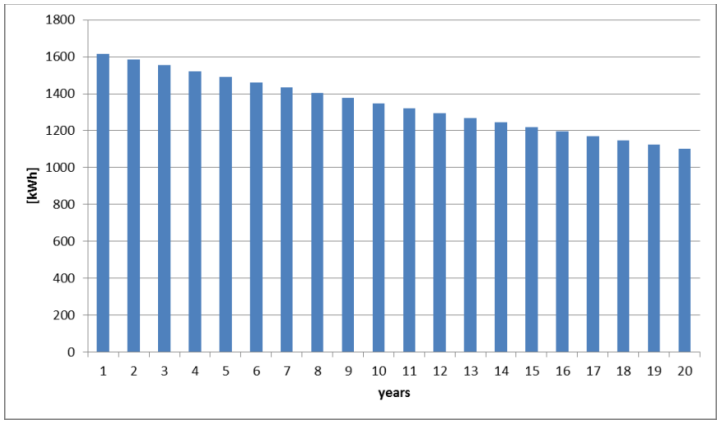

Figure 5.30 Trend of the annual energy generated by 1 kW_p of PV

Adopting these new profiles, the results of the optimizations with the different configurations are reported in the following tables. Adopting Li-ion batteries:

Configuration	PV [kW]	Wind [kW]	Battery [kWh]	Wasted energy [MWh]	LCoE [€/kWh]
PV+battery	1083		2017	306	0,280
Wind+battery		2500	2659	4334	0,578
PV+wind+battery	856	250	1687	550	0,265

Table 5.20 Summary results with Li-ion battery

Instead, adopting Pb-acid batteries:

Configuration	PV [kW]	Wind [kW]	Battery [kWh]	Wasted energy [MWh]	LCoE [€/kWh]
PV+battery	1219		2988	489	0,322
Wind+battery		2250	5443	3785	0,662
PV+wind+battery	856	250	2460	550	0,290

Table 5.21 Summary results with Pb-acid battery

Comparing the results of the case with the profiles repeated identically from year to year (Table 5.18 and Table 5.19) with the case with load increase and PV degradation (Table 5.20 and Table 5.21), it can be seen that the generation size has to be higher in the second case to face the increasing load. In particular the PV size increases by around 35% because of its degradation that can be seen as a lower average efficiency during the 20 years.

The best configuration is again the one that adopts both PV and wind turbines and the same arguments can be done about the cost and the wasted energy of the wind+battery configuration.

The execution of the procedure takes 1 minute to optimize the micro-grid that adopts PV and battery (the simplest), it takes 2 minutes to optimize the configuration with wind turbines and battery (the study of the database takes some time) and the optimization of the micro-grid that adopts PV panels, wind turbines and batteries takes 5 minutes (the procedure has to minimize the objective function for some turbines that is a time-consuming operation and then generate the space of analysis). This fulfills the constraint given by CESI about the computation time of the tool.

Chapter 6

6 Conclusions

In this thesis it was studied a procedure to optimize the design of a micro-grid for rural area electrification.
In order to guarantee the access to electricity to the rural areas of the poorest countries in the world the right choice is to adopt an off-grid system that connects the houses of a small village exploiting renewable energy sources. Therefore, it is necessary to develop a procedure to optimize a micro-grid, that has to be able to find the best configuration and the optimal size of the components.
The micro-grid optimization procedure has been implemented in a tool developed Excel VBA that has to support the decision-making of non-technical personnel, according to the guidelines given by CESI (Centro Elettrotecnico Sperimentale Ialiano), where the author undertook an internship.
Knowing the load and the meteorological data, the load profile and the technical data of the components, the tool aims to find the sub-optimal solution for a micro-grid. The general approach is to find an intuitive sizing of the components, that is a fist staring point calculated by means of simple equations. Then, the space of analysis is generated varying the sizes of the components starting from the intuitive ones. The configurations present in the space of analysis are simulated and their results are compared. For each configuration it is possible to calculate the reliability and the cost: the configuration' reliability is evaluated by means of the LLP, while the cost is represented by the LCoE. Therefore, the techno-economic optimum is the configurations within the space of analysis that has the lowest LCoE and the LLP lower than the maximum accepted.
The main topics studied by the author and implemented in the tool are the development of an advanced battery model, the study of a micro-grid exploiting wind turbines and battery and the study of a micro-grid that mixes the generation of PV with wind turbines.
It is important to have an accurate battery model because it is essential to simulate the energy exchanged in order to optimize the battery size. The optimization of the battery is important since it is an expensive component of the system and it is fundamental to provide energy when the unpredictable renewable energy sources are not present. The model adopted is an analytical model that calculates the charge and discharge efficiency of the battery as a function of the operating parameters. It also considers the capacity fade that is useful to model the battery degradation during utilization.

An alternative to the well-known PV+battery architecture is the adoption of a configuration that exploits wind turbines and battery. The main issue dealing with the wind turbines is that different turbines present different behaviors with respect to the wind speed. Therefore, a database of wind turbine power curves is implemented in the tool. For each turbine in the database it is possible to calculate the intuitive number of turbines and a relative space of analysis. From this the optimal configuration can be found, choosing the optimal turbine and the optimal sizing.

The adoption of a micro-grid that exploits more than an energy source is interesting to reduce the costs optimizing the different sources. Indeed, using different sources it is possible to reduce the battery size and so also the plant costs. In the tool it was developed and implemented a procedure to optimize a micro-grid based on PV, wind turbines and battery. Here the main issue to be faced is the optimization of the mix. At first a technical optimization is performed looking for the ratio between the two sources that minimize the battery size and the best turbine is chosen. Then the best configuration according to the techno-economic parameters is found in a space of analysis where PV, wind a battery are varied.

The procedures proposed were validated using the PV production profile and the wind speed profile given by Renewables.ninja, an online database of meteorological data for all the world. Instead, the load implemented is the measured load of the St. Mary's Lacor Hospital, in Uganda. It resulted that the most cost-effective solution for the case study is the adoption of a micro-grid that exploits PV panels, wind turbines and Li-ion batteries. Even though the Pb-acid batteries present a lower cost per kWh, the Li-ion battery are cheaper considering plant lifetime since they present lower degradation processes. The adoption of PV and wind allows to reduce the costs optimizing the sources and reducing the battery size required.

Further development of the tool can be related to the introduction of other renewable generation sources (for example the hydro) and couple them with non-renewable sources like diesel and implement different dispatching methods.

List of figures

List of symbols

AC	Alternating current
C	Capacity of the battery
cf	Capacity fade
DC	Direct current
DoD	Depth of discharge
E_b	Residual energy stored in the battery
$E_{PV,1kW}$	Hourly average generation profile for a 1-kWp PV
ESS	Energy storage system – Nominal battery size
η	Efficiency
E_{turb}	Hourly average generation profile for a turbine
h_{eq}	Equivalent hours
LL	Loss of load
LLP	Loss of load probability
MPPT	Maximum power point tracker
NPC	Net present cost
N_{turb}	Number of turbines
Ny	Lifespan in years
OF#	Objective function
PE	Power/energy fraction limit
$P_{nom,turb}$	Nominal power of a turbine
$P_{nom,w}$	Total nominal power of the wind turbines
$P_{PV,1kW}$	Power generation profile for a 1-kWp PV
P_{turb}	Power generation profile for a turbine
PV	Photovoltaic panels
PV_{peak}	Nominal power of the PV
$\left(\frac{PV}{wind}\right)_{ratio}$	Ratio between the nominal power of the PV and the total nominal power of the wind turbines
SoC	State of charge of the battery
SoH	State of health of the battery
t	Time step (1 hour)
T	Lifespan in hours (number of time step in the simulation)
y	Year
#turb	Number of turbines

References

[1] United Nations, "Transforming our world: the 2030 Agenda for Sustainable Development," in *General Assembly Resolution 70/1, 25 September 2015*, 2015.

[2] The World Bank, "State of electricity access report," 2017.

[3] E. Colombo, S. Bologna and D. Masera, "Renewable energy for unleashing sustainable development," 2013.

[4] C. Shyu, "End-users' experiences with electricity supply from stand alone mini-grid solar PV power stations in rural areas of western China," *Energy Sustainable Development,* vol. 17, pp. 391-400, 2013.

[5] M. Y. Suberu, M. W. Mustafa, N. Bashir, N. A. Muhamad and A. S. Mokhtar, "Power sector renewable energy integration for expanding access to electricity in sub-Saharan Africa," *Renewable and Sustainable Energy Reviews,* vol. 25, pp. 630-642, 2013.

[6] M. Welsch et al., "Smart and just Grids fro sub-Saharan Africa: Exploring options," *Renewable Sustainable Energy Reviews,* vol. 20, pp. 336-352, 2013.

[7] G. Pepermans, J. Driesen, D. Haeseldonckx, R. Belmans and W. D'haeseleer, "Distributed generation: definition, benefits and issues," *Energy Policy*, vol. 33, no. 6, pp. 787-798, 2005.

[8] T. Ackermann, G. Andersson and L. Söder, "Distributed generation: a definition," *Electric Power Systems Research*, vol. 57, no. 3, pp. 195-204, 2001.

[9] J. Turkson and N. Wohlgemuth, "Power sector reform and distributed generation in sub-Saharan Africa," *Energy Policy,* vol. 29, pp. 135-145, 2001.

[10] R. B. Hiremath, B. Kumar, P. Balachandra, N. H. Ravindranath and B. N. Raghunandan, "Decentralised renewable energy: Scope, relevance and applications in the Indian context," *Energy for Sustainable Development,* vol. 13, no. 1, pp. 4-10, 2009.

[11] C. Patrascu, C. L. Rat, D. Hulea, D. Vitan and N. Muntean, "Mixed PV-Wind Small Power Microgrid," 2017.

[12] S. Sinha and S. S. Chandel, "Review of software tools for hybrid renewable energ ysystems," *Renewable and Sustainable Energy Reviews,* no. 32, pp. 192-205, 2014.

[13] D. Connolly, H. Lund, B. V. Mathiesen and M. Leahy, "A review of computer tools for analysing the integration of renewable energy into various energy systems," *Applied Energy,* vol. 87, no. 4, pp. 1059-1082, 2010.

[14] G. S. Dell'Orto, "Rural electrification, a tool for the microgrids," *Master thesis.*

[15] HOMER energy, "User manual," 2017.

[16] D. W. Dees, V. S. Battaglia and A. Bélanger, "Electrochemical modeling of lithium polymer batteries,"

Journal of Power Sources, vol. 110, 2002.

[17] National Renewable Energy Laboratory (NREL), "HOMER - Hybrid Renewable and Distributed Generation System Design Software," 2010.

[18] M.R. Jongerden and B.R. Haverkort, "Which battery model to use?," *IET Software*, vol. 3, 2009.

[19] L. Tao, J. Ma, Y. Cheng, A. Noktehdan, J. Chong and C. Lu, "A review of stochastic battery models and health management," *Renewable and Sustainable Energy Reviews*, vol. 80, pp. 716-732, 2017.

[20] C. Brivio, "Battery Energy Storage Systems: Modelling, Applications and Design Criteria," *PhD thesis, Politecnico di Milano, Energy department*, 2017.

[21] Sonnenschein, "Handbook for Gel-VRLA-Batteries - Part 2: Installation, Commissioning and Operation," [Online]. Available: http://www.sonnenschein.org/PDF%20files/GelHandbookPart2.pdf.

[22] M. Fadaee and M.A.M. Radzi, "Multi-objective optimization of a stand-alone hybrid renewable energy system by using evolutionary algorithms: A review," *Renewable and Sustainable Energy Reviews*, vol. 16, 2012.

[23] J. F. Manwell, J. G. McGowan and A. L. Rogers, Wind energy explained - theory, design and application, Wiley, 2009.

[24] Energy & Strategy Group, "Renewable energy report 2018 - Il futuro delle rinnovabili in Italia," 2018.

[25] A. Chauhan and R. P. Saini, "A review on Integrated Renewable Energy System based power generation for stand-alone applications: Configurations, storage options, sizing methodologies and control," *Renewable and Sustainable Energy Reviews*, no. 38, pp. 99-120, 2014.

[26] T. Khatib, A. Mohamed and K. Sopian, "A review of photovoltaic systems size optimization techniques," *Renewable and Sustainable Energy Reviews*, no. 22, pp. 454-465, 2013.

[27] S. Sinha and S. S. Chandel, "Review of recent trends in optimization techniques for solar photovoltaic–wind based hybrid energy systems," *Renewable and Sustainable Energy Reviews*, no. 50, pp. 755-769, 2015.

[28] O. Erdinc and M. Uzunoglu, "Optimum design of hybrid renewable energy systems: Overview of different approaches," *Renewable and Sustainable Energy Reviews*, no. 16, pp. 1412-1425, 2012.

[29] E. Koutroulis, D. Kolokotsa, A. Potirakis and K. Kalaitzakis, "Methodology for optimal sizing of stand-alone photovoltaic/wind-generator systems using genetic algorithms," *Solar Energy*, no. 80, pp. 1072-1088, 2006.

[30] Y. S. Zhao, J. Zhan, Y. Zhang, D. P. Wang and B. G. Zou, "The optimal capacity configuration of an independent wind/PV hybrid power supply system based on improved PSO algorithm," 2009.

[31] O. Ekren and B. Y. Ekren,, "Size optimization of a PV/wind hybrid energy conversion system with battery storage using simulated annealing," *Applied Energy*, no. 87, pp. 592-598, 2010.

[32] S. H. Karaki and R. B. Chedid, "Probabilistic Performance Assessment of Autonomous Solar-Wind

Energy Conversion Systems," *IEEE Transactions on Energy Conversion*, vol. 14, no. 3, 1999.

[33] T. Markvart, "Sizing of hybrid photovoltaic-wind energy systems," *Solar Energy*, vol. 57, no. 4, pp. 277-281, 1996.

[34] W. D. Kellogg, M. H. Nehrir, G. Venkataramanan and V. Gerez, "Generation unit sizing and cost analysis for stand-alone wind, photovoltaic, and hybrid wind/PV systems," *IEEE Transactions on Energy Conversion*, vol. 13, no. 1, 1998.

[35] P. Toma, P. Dorin, E. Radu and M. Daniel, "Sizing photovoltaic-wind smart microgrid with battery storage and grid connection," 2014.

[36] EngineerExcel.com, "Excel solover: which solving method should I choose?," [Online]. Available: http://www.engineerexcel.com/excel-solver-solving-method-choose/.

[37] A. Alaimo and A. M. Zanolini, "Design of a model for micro-grid simulations: the case of St. Mary's Lacor Hospital," *Master thesis.*

[38] IRENA, "Battery storage for renewables: market status and technology outlook," 2015.

[39] Agora Energiewende, "Future Cost of Onshore Wind," 2017.